METAL ION-MEDIATED FOLDING AND CATALYSIS OF THE HAMMERHEAD RIBOZYME

by

WILLIAM LUKE WARD

A DISSERTATION

Presented to the Department of Chemistry
and the Graduate School of the University of Oregon
in partial fulfillment of the requirements
for the degree of
Doctor of Philosophy

June 2012

DISSERTATION APPROVAL PAGE

Student: William Luke Ward

Title: Metal Ion-Mediated Folding and Catalysis of the Hammerhead Ribozyme

This dissertation has been accepted and approved in partial fulfillment of the requirements for the Doctor of Philosophy degree in the Department of Chemistry by:

Andrew J. Berglund	Chairperson
Victoria J. DeRose	Advisor
Tom H. Stephens	Member
Diane K. Hawley	Member
Alice Barkan	Outside Member

and

Kimberly Andrews Espy	Vice President for Research& Innovation/Dean of the Graduate School

Original approval signatures are on file with the University of Oregon Graduate School.

Degree awarded June 2012

DISSERTATION ABSTRACT

William Luke Ward

Doctor of Philosophy

Department of Chemistry

June 2012

Title: Metal Ion-Mediated Folding and Catalysis of the Hammerhead Ribozyme

The factors that determine RNA structure formation, stability, and dynamics are inexorably linked to RNA function. The Hammerhead ribozyme (HHRz) has long served as a model for studying metal-dependent folding and catalysis in RNA. The HHRz consists of three helices meeting at a common junction of conserved nucleotides that form the active site of the ribozyme. Current models of metal-dependent HHRz function involve a requirement for divalent metals to globally fold the ribozyme at low metal concentrations, followed by a second metal-dependent process which activates the HHRz for catalysis. The exact role of metal ions in activating HHRz catalysis is still a subject of investigation. We used 2-aminopurine substitutions near the active site of the ribozyme to determine if this second metal-dependent process involves a conformational rearrangement in the core of the ribozyme. We find evidence for a conformational change beyond global folding in the core of the ribozyme that not only correlates with metal activated catalysis but is also sensitive to the identity of the metal ions used for folding. Though phosphorothioate substitutions indicate that a ground-state coordination of a catalytic metal to the scissile phosphate is required for efficient catalysis, our folding studies show that this coordination event is not absolutely required for folding of the HHRz core. To investigate possible roles for metal ions in general acid-base catalysis, we tested the pH dependence of the HHRz rate using a

variety of metal ions. We find the pH dependent rate profile of the ribozyme is shifted by transition metal ions, whereas other group II metals show similar profiles to Mg^{2+}. Combined these data suggest there is a non-specific requirement for divalent metal ions to fold the core of the ribozyme, while the specific characteristics of metal ions affect the architecture of the active site and dictate the effects of metals ions on the catalytic mechanism. This dissertation includes previously published and un-published co-authored material.

CURRICULUM VITAE

NAME OF AUTHOR: William Luke Ward

GRADUATE AND UNDERGRADUATE SCHOOLS ATTENDED:

University of Oregon, Eugene, Oregon

University of Missouri, Columbia, Missouri

DEGREES AWARDED:

Doctor of Philosophy, Chemistry, 2012, University of Oregon

Bachelor of Science, Biochemistry, 2006, University of Missouri

AREAS OF SPECIAL INTEREST:

RNA Structure, Function, and Catalysis

Molecular Biophysics

PROFESSIONAL EXPERIENCE:

NSF GK-12 Teaching Fellow, Materials Science Institute, University of Oregon, Eugene, Oregon, 2010-2012

Graduate Teaching Fellow, University of Oregon, Eugene, Oregon, 2006-2007

GRANTS, AWARDS, AND HONORS:

NIH Molecular Biology Training Grant, Institute of Molecular Biology, University of Oregon, Eugene, Oregon, 2007-2010

Undergraduate Research Grant, University of Missouri, Columbia, Missouri, 2005-2006

PUBLICATIONS:

Ward, W.L. and DeRose, V.J. 2012. Ground-state coordination of a catalytic metal to the scissile phosphate of a tertiary-stabilized Hammerhead ribozyme. *RNA-a Publication of the RNA Society* **18**(1): 16-23.

Osborne, E.M., Ward, W.L., Ruehle, M.Z., and DeRose, V.J. 2009. The identity of the nucleophile substitution may influence metal interactions with the cleavage site of the minimal hammerhead ribozyme. *Biochemistry* **48**(44): 10654-10664.

ACKNOWLEDGMENTS

I would like to express my gratitude to Dr. Victoria DeRose for her guidance and support through my graduate school career. I would also like to thank the members of my committee and Dr. Pete von Hippel for their scientific and professional guidance throughout my time at the University of Oregon. Additionally, I gratefully acknowledge funding by the University of Oregon Institute of Molecular Biology NIH Training Grant (GMGM007759-29) and The Material Science Institute NSF GK-12 Fellowship (DGE-0742540).

I would also like to thank the members of the DeRose and the von Hippel Labs for their contributions to my experience. In particular, I thank Dr. Erich Chapman for his significant impact on my time here in Eugene, both inside the lab and out. Additionally, I would like to thank my incredible friends in the many different circles of my life; you have made my time here in Eugene extraordinary.

Finally, I thank my family, particularly my parents Dr. Mark and Katy Ward for their unending love and support.

This dissertation is dedicated to the teachers in my life.

TABLE OF CONTENTS

Chapter Page

LIST OF FIGURES

Figure Page

LIST OF TABLES

Table Page

LIST OF SCHEMES

Scheme Page

CHAPTER I
INTRODUCTION

Emerging fields of functional RNA

While RNA may be best known for its role in transferring information from DNA for translation into proteins, new classes of functional RNAs continue to be discovered and are not only re-shaping the view of RNA's role in the essential functions of life, but its role in the creation of life itself. In 1982-83, the labs of Thomas Cech and Sydney Altman reported protein independent catalysis of phosphodiester bond cleavage by the RNA components of the Group I intron and RNaseP enzyme, respectively (Kruger et al. 1982; Guerrier-Takada et al. 1983). Since this initial discovery, several other catalytic RNA systems have been discovered. Known as ribozymes, these functional catalytic RNAs represented a paradigm shift in molecular chemistry, as the role of biological catalyst no longer fell solely in the realm of proteins.

Ribozymes are found throughout all domains of life and are part of a range of essential biochemical processes. The RNaseP ribozyme, for instance, is composed of a highly conserved catalytic RNA subunit and a variable number of associated proteins. The catalytic RNA subunit of RNaseP is conserved throughout all domains of life and forms the active site, which cleaves RNA as a step of tRNA maturation. Another ubiquitous ribonucleoprotein complex, the ribosome, also has an all RNA active site, and is therefore also considered to be a ribozyme (Nissen et al. 2000). The group I and group II introns are ribozymes involved in mRNA maturation through their ability to specifically cleave and then ligate the phosphodiester backbone during intron removal (Kruger et al. 1982; Michel and Dujon 1983). Interestingly, the excised sequence of the group II intron can contain open reading frames, which encode proteins that enable the group II intron to exist as mobile retroelements, a finding that has great implications for the evolution of introns and retroviral species (for review see (Mohr et al. 2010)). The remaining naturally occurring ribozymes are of the small endonucleolytic ribozyme family. Most ribozymes of this family function in genomic processing of sub-viral

elements (for review see ((Cochrane and Strobel 2008; Fedor 2009). While the members of this family all perform the same type of reaction, they are diversified in sequence and structure. One member of this group, the GlmS ribozyme, stands out due to its dual nature as a ribozyme and a riboswitch. The GlmS ribozyme is found in the 5' UTR of the bacterial *glmS* gene and switches conformations in response to the presence of glucosamine-6-phosphate (Winkler et al. 2004). The binding of this co-factor stabilizes the catalytic conformation and is also a required component of the catalytic mechanism (Klein and Ferre-D'Amare 2006). The discovery of the GlmS ribozyme/riboswitch represents a significant extension of the ribozyme field into the potential for ribozyme systems to participate in genetic regulation. The discovery of new ribozymes and increasing diversity of ribozyme capabilities has strengthened the concept of an RNA world, in which it is hypothesized that as a bio-molecule capable of both catalysis and information storage, RNA may represent the sole component of the first self-replicating biological systems (Gesteland et al. 2006).

Our understanding of the physical and chemical principles that enable RNA systems to form complex active sites capable of catalysis continues to evolve. The scientific community has still not defined the limits of ribozyme catalysis, as new ribozymes are still being discovered. The discovery of new ribozymes in nature and the evolution and engineering of ribozyme systems in the laboratory environment demonstrates the depth of ribozyme capabilities and their potential as molecular tools and medicinal therapies. A thorough understanding of ribozyme structural biology and biochemistry will be necessary to safely and effectively harness the exciting potential of this class of functional RNA.

RNA structure and catalysis

Ribozymes, like protein enzymes, use a variety of strategies in order to overcome the energetic barriers of chemical reactions (Cochrane and Strobel 2008; Fedor 2009). Perhaps the most ubiquitous of these strategies is the creation a specific active site that binds reactive species and thereby provides substantial energetic gains. Within the active site, solvent and functional groups are precisely positioned in order to interact with the reactive bonds of the substrates. The use of general acid-base chemistry is a common

strategy for nucleophile activation and protonation of leaving groups in natural ribozymes (DeRose 2002). The effective positioning and alignment of the nucleophile and electrophile is necessary to overcome the electrostatic and geometric barriers of reaching the transition state. Typically, the active site is protected from bulk solvent allowing the electrostatic environment of the active site to be tuned to either destabilize the ground state, and/or stabilize the transition state. While these are common and well understood strategies for enzymes, there are particularly challenging aspects in regards to the nature of ribonucleic acids that ribozymes must overcome to form an active site and catalyze chemical reactions (Fedor and Williamson 2005).

Perhaps the most glaring differences between RNA and proteins are the very components that make up each polymer. Proteins employ a variety of side chains, branching off a peptide backbone, that interact to stabilize protein structure and fine-tune the chemical environment of active sites. RNAs, on the other hand, are much more limited in the variety of polymeric units, with only 4 common nucleobases and a negatively charged phosphodiester backbone (**Figure 1.1**). Despite these limitations, RNA is able to fold into a variety of secondary structural motifs such as helices, pseudoknots, stem-loops, and unpaired bulges. These motifs interact with each other and often times with protein co-factors, to form a stable tertiary structure. To form both secondary and tertiary structure, however, RNA must overcome significant charge repulsion by the polyanionic phosphodiester backbone. To overcome this strong charge repulsion, RNA is dependent on the presence of cations for structural stabilization.

Cations interact with RNA on several levels (for review see (Misra and Draper 2002; Sigel and Pyle 2007)). On a very basic level, cations condense around RNA due to electrostatic attraction to the negatively charged phosphodiester backbone. This increases the local concentration of cations and creates a diffuse cationic cloud that provides a basic level of charge shielding, allowing RNA to form secondary structures. While monovalent cations (normally Na^+ or K^+) are sufficient for this effect, divalent metal ions, such as Mg^{2+}, are able to aid in folding much more effectively due to increased charge density. The increased charge density of divalent metals also allows a single metal ion to shield charges from multiple phosphate groups in a tight space. These highly electronegative regions, therefore, form non-specific metal cation-binding pockets.

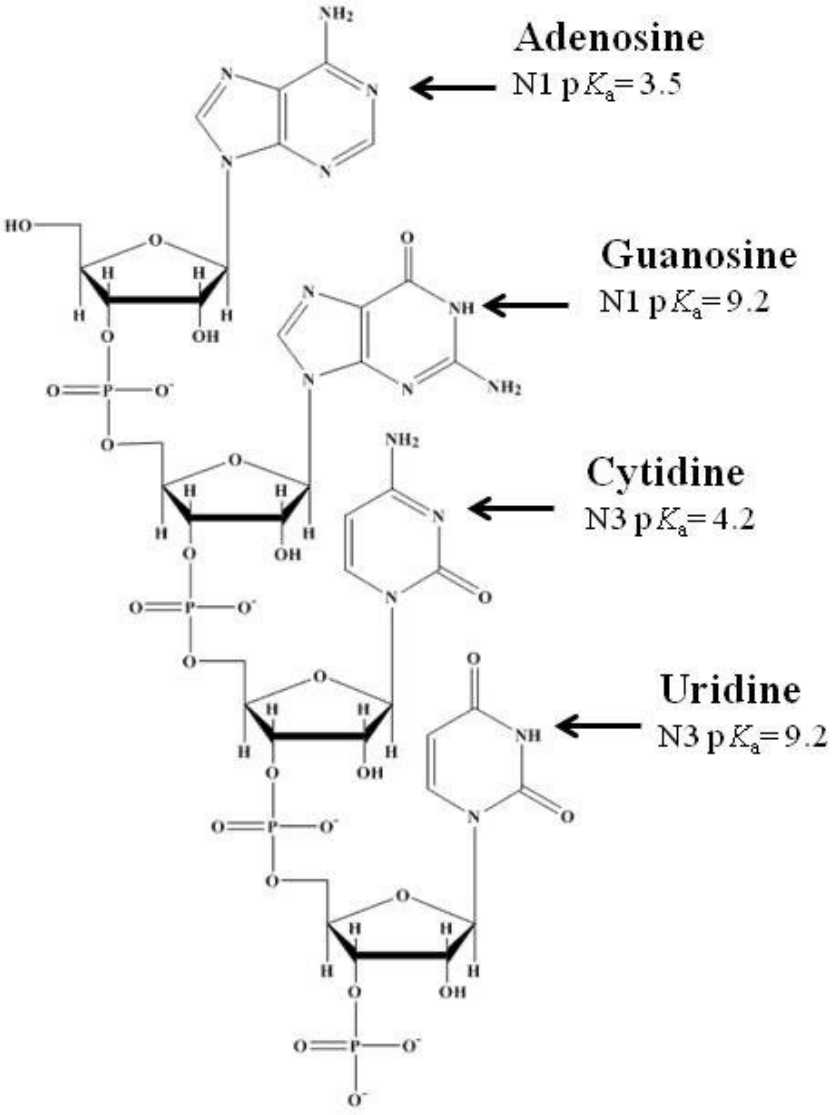

Figure 1.1. The basic components of RNA. The four nucleobases adenosine, guanosine, cytidine, and uridine are attached to ribose sugars which are linked via negatively charge phosphodiester bonds. The most common protonatable groups for each base, indicated by arrows, have pK_a values well outside of neutrality (pK_a values from (Fedor and Williamson 2005)).

While non-specific binding of divalent cations to RNA can sufficiently stabilize some tertiary structure formation, divalent metal ions can offer a greater level of stabilizing interactions through their coordination spheres. Outer sphere coordination

interactions are formed via hydrogen bonding of metal-bound water molecules to RNA ligands. Inner sphere coordination is formed by direct coordination of the metal ion to an RNA ligand. Combinations of coordination interactions of a single metal ion to multiple RNA ligands can provide significant levels of structural stability and can often times form bridging interactions between sequentially distant domains. Specific coordination of metal ions within the active sites of ribozymes offers a variety of potential chemical advantages for the promotion of catalysis beyond the stabilization of the local architecture, including direct participation in the catalytic mechanism, electrostatic tuning of the chemical environment of the active site, and alteration of nucleobase pK_as via Lewis acidity (Sigel and Pyle 2007).

At first approximation, RNA seems ill-suited for biological catalysis. Aside from electrostatic repulsion by the phosphodiester backbone, the functional groups of RNA nucleobases have pK_a values well out of the range of physiological pH (Fedor and Williamson 2005), suggesting that these groups could not effectively participate in general acid or general base chemistry (**Figure 1.1**). Instead, it was theorized that RNA acted as a scaffold for metal ions, which when specifically bound in the active site would promote catalysis via metal-bound water molecules participating in acid-base catalysis and metal-coordination providing charge stabilization of the transition state (Steitz and Steitz 1993). This model of metal-mediated catalysis is exemplified by the extensive participation by Mg^{2+} ions in the Group I ribozyme mechanism (Shan et al. 2001). However, investigations into the mechanisms of the type II family of small ribozymes have shown that ribozymes use a variety of catalytic strategies and do not strictly rely on divalent metal ions.

The type II family of small ribozymes perform endonucleolytic cleavage of a specific phosphodiester bond via general acid-base catalyzed nucleophilic attack of a 2'-OH on the proximal 3' –phosphate, resulting in a 2', 3' –cyclic phosphate and a 5'-OH leaving group (**Figure 1.2**). This ribozyme family consists of the Hammerhead ribozyme (HHRz), HDV ribozyme, hairpin ribozyme, VS ribozyme, and the GlmS riboswitch/ribozyme. Each member of this family seems to perform general acid-base catalysis differently (Cochrane and Strobel 2008; Fedor 2009). Strategies include combinations of the use of metal ion-mediated catalysis, nucleobase functional groups

with perturbed pK_a values, and/or non-metal co-factors. Even though the HHRz was the first member of this family to be discovered (Buzayan et al. 1986), and has long been a model system for investigating RNA folding and catalysis, the exact details of the HHRz mechanism remain incompletely elucidated.

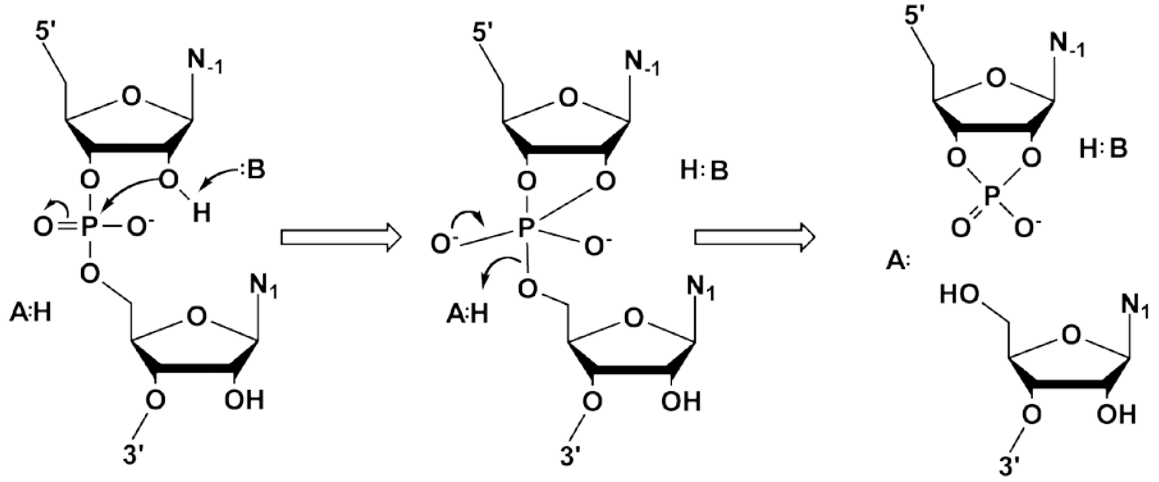

Figure 1.2. Proposed mechanism of cleavage by small nucleolytic ribozymes.

The Hammerhead Ribozyme

The Hammerhead ribozyme was first discovered as a component of the reproduction cycle of the subviral RNA plant pathogens known as viroids (Buzayan et al. 1986). These extremely small (200-400nt), circular, RNA-based viroids invade plant cells and recruit host polymerases to reproduce via rolling circle replication (Flores et al. 2005). During polymerization a multimeric strand of genomic RNA is produced, which subsequently is processed through HHRz catalysis. Once per copy of the genome, the HHRz motif transiently forms in order to cleave a specific phosphodiester bond, leaving monomeric copies of the viroid genome to be re-circularized either via ligation enzymes or the reverse HHRz cleavage reaction. Upon circularization, the HHRz motif is sequestered by base pairing, preventing the reformation of the active ribozyme motif.

Though the HHRz motif was first known to function in viral plant pathogens, the motif has since been found in several other species. Initial searches found HHRz motifs in the genomes of several amphibious species, where they reside in tandem repeats of satellite DNA (Epstein and Gall 1987; Zhang and Epstein 1996). HHRz motifs were subsequently found in satellite DNA of blood flukes (*Schistisoma*) and cave crickets

(Ferbeyre et al. 1998). More recently, the wealth of data that has been produced by genomic sequencing has been computationally mined to predict functional RNA motifs such as the HHRz (Hammann et al. 2012), leading to discoveries of genomic HHRz motifs in all domains of life, including human (de la Pena and Garcia-Robles 2010). Despite their widespread distribution and sequence conservation, the biological function of the HHRz motif is unknown outside of the plant pathogens, suggesting that these motifs might merely be genetic fossils.

The HHRz motif is composed of three variable length helices meeting at a common junction of highly conserved nucleotides, which form the active site. For several years, the HHRz was studied in its most simplified form, in which the motif was separated into a "substrate" strand (containing the scissile phosphate), and an "enzyme" strand. The helices surrounding the active core were truncated, leading to the "minimal" or "truncated" HHRz systems (**Figure 1.3A**) (Ruffner et al. 1990). A wealth of biochemical data was derived by experimentation on minimal HHRz constructs. However, there was widespread disagreement about the details of the HHRz catalysis, as structural and biochemical data were essentially irreconcilable (Blount and Uhlenbeck 2005). It was therefore hypothesized that the catalytically active conformation of the HHRz was very different from the structure described by crystallography (Peracchi et al. 1997).

In 2003, it was discovered that the inclusion of un-basepaired loop and/or bulge motifs in helices I and II of the HHRz is essential for in vivo activity (**Figure 1.3B**) (Khvorova et al. 2003). These unpaired regions, constitutively found in native HHRz sequences, had long been ignored due to the extremely high variability of the positioning and sequence of the motifs (Dufour et al. 2009). The inclusion of these unpaired regions led to significant increases in HHRz catalytic rates, while also greatly reducing the concentration of divalent metals needed to achieve such rates (De la Pena et al. 2003; Canny et al. 2004). HHRz catalysis studies, along with folding studies, led to the conclusion that the unpaired motifs in helices I and II of the HHRz formed tertiary interactions which aid in stabilization of the active site.

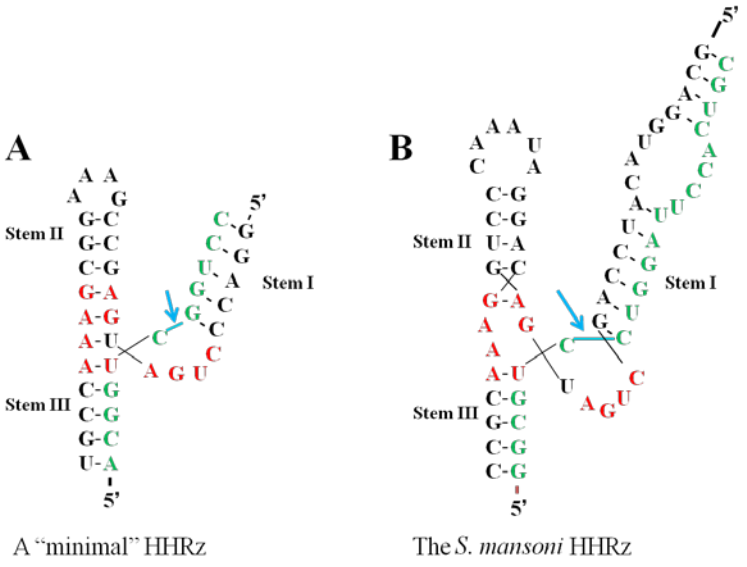

Figure 1.3. Two derivations of the HHRz. A) The minimal form of the HHRz contains only the core nucleotides with three helical stems. B) A native HHRz, based on the *Schistosoma mansoni* sequence, includes unpaired loop structures in Stems I and II. The substrate strand is labeled in green, with the scissile bond highlighted by the blue arrow. The enzyme strand is labeled in black. The conserved nucleotides of the core are red.

In 2006, a crystal structure of a native HHRz confirmed tertiary interactions between helices I and II, and provided a view of the HHRz tertiary structure and active site that is entirely different from that of the minimal HHRz (**Figure 1.4**) (Martick and Scott 2006). This new structural view of the active site did much to reconcile mechanistic models based on biochemical experimentation, which previously were not in agreement with models that were based on structures of minimal HHRzs (for review see (Nelson and Uhlenbeck 2008b)). At the same time, this structure brought up several new questions regarding the HHRz mechanism. Of particular relevance is the dependence of metal ions for folding and catalysis (Kim et al. 2005). The HHRz has long been known to use divalent metal ions in the catalytic mechanism. However, while the minimal HHRz was absolutely dependent on divalent metals, the native HHRz does not show an absolute requirement for divalent metals *in vitro*, as appreciable rates of catalysis are achieved in

high concentrations of monovalent ions (for review see (Leclerc 2010). Despite this, it is likely that under physiological ionic conditions, the HHRz utilizes Mg^{2+} ions in the catalytic mechanism. Exactly how metal ions are utilized by the HHRz, however, is still unknown.

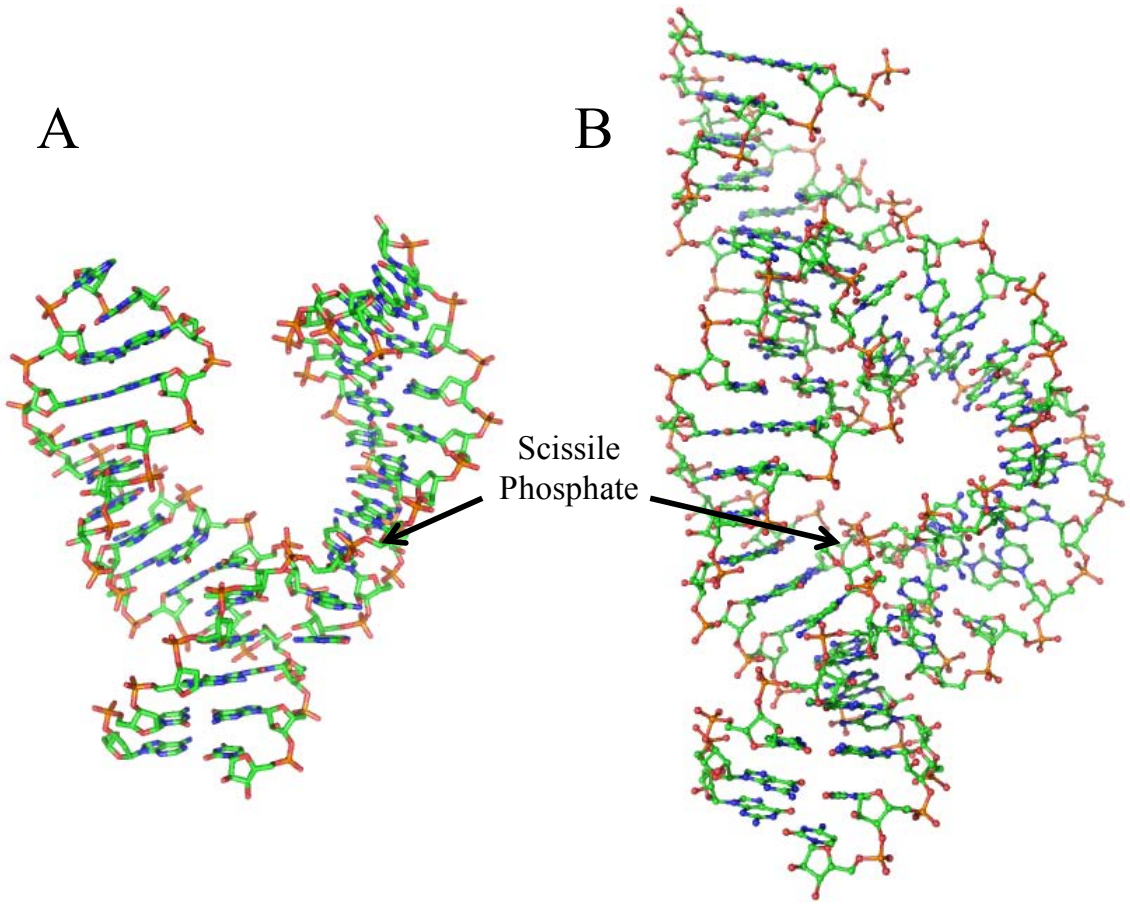

Figure 1.4. Crystal structures of two HHRzs. A) a minimal HHRz (pdb ID 1HMH (Pley et al. 1994)) and a (B) native HHRz (pdb ID 2GOZ (Martick and Scott 2006)). While the minimal HHRz shows an open conformation, the native HHRz demonstrates "docking" of loop regions of stems I and II which impart a significant change on the structure of the core. The cleaved phosphate is indicated by arrows.

Overview and acknowledgment of contributions by others to this dissertation

This dissertation describes research done in the lab of Dr. Vickie DeRose aimed at elucidating the roles of metal ions in stabilizing HHRz structure and how metal ions participate in the catalytic mechanism. This document includes the contributions of

several co-workers and all experiments were co-developed and all material was co-written with Dr. DeRose. The second chapter contains material that was published in RNA regarding the interactions with metal ions with the scissile phosphate of a native HHRz construct (Ward and DeRose 2012). Chapter III reports the use of the fluorescent nucleobase analog 2-aminopurine as a structural probe for conformational changes in the core of the HHRz. The idea for this work stemmed from conversations with my co-worker Dr. Erich Chapman. From these initial ideas, I developed the experimental strategy and performed all the bench work. This work has been submitted for publication in *RNA* (Ward and DeRose Submitted). In Chapter IV, I describe investigations into the role of metal ions on general acid catalysis for the HHRz. For this chapter I worked with Dan Morris, Matthew Hendricks, and Greg Solis as they performed the majority of the bench work under mine and Vickie's mentorship. Additionally, Dr. Barb Golden suggested that A6 might play a role in general acid catalysis, inspiring us to determine the pH profile of A6 mutants. The project was planned and guided by Vickie and myself and will be submitted for publication in *Biochemistry*. Finally, Chapter V is a project that was mostly performed by Dr. Edith Osborne at Texas A&M and represents a major component of Edith's doctoral dissertation. This work involves the use of phosphorous NMR to study metal ion interactions with components of the HHRz active site. The project was finished at the University of Oregon. While I helped Vickie in planning the necessary experiments to finish the project, the bench work performed in Oregon was done by Max Z. Ruehle under the guidance of Vickie and myself. The manuscript, published in *Biochemistry* (2009), was co-written by Edith, Vickie, and myself (Osborne et al. 2009). I would like to thank all those involved with these projects for their work and contributions to this dissertation.

CHAPTER II

GROUND-STATE COORDINATION OF A CATALYTIC METAL TO THE SCISSILE PHOSPHATE OF A TERTIARY-STABILIZED HAMMERHEAD RIBOZYME

Overview

This chapter was co-written with Dr. Victoria DeRose and includes work published in *RNA* (Ward and DeRose 2012). Dr. DeRose conceived of this project. I performed all the experiments and helped to refine the project strategy in regards to using lower cation concentrations to better analyze metal-dependent HHRz rates. As my first project as a member of the DeRose Lab, this work represents my introduction to the HHRz and helped to guide my experimental goals for this dissertation.

Introduction

A continuing challenge in the field of ribozyme enzymology is the precise determination of the contributions of metal ions to RNA catalytic activity. RNA has a general electrostatic requirement for cations for proper folding, and metal ions can specifically bind RNA ligands via inner or outer sphere coordination to provide a deeper level of structural stabilization. Site-specifically bound divalent metal ions can have a direct role in the chemical mechanism of the ribozyme as well (Sigel and Pyle 2007). Using RNaseP and the group I intron as model ribozymes, Steitz and Stietz proposed that ribozymes might rely on bound metal ions to perform general acid/base chemistry (Steitz and Steitz 1993). However, insights into the mechanisms of small nucleolytic ribozymes have indicated that the nucleobase functional groups of RNA can also play critical roles in catalysis, with the extreme example of the hairpin ribozyme which is proposed to catalyze phosphoryl transfer in the complete absence of metal ion participation in the chemical mechanism (Nesbitt et al., 1997; Bevilacqua, 2003). A thorough understanding of the range of mechanisms employed by ribozymes has not yet been realized, as the

detailed mechanisms including the specific roles of metal ions in ribozyme active sites are difficult to ascertain.

The Hammerhead Ribozyme (HHRz) has been a particularly challenging system with regards to determining the roles of metal ions in structure and catalysis. The HHRz is a small nucleolytic ribozyme that catalyzes the site-specific nucleophilic attack of a 2'-OH on its 3'-phosphodiester bond, resulting in strand cleavage. Hammerhead ribozymes were originally discovered as the genome processing component of RNA-based viroids and have since been found in genomes throughout the domains of life (Buzayan et al. 1986; de la Pena and Garcia-Robles 2010). In medium ionic strength, HHRz activity is extremely sensitive to the concentration and identity of divalent metals (Boots et al. 2008). Moderate rates of catalysis can also be achieved in molar concentrations of monovalent cations alone, an important property that helped to uncover the critical roles of nucleobases in the HHRz reaction mechanism (Murray et al., 1998; O'Rear et al., 2001; Bevilacqua et al., 2004). At physiological ionic strengths, the HHRz requires divalent ions for appreciable rates of catalysis; therefore it is reasonable to assume that the divalent metal-dependent channel is the primary mode of catalysis in nature (Khvorova et al. 2003).

The HHRz was studied for years in its simplest active form, as 3 short helices meeting at a junction of conserved nucleotides that form the active site of the ribozyme (reviewed in Blount and Uhlenbeck, 2005). Studies using this 'truncated' form of the HHRz (trHHRz) led to a model of catalysis in which a catalytic metal in the P9/G10.1 site coordinates the *pro*-R oxygen of the scissile phosphate, presumably to stabilize the negative charge of the phosphorane transition state (Peracchi et al. 1997a; Wang et al. 1999b). Based on detailed metal-rescue experiments, Wang and coworkers predicted that the metal ion coordinates to the P9/G10.1 site in the ground-state, and bridges to the scissile phosphate in the transition state of the trHHRz reaction (Wang et al. 1999b). A ground state that is very different from the transition state is consistent with structural studies of the truncated HHRz, which in general did not show catalytically relevant atoms within appropriate distances of the active site (Blount and Uhlenbeck 2005). In these structures, the P9/G10.1 metal ion site is ~20 Å away from its predicted ligand during catalysis, the pro-R oxygen of the scissile phosphate (Pley et al. 1994; Scott et al. 1995).

To corroborate these seemingly conflicting data, it was proposed that the trHHRz periodically sampled a thermodynamically unstable 'active' structure in which the implicated functional nucleobases and metal ion would be in the correct position to stimulate catalysis (for review see (Blount and Uhlenbeck 2005)).

Hammerhead ribozymes contain non-conserved unpaired regions in helices I and II that interact to promote the formation of the active site in the helix junction. These tertiary interactions result in a higher population of functionally folded ribozymes, leading to higher observed rates and a significantly lower requirement for divalent metals *in vitro* as well as activity *in vivo* (Khvorova et al. 2003). New structures of constructs based on native HHRz's (2GOZ, 2OEU, 2QUS) largely satisfy predictions based on previous mutations, and also provide new hypotheses concerning players in the HHRz mechanism (Martick and Scott 2006a; Lee et al. 2007; Chi et al. 2008b). The conformation of the native HHRz in crystal-forming conditions is significantly different from that of the truncated HHRz. The native HHRz structures show a well-organized active site, with functional groups from the G8 and G12 guanosines in place to participate in general acid/base catalysis (**Figure 2.1**, next page). One fascinating aspect of these structures, however, is that even in this proposed 'active' conformation, the metal modeled at the P9/G10.1 site is still not making contact with functional groups directly involved in catalysis.

The extended HHRz from *Schistosoma mansoni* demonstrates Cd^{2+} rescue of P9 and scissile phosphorothioate substitutions, supporting the prediction that inner-sphere coordination of a metal ion to these phosphates is required for efficient catalysis in the stabilized HHRz (Osborne et al. 2005a). These prior studies were done with mixtures of phosphorothioates and fixed Cd^{2+} concentrations, and did not provide sufficient basis to determine ground-state affinities of the rescuing metal ions. Assuming the metal ion observed in the P9/G10.1 site of native HHRz's is the catalytically relevant ion implicated in coordinating the pro-R oxygen of the scissile phosphate, as is predicted by studies in the trHHRz, two simple models exist which might explain how this metal ion interacts with the active site during catalysis. In one model, named here the 'dynamic model', the metal ion could be recruited to the scissile phosphate at some point during the

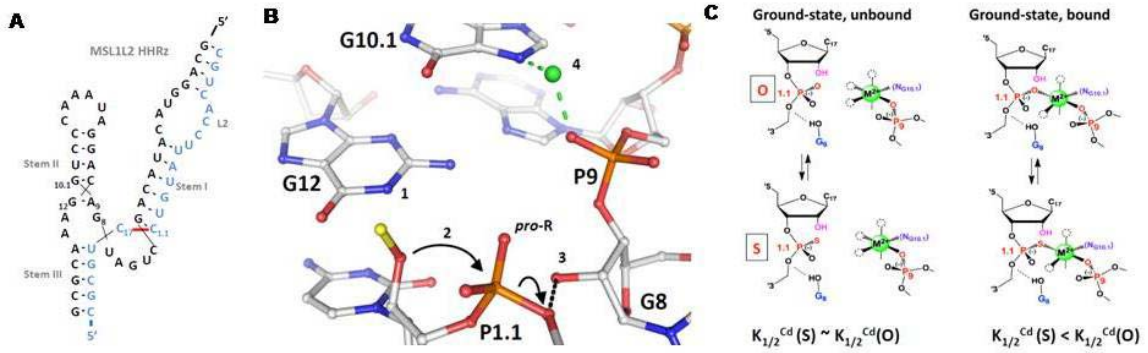

Figure 2.1. The MSL1L2 HHRz, active site model, and Cd^{2+} rescue principles. **A)** Secondary structure of the modified *Schistosome mansoni* HHRz (MSL1L2) ((Osborne et al. 2005a) used in these studies. **B)** Crystallographic active site of the *S.* mansoni HHRz (2OEU, Martick et al., 2008) showing (1) proximity of the G12 N1, proposed to act as general base for activation of the 2' nucleophile (2, a 2'-OMe in this structure) and the 2'-OH of G8 that has been proposed to act as a general acid for the 5'-O^- leaving group (3). The Mn^{2+} ion positioned in the P9/G10.1 active site (4) would be proposed to coordinate the pro-R oxygen (5) of the scissile phosphate based on these studies. **C)** Results expected for Cd^{2+} rescue of phosphorothioate substitution at the HHRz scissile phosphate. If there is no ground-state interaction between the metal and the substituted site (left), the value of $K_{1/2}$ (Cd^{2+}) for Cd^{2+} activation of the reaction should not change for the O and S substrates. For a ground-state interaction, $K_{1/2}$ (Cd^{2+}) should decrease to reflect the higher affinity of the Cd^{2+}-S interaction in the substituted site.

reaction resulting in stabilization of the negative charge of the phosphorane transition state (Wang et al. 1999b). This model, combined with native HHRz crystal structures, has been the basis for recent computational studies which calculated the position of the metal ion during different points along the HHRz reaction coordinate. These molecular simulations began with the crystallographically predicted P9/G10.1 metal site and predicted that a slight negative charge build-up resulting from nucleophile deprotonation is enough to rapidly and stably recruit the P9/G10.1 metal into a bridging coordination mode between the pro-R oxygen atoms of the P9 and scissile phosphates (Lee et al. 2008; Lee et al. 2009). Alternatively, the positioning of the metal ion may be specific to crystallography, in that the described structure is the most stable state under crystal-forming conditions. In solution, the most active form of the ribozyme may be slightly

different or be in equilibrium with the conformation observed in x-ray structures. A pre-initiation coordination (or an 'activated ground-state coordination') of the catalytically relevant metal ion to the scissile phosphate could theoretically provide a strong chemical advantage over the dynamic model via several methods. For instance, in a ground-state *pro*-R oxygen coordination position, the metal ion could lower the reaction barrier by stabilizing in-line attack geometry, activating the nucleophile via direct or indirect coordination, and/or withdrawing electron density from the phosphate thereby increasing the electrophilicity of the scissile phosphorus. Proximity of the metal ion may also lower the pK_a of the putative general base and/or nucleophilic 2'-OH. In the predicted mechanisms of other metal-dependent ribozymes such as the Group I intron, one or more metal ions are coordinated in the active site of the ribozyme without the need for metal recruitment during the reaction (Frederiksen and Piccirilli 2009).

We have performed detailed cadmium rescue experiments on HPLC-separated stereoisomers of a scissile phosphorothioate-substituted HHRz derived from *S.mansoni* in order to test whether a catalytic metal coordinates the scissile phosphate in the ground state or is instead recruited to the scissile phosphate during the transition state of the HHRz mechanism. Our results are consistent with a mechanism in which the rescuing metal makes a ground-state coordination with the pro-R oxygen of the scissile phosphate. These results differ from prior studies of cadmium rescue using trHHRz constructs, which demonstrated transition-state and not ground-state coordination (Peracchi et al. 1997; Wang et al. 1999b), indicating that the tertiary interactions in native HHRz constructs stabilize a ground-state that may be more advanced on the reaction coordinate. These results also imply that the current structural view of the HHRz, with a metal ion coordinated only in the P9/G10.1 site, may not represent the most active conformation of the HHRz active site. Instead, the crystal structure may represent just one of several conformations available to the HHRz core leading to catalytic activation, whereby the activating metal coordinates the pro-R oxygen of the scissile phosphate to stimulate catalysis.

Results and Discussion

Cd^{2+} Rescue in 100 mM Na^{+} and 15 mM Ca^{2+}

The HHRz has a general dependence on divalent metal cations for folding. In a background of 100 mM Na^{+}, the $K_{1/2}$for folding is approximately 1mM $M^{2+}$for a variety of metal cations (Kim et al. 2005; Boots et al. 2008; Ward and DeRose Submitted). Catalytic activation of the ribozyme occurs at much higher metal concentrations than does folding, however, and reaction rates vary greatly depending on cation identity (Kim et al. 2005; Boots et al. 2008; Ward and DeRose Submitted). For instance, Cd^{2+} is an especially stimulatory cation while Ca^{2+} is a poor stimulator of activity (Boots et al., 2008). We used these relationships in thiophosphate substitution-Cd^{2+} rescue experiments to separate the effects of Cd^{2+} on catalytic rescue from its contributions to global folding. HHRz kinetic experiments were performed in a background of 15 mM $Ca^{2+}$and 100 mM Na^{+}, which supports a folded ribozyme population with very low activity, and the ability of Cd^{2+} to stimulate WT and thiophosphate-substituted samples was compared.

Stereosiomers (R_p and S_p) of the scissile phosphorothioate-substituted HHRz substrate strand were separated by reverse-phase HPLC for use in Cd^{2+} rescue titrations alongside the wild type scissile phosphate construct (WT). The rate for each construct in 15 mM Ca^{2+} and 100 mM Na^{+} is very low, reaching only 0.04 min^{-1} for the WT construct (**Figure 2.2,** next page). The S_p construct has a rate reduction of one-half the WT rate ($k = 0.02\ min^{-1}$) , indicating that the S_p construct is only slightly inhibited by the sulfur substitution. By contrast, the R_p construct cleaves 100-fold more slowly than the WT construct under these conditions ($k = 0.0004\ min^{-1}$). General catalytic inhibition by a phosphorothioate substitution is possible in ribozymes (Forconi and Herschlag 2009) and could be due to slight structural perturbation due to the larger sulfur atom in place of an oxygen atom. Additionally, the less electronegative sulfur atom may withdraw less electron density from the phosphorus causing the phosphorus to have a lower electrophilicity than the native phosphate, leading to a lower intrinsic reaction rate (Erat and Roland 2011).The 50-fold additional inhibition from the R_p thio substitution in comparison with the S_p isomer is consistent with further loss of activity that may be due to the very low affinity of the hard Ca^{2+}ion for the R_p sulfur.

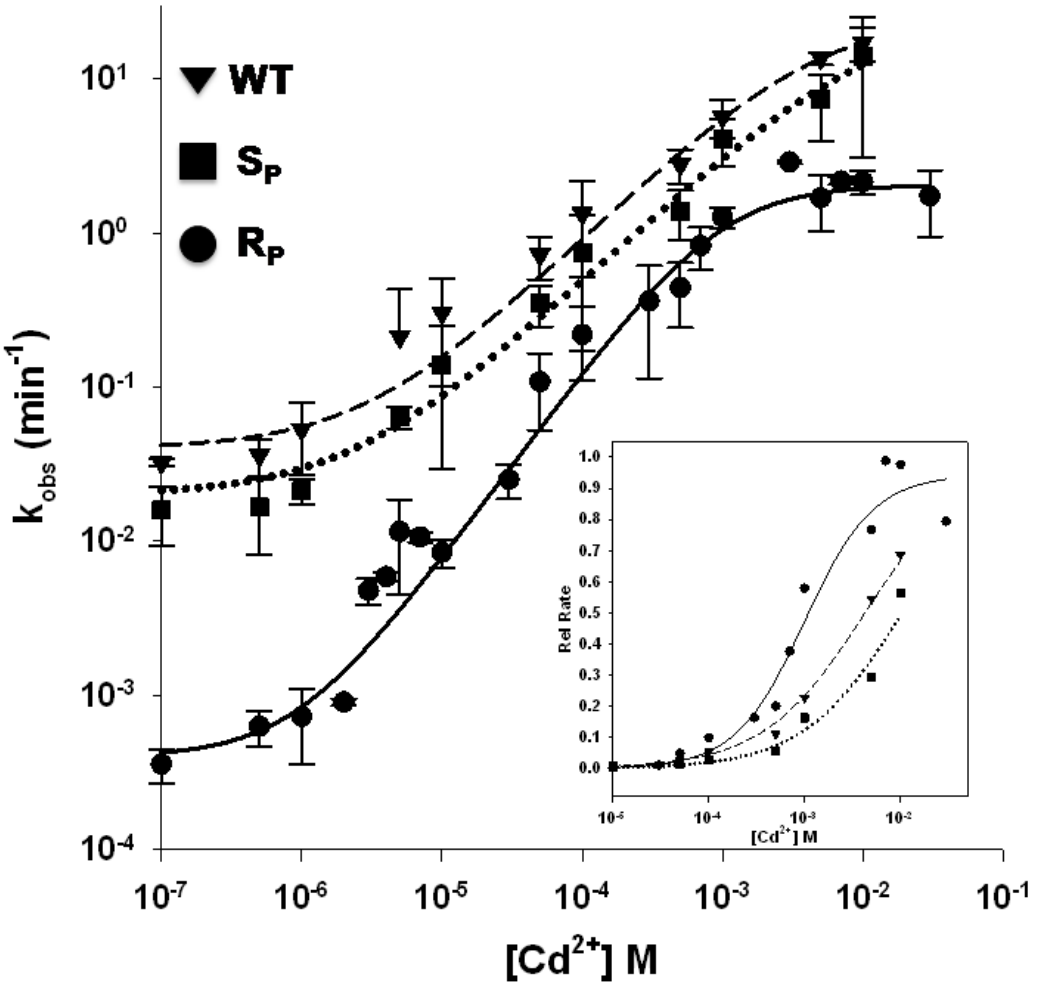

Figure 2.2. Cadmium rescue of HHRz constructs in 100 mM Na^{+} and 15 mM Ca^{2+}. The WT (triangles) and S_p phosphorothioate construct (squares) show similar Cd^{2+} profiles compared to the R_p phosphorothioate construct (circles), which is significantly inhibited in absence of Cd^{2+}. The rates in 0 mM Cd^{2+} are 0.04 min^{-1} for WT, 0.02 min^{-1} for S_P construct and 0.0004 min^{-1} for the R_P construct. The data were fit to equation A.3 to give apparent binding affinities of the rescuing Cd^{2+} of WT $K_{1/2}$ = 4 ± 1 mM, S_p $K_{1/2}$ = 10 ± 7 mM, R_p $K_{1/2}$ = 900 ± 300 uM. The inset presents the data using rates normalized to the predicted k_{max} in order to highlight the differences in $K_{1/2}$ values.

The addition of Cd^{2+}, which supports faster reaction rates in comparison with both $Mg^{2+}$and Ca^{2+}, causes a rate increase for each HHRz construct. Upon titration withCd^{2+}, the activity of the S_p construct approximately mirrors that of the WT, with the S_p phosphorothioate causing a small and constant rate reduction (**Figure 2.2**). Due to the

limits of manual kinetics techniques, rates for the S_p and WT ribozyme were not collected above 10 mM Cd^{2+}. The data were fit to equation A.3 (materials and methods of this chapter), and give a predicted k_{max} of approximately 25 min^{-1} for both ribozymes, which likely represents a lower limit for the k_{max} values. The stimulation of WT activity over this range of Cd^{2+} concentrations is ~600-fold. Over the same range of Cd^{2+} concentrations, the initial inhibition in the R_p construct is almost completely rescued, ending in a saturated activity curve with a k_{max} that is ~10-fold lower than the WT ribozyme. Incomplete rescue of the R_p construct to the WT rates may be due to the properties of phosphorothioate substitutions mentioned above. The 5000-fold stimulation in R_p activity, however, is consistent with the rescue of an essential metal coordination with the pro-R position of the scissile phosphate.

The $K_{1/2}$ value of activity stimulation can be considered to reflect the apparent affinity of the activating metal to the HHRz in the ground state. Therefore, if the coordination environment of the metal ion in the activated complex is changed such that the affinity between a metal ion and the respective ligand is increased, this should be reflected as a decrease in the $K_{1/2}$ of stimulation (**Figure 2.1C**). The WT ribozyme represents the standard state of the metal binding pocket, with the "rescuing" or "stimulating" metal ion coordinating a given set of ligands. If the metal ion coordinates a scissile phosphate oxygen in the ground state, then in the thio-substituted construct the increased affinity of a Cd^{2+}-S bond over a Cd^{2+}-O bond should be reflected in an increased affinity of the rescuing metal. Based on the data of Figure 2, the WT and S_p constructs have predicted stimulation $K_{1/2}$ values of 4 ± 1 mM and 10 ± 7 mM respectively for Cd^{2+}stimulation in a background of 15 mM Ca^{2+}/100 mM Na^{+}. Due to incomplete saturation of k_{max}, these values likely represent lower limits for the apparent $K_{1/2}$ of the catalytically stimulating metal. For the R_p construct, a $K_{1/2}$ = 900 ± 300 uM Cd^{2+} is measured, which is 4-10 fold lower than the constructs with a pro-R oxygen. This increased affinity of the rescuing metal for the R_p thio-construct is consistent with coordination of the activating metal to the pro-R position of the scissile phosphate in the ground state of the HHRz.

In model nucleotide systems, the binding affinity of Cd^{2+} to a phosphorothioate is 20-100 fold tighter than the affinity to a phosphate oxygen (Pecoraro et al. 1984; Sigel et

al. 1997). The affinity increase in these model systems calls into question whether a 4-10 fold increase can correctly be considered to reflect a "ground-state" coordination. Consideration should be given to the fact that the rescuing metal ion in our experiment competes with 15 mM Ca^{2+} and 100 mM Na^{+} for positioning in the active site. Wang and co-workers, using similar ionic conditions of 10 mM Ca^{2+}/100 mM Na^{+}, measured a 4-fold increase in apparent affinity for Cd^{2+} stimulation of activity in a trHHRz with an A9 R_p-S substitution, leading to the conclusion that the rescuing metal ion made a ground state interaction with the A9 pro-R oxygen (Wang et al. 1999b). For the same P9 substitution but in a background of 10 mM Mg^{2+}, Perrachi and coworkers found an 8.8-fold increased $K_{1/2}$ for stimulating Cd^{2+} (Peracchi et al. 1997). Metal coordination to the A9/G10.1 site in activity-inhibited constructs has also been spectroscopically measured, providing further support for the description of the A9 interaction as a ground state interaction (Horton et al. 1998; Hunsicker and DeRose 2000; Suzumura et al. 2002; Vogt et al. 2006). Additionally, in the present study, the $K_{1/2}$ values for Cd^{2+} activity stimulation in the WT and S_p constructs likely represent low estimates of the actual $K_{1/2}$values in this ionic background. Therefore, it is likely that the $K_{1/2}$ difference between the Rp and the pro-R oxygen constructs is also a lower limit. The 4-10 fold increase in the affinity of Cd^{2+} for the R_P scissile phosphorothioate in the native HHRz is, therefore, consistent with affinity increases of other characterized ground-state interactions in the HHRz.

Cd^{2+} rescue in 20 mM Na^{+} and 5 mM Ca^{2+}

Metal coordination is subject to general cation competition, and therefore the presence of high concentrations of Na^{+} and Ca^{2+}, while intended to de-convolute the role of Cd^{2+} in metal rescue, also raise the level of Cd^{2+} required for achieving maximum activities. We have recently used 2-aminopurine fluorescence to measure global HHRz folding in a reduced ionic background of 20 mM Na^{+}, and find a $K_{1/2,fold}^{Ca}$ value of 230 ± 20 uM (Ward and DeRose Submitted). The lowered Na^{+} background also reduces the k_{max} and $K_{1/2}$ for Mg^{2+} activation. By reducing the background Na^{+} and Ca^{2+} concentrations, competition for the rescuing Cd^{2+} ion should be reduced in the HHRz active site while still satisfying the general ionic requirements for global folding. We

therefore repeated the Cd^{2+} activity titrations for the WT and R_p constructs in a background of 20 mM Na^+ and 5mM Ca^{2+}(**Figure 2.3**).

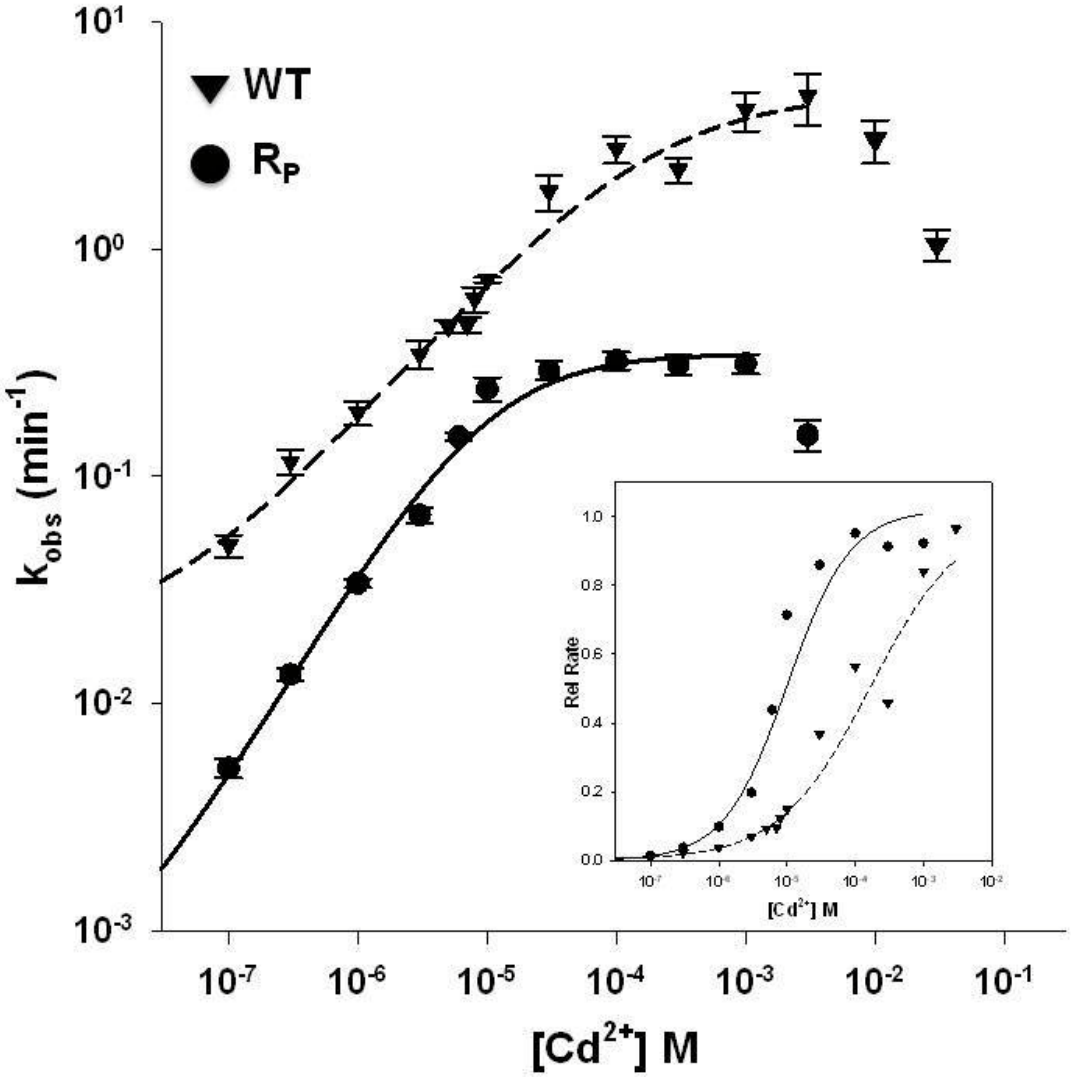

Figure 2.3. Cadmium rescue of HHRz construct in 20 mM Na^+ and 5 mM Ca^{2+}. WT (triangles) and R_p phosphorothioate construct (circles) both experience catalytic inhibition phases at $[Cd^{2+}] > 3$ mM. The rates in 0 mM Cd^{2+} are 0.02 min^{-1} for WT and <0.0004 min^{-1} for the R_P construct. The data, excluding inhibited points, were fit to equation A.3 to give apparent binding affinities of the rescuing Cd^{2+} of WT $K_{1/2}$ = 170 ± 10 uM and R_p $K_{1/2}$ = 10 ± 3 uM. The inset presents the data using rates normalized to the predicted k_{max} in order to highlight the differences in $K_{1/2}$ values.

Under these lower background ionic conditions, the k_{max}^{app} for stimulating Cd^{2+} is reduced in each construct, consistent with observations for Mg^{2+} activation in reduced Na^{+} (Ward and DeRose Submitted). With added Cd^{2+} the activity of the WT construct increases and then peaks at ~3 mM Cd^{2+}, followed by catalytic inhibition at higher concentrations of Cd^{2+}. Inhibition could be explained by the presence of a relatively low affinity metal coordination site that stabilizes an inactive conformer of the HHRz at high concentrations of Cd^{2+}. Catalytic inhibition by soft metals is a known problem due to the propensity for non-native site binding (Forconi and Herschlag 2009), and Cd^{2+} inhibition of the trHHRz has been observed as well (Wang et al. 1999b). The R_p construct is able to reach a saturated k_{max} at low uM Cd^{2+} concentrations, and it too begins to show catalytic inhibition at 3mM Cd^{2+}, supporting this inhibition as a general effect of high Cd^{2+} on the HHRz in these background ionic conditions. Since this inhibitory effect was not observed in 100 mM Na^{+} and 15 mM Ca^{2+}, it may indicate that the inhibitory metal is effectively out-competed by higher background ionic conditions. Additionally, as it is also not observed for Mg^{2+} (Kim et al., 2005), this inhibitory effect may be specifically attributed to the binding of soft metal ions or transition metal ions.

The WT and R_p Cd^{2+} rate profiles, excluding the inhibition phase, were fit to equation A.3. The reduced cation competition clearly amplifies the differences in $K_{1/2}$ values for Cd^{2+} stimulation of activity in these constructs. In 5 mM Ca^{2+}/20 mM Na^{+}, the $K_{1/2}$ for Cd^{2+} stimulation of WT activity is 170 ± 10 uM, while the $K_{1/2}$ for the R_p construct is now 10 ± 3uM. This 17-fold increase of Cd^{2+} affinity for the R_p-thio construct over the WT phosphate strongly supports a ground state metal coordination to the pro-R oxygen of the HHRz.

Conclusions

The HHRz relies on divalent metal ions to achieve appreciable rates of catalysis in physiological ionic strength. We investigated the catalytically important coordination of a metal ion to the scissile phosphate using Cd^{2+} rescue titrations under ionic conditions in which the HHRz is globally folded with low background catalytic activity. Consistent with previous work on minimal HHRz constructs, we find that Cd^{2+} rescue is stereo-specific for the pro-R position of the scissile phosphate. However, we also find a 4-17

fold increased affinity of the rescuing Cd^{2+} for the R_p-phosphorothioate construct. This increased affinity of the rescuing metal supports a model in which a catalytic metal coordinates the pro-R oxygen of the scissile phosphate in the ground state of the HHRz mechanism, a result that differs from current mechanistic models derived from trHHRz data in combination with crystallographic structures of native HHRz's (Wang et al. 1999b; Lee et al. 2009).

The 'minimal' trHHRz that lacks tertiary interactions is proposed to predominantly occupy an "open" state that requires a conformational change to a "closed" or active state for catalysis. This closed form seems to be only transiently populated, meaning that 'ground-state' pre-equilibration of metal occupancies in the trHHRz would mainly reflect the open conformation. Both structure ((Scott et al. 1995) and spectroscopic measurements (Maderia et al. 2000b; Vogt et al. 2006; Osborne et al. 2009) indicate higher-affinity population of the P9/G10.1 metal ion site in the trHHRz. Thus, metal-rescue studies of the trHHRz that predict metal coordination to the P9 site in the ground state, and the scissile phosphate at a later point on the reaction pathway, are consistent for that system.

Native HHRz constructs, however, stabilize a "closed" conformation through tertiary interactions. Given the higher stability of this closed conformation, and that P9 and scissile phosphate oxygens are much closer in native HHRz crystal structures, a bridging coordination mode for the catalytic metal ion seems to be achievable in the ground state of these constructs. Despite this, current crystallographic models locate a Mn^{2+} ion only in the nearby P9/G10.1 coordination site (Martick et al., 2008) or not strongly localized in the case of Mg^{2+} (Martick and Scott, 2006; Chi et al., 2008). In contrast, the data presented here strongly support a ground-state metal coordination to the scissile phosphate. A caveat to thio-substitution and Cd^{2+} rescue experiments is the potential creation of a non-native coordination environment due to the increased affinity of Cd^{2+} for sulfur over oxygen. The potential drawbacks of metal-rescue methods for ribozyme mechanistic studies are well discussed in the literature (Forconi and Herschlag 2009; Frederiksen and Piccirilli 2009; Erat and Roland 2011). While caveats must be considered, such methods have been used successfully to identify important coordination sites for several ribozymes (Frederiksen and Piccirilli 2009). A quantitative analysis of

the apparent affinity of the rescuing metal, such as performed here, expands the information gained to allow identification of the state of the ribozyme in which the metal and substituted ligand are in contact. The 4-17-fold increase in affinity for Cd^{2+} for the substituted R_p scissile phosphorothioate observed for this native HHRz is very similar to results previously obtained for the P9/G10.1 site in the trHHRz, whose occupancy has been corroborated by crystallography and spectroscopic methods. The simplest interpretation of the current data is therefore that the HHRz has a catalytic metal ion bound to the scissile phosphate.

Summary and bridge to Chapter III

Although current crystallographic results place a metal ion in the nearby P9/G10.1 position, simulations in which this metal has moved to bridge to the scissile phosphate show small structural changes including an increase in the in-line fitness for nucleophilic attack (Lee et al., 2008). Our data suggest that this metal ion coordinates the scissile phosphate prior to catalysis. This calls into question whether coordination of a metal ion to the scissile phosphate causes a conformational change in the HHRz core. Structural changes, along with beneficial electrostatic effects, would enhance the catalytic potential of the ribozyme. We propose, therefore, that the most active form of the HHRz involves a ground-state coordination of an activating metal ion to the pro-R oxygen of the scissile phosphate, which is then expected to aid catalysis throughout the reaction coordinate. In chapter III, we introduce the use of the fluorescent nucleotide analog 2-aminopurine to investigate metal dependent conformational changes in the core of the HHRz.

CHAPTER III

METAL DEPENDENT STRUCTURAL TRANSITIONS MEASURED BY 2-AMINOPURINE IN THE THREE HELIX JUNCTION OF THE HAMMERHEAD RIBOZYME

Overview

This chapter describes the use of 2-aminopurine (2AP) as a reporter of conformational changes of the HHRz three helix junction. Two of the 2AP HHRz systems are established as effective probes for HHRz structural transitions with the goal that these systems will be used in more detailed spectroscopic investigations into the folding and dynamics of the HHRz. We also present two 2AP substitutions that may not accurately represent the native structural transitions of the HHRz core, which in and of themselves present interesting systems for further investigation. I conceived of and designed this project with the guidance of Dr. DeRose. This work has been submitted for publication in *RNA*.

Introduction

RNA has the potential to form complex tertiary structures capable of performing catalysis or functionally interacting with other molecules to affect cellular processes. The factors that determine RNA structure formation, stability, and dynamics are therefore inextricably linked to the functional capabilities of RNA, and a general understanding of RNA folding processes will be important in determining the roles of the growing list of functional non-coding RNA classes. A major factor in RNA folding and stability is the dependence of RNA structure on metal cations, as cations are necessary for charge shielding of the phosphodiester backbone and can make significant contributions to stability through non-specific and site specific coordination, particularly in the case of divalent metals (For review see (Draper 2004; Woodson 2005)). In addition to roles in RNA structure, metal cations can influence the chemical steps of ribozyme mechanisms through specific and nonspecific effects (Review see (Sigel and Pyle 2007)). Determining

the particular role of divalent metals in affecting RNA catalysis can often be difficult due to the dual nature of metal ion functionality.

The Hammerhead ribozyme (HHRz) is one of the most studied of the small ribozymes and has long served as a model system for studying ribozyme mechanisms and relationships between RNA structure and function. The HHRz was originally discovered in plant viroids as the genome processing component of rolling circle replication where it performs endonucleolytic cleavage of a specific phosphodiester bond (Buzayan et al. 1986; Hutchins et al. 1986). The HHRz motif has since been found throughout all the domains of life (de la Pena and Garcia-Robles 2010), including mammals (Martick et al. 2008a) and long terminal repeats of the blood fluke *Schistosome* (Ferbeyre et al. 1998). Although they are capable of catalysis, the biological function of the HHRz motifs outside of those in viroids is unknown.

The canonical HHRz motif is composed of 3 relatively short helices meeting at a common junction of 13 conserved nucleotides, which compose the catalytic core of the ribozyme (Ruffner et al. 1990) (**Figure 3.1A**). Early studies of the HHRz used minimal, or truncated HHRz constructs (trHHRz), which contain the catalytic core and three truncated helices. It was later found, however, that tertiary interactions between unpaired or 'unstructured' regions in helices I and II of native HHRz constructs promote ribozyme activity, presumably by stabilizing the active conformation of the HHRz over inactive intermediate states, thereby allowing the ribozyme to exhibit maximal catalytic activity in physiologically relevant ionic conditions (De la Pena et al. 2003; Khvorova et al. 2003). X-ray crystal structures of the HHRz have modeled the predicted tertiary interactions and also indicate a well-organized catalytic core (Martick and Scott 2006; Chi et al. 2008) (**Figure 3.1B**). While the crystal structure has been helpful in determining a specific state of the ribozyme, questions remain about the dynamic processes of metal dependent HHRz folding in solution, particularly how the distal loop-loop interactions exact long-range effects on the folding processes, structural stability, and structural dynamics at the HHRz three-helix junction.

Several groups have used probes in the HHRz helices to investigate the metal dependence of conformational changes based on the changing orientations of the three helices, which is referred to as HHRz 'global' folding. Penedo and co-workers (2004)

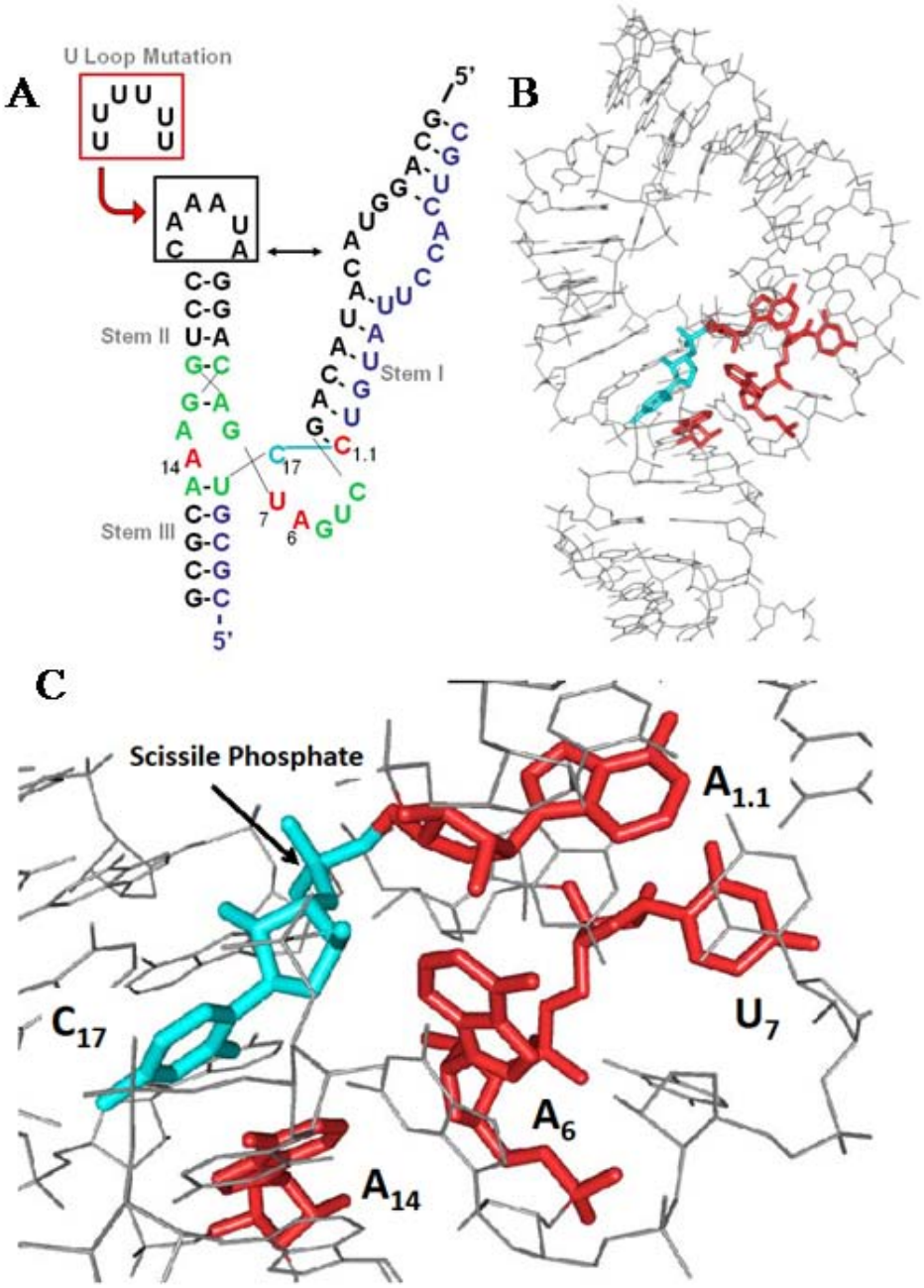

Figure 3.1. 2-aminopurine substitutions in the core of the MSL1L2 HHRz. A) The secondary structure of the MSL1L2 HHRz, with the highlighted conserved core (green), the selected 2-AP sites (red), and the alternate loop of stem II to create the U Loop mutant. B) A crystal structure of a native HHRz (2GOZ). C) The core of the HHRz as modeled by the crystal structure with the 2AP substitutions positions in red and the scissile position in blue.

used FRET to measure the proximity of helices I and III of an HHRz construct based on the *Schistosoma mansoni* HHRz and found a single Mg^{2+} dependent folding step with a $K_{1/2}$ of 160μM Mg^{2+} in the absence of added Na^{+}. When the loop interactions of helices I and II were disrupted by mutation, the 2-state folding model of the WT system reverted into a 3-state folding process observed in 'truncated' HHRz systems (Penedo et al. 2004). In the 3-state model, co-axial alignment of helices II and III happens with a $K_{1/2}^{Mg}$ value of 55uM and formation of the uridine turn follows, with a $K_{1/2}^{Mg}$ of 2mM (no added Na^{+}). Similarly, if folding of the native HHRz was initiated by the addition of only monovalent ions, a 3-state folding process was also observed, demonstrating the increased efficiency divalent metal-mediated folding. Penedo and co-workers (2004) offer the model that the loop-loop interactions increase the relative stability of the final folded state so that in ensemble steady-state experiments, the intermediate folding state observed in trHHRz and loop-disrupted HHRz constructs is effectively abolished. Global folding of the *S. mansoni* HHRz has also been measured by the increase in proximity of loops I and II through FRET (Boots et al. 2008) and EPR (Kim et al. 2005; Kim et al. 2010), where it was also found that the HHRz folds in a single step with a $K_{1/2}$ of 0.7 – 1.2 mM Mg^{2+} in 0.1M Na^{+}. The loop I-II interactions were also destabilized by mutation, leading to an increased $K_{1/2}^{Mg}$. A 3-state folding model was not observed by these experiments. In the context of the intermediate state model offered by Penedo and co-workers, these data suggest that the average distance between helices I and II of the native HHRz is only affected by a single metal dependent conformational change.

Stimulation of HHRz catalytic activity occurs with a $K_{1/2}^{Mg}$ much greater than global folding of the HHRz. Though folding experiments indicate that the native HHRz is stably folded with a $K_{1/2}^{Mg}$ of ~1mM in 100mM Na^{+}, the HHRz reaches maximal activity with a $K_{1/2}^{Mg}$ greater than 1mM (Canny et al. 2004; Kim et al. 2005)(and results described below). This implies that either a previously undetected metal-dependent structural transition activates the ribozyme, and/or a low affinity specific metal site necessary for catalysis is increasingly occupied once the HHRz has globally folded into its activated structure. Time-resolved (tr) and single-molecule (sm) FRET experiments using an HHRz derived from the Avocado Sunblotch Viroid (ASVd), with FRET dyes on stems I and II, reveal a multi-step folding process that was fit to bi-phasic Mg^{2+}

dependence with $K_{1/2}^{Mg}$ values of 0.23mM and 4.2mM in 100mM Na^+ (McDowell et al. 2010). The second observed folding phase is correlated with metal-dependent catalytic activation of the HHRz. Through smFRET, they show that the globally folded ribozyme dynamically samples a range of conformational space under conditions in which the ribozyme is considered globally folded. They find that the HHRz tends to populate particular FRET states and that compared with the FRET states allowed in 1mM Mg^{2+}, at 10mM Mg^{2+} a new FRET state is populated and is associated with catalytic activity. Based on the multiple states revealed by smFRET, the second folding phase measured by trFRET may indicate a transition into a sparsely or transiently populated, yet fully activated conformation. The extent of the tertiary interactions affected the ability of the ribozyme to populate this new FRET state. Additionally, McDowell and co-workers (2010) used MD simulations to demonstrate that varying tertiary interactions physically translate to conformational heterogeneity in the core of the ribozyme, and that constructs showing high catalytic rates *in vitro* more frequently sample favorable catalytic geometries *in silico*. These experiments provide evidence that the globally folded native HHRz is structurally dynamic and may populate active conformations in a metal-dependent fashion. Population of these more active conformations is not readily detected by steady-state FRET or EPR measurements of helix orientation. smFRET and trFRET experiments to date, however, do not directly address changes in the structure of the catalytic core or the mechanism for metal dependent catalytic activation in the core of the HHRz.

Here, we describe the use of the fluorescent base analog 2-aminopurine (2AP) as a reporter for local conformational changes in the core the MSL1L2 HHRz derived from *S. mansoni* (**Figure 3.1A**)(Osborne et al. 2005a). 2AP has been widely used in structural studies of RNA (Walter et al. 2001; Hall 2009), including studies on 'truncated' HHRz systems (Menger et al. 1996).We used the recent x-ray crystal structures of the HHRz along with information gained from *in vitro* folding and catalysis experiments on trHHRz constructs (Nelson and Uhlenbeck 2008b)to predict positions in the conserved catalytic core of a native HHRz that should be least sensitive to mutation (**Figure 3.1C**).Based on this analysis, we chose 2AP substitutions in positions 1.1, 6, 7, and 14. These four mutations represent positions on each strand of the three helix junction, with 2AP1.1 on

the scissile "substrate" strand, 2AP6 and 7 on the uridine turn, and 2AP14 on the third unpaired region consisting of A13-15 (**Figure 3.1A**).The catalytic activity of each of the 2AP substitutions was compared to WT activity under identical conditions to determine the viability of the mutant as a model for wild type folding. The fluorescence of each substitution in a non-cleavable HHRz system was then measured as a function of metal concentration. The 2AP mutants were paired with a tertiary destabilizing U Loop mutation (Kim et al. 2005; Osborne et al. 2005b; Kim et al. 2010) to test the relationship between core folding/stability and loop interactions. We also tested the effect of mutations in the core of the HHRz that would be expected to change coordination of metals near the scissile phosphate. We find that the core of the HHRz has a structural transition that is dependent on the interaction of loops I and II. We also find evidence for a second folding phase detected by 2AP substitution in the uridine turn, and which is correlated with catalytic activation of the native HHRz. Additionally, single atom substitutions in the core of the HHRz were found to influence the metal-dependent folding of the HHRz, indicating the sensitivity of the HHRz motif to relatively conservative perturbations.

Results

2AP7 fluorescence is sensitive to global folding and a second local conformational change

The catalytic core of the HHRz is a highly conserved motif with a complex network of hydrogen bonds that can be disrupted by even single atom substitutions (for review see Nelson and Uhlenbeck 2008). We selected positions for 2AP substitution that should minimally disrupt the core of the ribozyme. We used the relative catalytic activity (k_{rel}) of the substituted HHRz construct to determine if the ribozyme would likely imitate the native structure. A $k_{rel} \leq 0.01$ is considered a debilitating mutation and is expected to disrupt the stability a folded state, alter the native architecture of the core, and/or remove specific components directly involved in the chemistry of catalysis.

Position 7 of the Uridine turn has been reported as a mutable base (Ruffner et al. 1990) and is not completely conserved in natural HHRz motifs (de la Pena and Garcia-Robles 2010). Based on the crystal structure of the native HHRz, none of the U7 nucleobase functional groups are predicted to make hydrogen bonds. The crystal

structures of native HHRz systems (2GOZ, 2QUS) also predict thatU7 is partly solvent exposed on one face and stacked with the C3-G8 base pair on the other. We find that 2-AP in this position (2AP7) results in a k_{rel} of 0.46, indicating that this mutant should report on native folding pathways (**Table 3.1** and **Figure B1** (appendix B)).

Table 3.1 Catalytic activity and metal-dependent folding of *S. mansoni* Hammerhead ribozyme and 2AP variants

Variant	k_{rel} (min^{-1})[a]	% Fast Pop[b]	$K_{1/2}^{Mg}$ [c]
WT Rate	1	40	17 ± 4 mM
2AP7	0.46	39	80 ± 10 uM >1.5 mM[d]
2AP1.1	0.55	36	170 ± 40 uM
2AP6	0.008	43	100 ± 3 uM
2AP14	0.01	34	270 ± 6 uM
2AP1.1/Pul4	0.06	38	170 ± 5 uM >100mM[e]

[a] Apparent rate constant compared to the WT rate under identical conditions (see Materials and Methods)
[b] Fraction of total ribozyme cleavage that is attributed to the faster cleaving population in the biphasic fit of single turnover cleavage experiments
[c] The concentration of Mg^{2+} required for half maximal activity (WT rate) or folding (2AP variants). The error for folding is the standard deviation from averaging the values derived from non-linear regression of individual titrations, repeated 3-6 times.
[d] 2AP7 titrations were fit to a bi-phasic folding model. The reported values are for the first transition and the second transition, which represents a lower limit for this transition as the data did not reach saturation
[e] 2AP14 data were fit to a bi-phasic folding model.

Global folding of the *S. mansoni* HHRz has been characterized as a function of Mg^{2+} by measuring the proximity of loops I and II via FRET or EPR in a background of 100 mM Na^{+} (Kim et al. 2005; Boots et al. 2008; Kim et al. 2010). These techniques show that global folding occurs in a single step with a $K_{1/2}$ of 0.7 - 1 mM Mg^{2+}. In order to directly compare global folding studies of the *S. mansoni* HHRz to changes within the

three helix junction, we measured the steady state fluorescence of 2AP7 as a function of Mg^{2+}concentration in100 mM Na^{+} in the context of a deoxy-C17 mutation, which prevents ribozyme cleavage. We find that the addition of Mg^{2+} causes a decrease in 2AP7 fluorescence (**Figure 3.2**). Decreasing 2-AP fluorescence is generally associated with increased base stacking interactions (Rachofsky et al. 2001; Ballin et al. 2007). Assuming this mechanism, the Mg^{2+} induced quenching of 2AP7 suggests that as the globally folded conformation of the HHRz is stabilized by addition of Mg^{2+}, position 7 stacks with neighboring bases. One source of this stacking could be formation of the uridine turn, causing stacking with the C3-G8 base pair as seen in the crystal structures of native HHRzs.

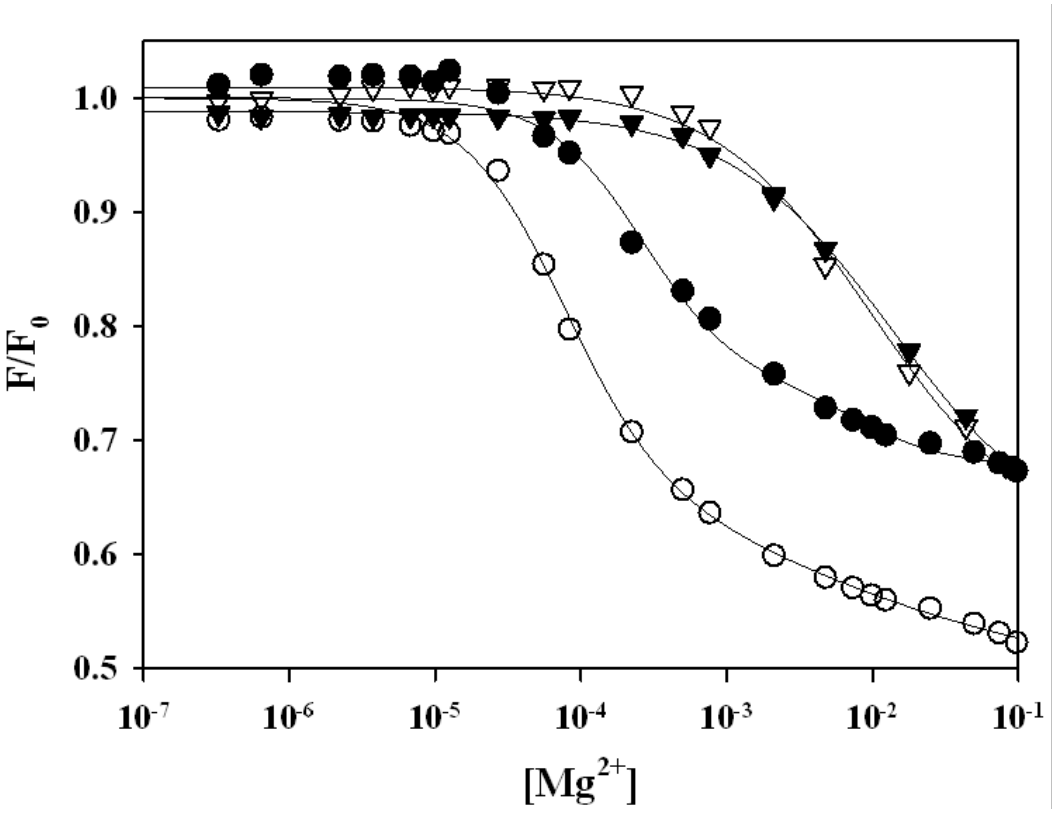

Figure 3.2. Metal-dependent 2AP7 fluorescence. The relative fluorescence (F/F_0), of 2AP7 with WT tertiary interactions (circles) and the U Loop mutant (triangles) indicate the dependence of the core structure on tertiary interactions. Data were taken in 50mM Tris pH 7.5 and 100 mM Na^{+} (black symbols) and 20mM Na^{+} (open symbols) indicate Na^{+} concentration has a mild effect on the metal dependence. The lines are the non-linear fits of a single data set to equation B5 (WT loops) and equation B4 (U Loop). The metal dependence of HHRz folding is derived from the average parameters of multiple data sets and are given in Table 3.2.

We fit the quenching data to a model in which it is assumed that the HHRz exists in only two detectable states, unfolded and folded (Scheme B1, Appendix B). Fitting the data to this model yields a $K_{1/2}^{Mg}$ of 340 uM (**Table 3.2).** While the quenching data are statistically well described by a two state model (R^2= 0.99), the data under these and other conditions (discussed below) consistently show continued fluorescence quenching at higher Mg^{2+} concentrations that is not fit by this model (**Figure B3, Appendix B**). This aspect of the quenching curve is better fit by a three state folding model (Scheme B2, Equation B5, appendix B) in which a large initial fluorescence decrease with a $K_{1/2}^{Mg}$ of 270uM is followed by a lower magnitude quenching phase that does not reach saturation by 100 mM Mg^{2+} (the point to which we limited our titrations, see Methods (appendix B). Due to the lack of saturation, the second phase can only be estimated to have a $K_{1/2} \geq$ 11 mM Mg^{2+}. This second folding phase correlates well with the metal dependent increase in HHRz activity (Canny et al. 2004; Kim et al. 2005), suggesting a possible structural component to HHRz activation (discussed below).

Table 3.2. Metal dependence of WT activity and 2AP7 folding variant

Signal	Background Na^+	$K_{1/2}$	n=
WT Rate[1]	100mM Na^+	>40 mM	NA
2AP7	100 mM Na^+	340 ± 20 uM	4
2AP7 U Loop	100 mM Na^+	>8 mM	2
WT Rate	20 mM Na^+	17 ± 4 mM	3
2AP7	20 mM Na^+	80 ± 10 uM	6
2AP7 U Loop	20 mM Na^+	>6 mM	3
2AP7 Ca^{2+}	20 mM Na^+	70 ± 20 uM	4
2AP7 Sr^{2+}	20 mM Na^+	200 ± 100 uM	6
2AP7/R_p1.1	20 mM Na^+	140 ± 5 uM	3
2AP7/S_p1.1	20 mM Na^+	130 ± 8 uM	3

[1] From Canny et al 2004

In order to directly test the relationship between core folding and loop interactions of the extended HHRz, 2AP7 fluorescence was measured in the context of a tertiary disrupted "U-Loop" mutant HHRz (**Figure 3.1A**). The U Loop mutation removes tertiary interactions between helices I and II which, in turn, is predicted to destabilize folding of the three helix junction, as evidenced by decreased rates of catalysis compared to the native HHRz (Kim et al. 2005; Osborne et al. 2005b). The removal of loop interactions also exposed multiple metal dependent folding steps when measured by steady state FRET between probes in helices I and III (Penedo et al. 2004). Multiple folding steps were not observed in experiments that measured global folding of loop mutants via reporters in helices I and II (Boots et al. 2008; Kim et al. 2010). We find that folding of the 2AP7 U Loop HHRz construct has an increased Mg^{2+} dependence as measured by fluorescence quenching (**Table 3.2, Figure 3.2**), indicating that the stability of the folded core is weakened by loss of tertiary interactions between helices I and II, consistent with proposed models of HHRz structural activation (Nelson and Uhlenbeck 2008). Quenching of 2AP7 does not reach saturation by 100 mM Mg^{2+} and the $K_{1/2}$ of the initial quenching phase increased to >10 mM Mg^{2+}, consistent with previous observations of global folding based on FRET (Boots et al. 2008; Kim et al. 2010) and DEER (Kim et al. 2010).

The first quenching phase of the 2AP7 titrations is dependent on tertiary loop interactions of the HHRz and is therefore associated with the "global folding" step. The second quenching phase, though subtle, could reflect a local structural transition in the HHRz core that has not been observed previously. While global folding of the HHRz occurs in sub-millimolar concentrations of Mg^{2+}, the metal dependent activation of the *S. mansoni* HHRz has a $K_{1/2}^{Mg}$ >40 mM in 100 mM Na^{+} (Canny et al. 2004; Kim et al. 2005). Activation of the HHRz has therefore been attributed to the population of a low affinity metal site and/or increased stability of a transiently populated, fully activated structure. Based on this model, we propose that at higher Mg^{2+} concentrations, 2AP7 fluorescence is sensing the accumulation of the fully activated HHRz structure.

If catalytic activation is due to a structural change in the HHRz core, saturation of the final folded state may not be observable within the limits of our titrations, as the

metal dependence of activation is unsaturated at 100mM Mg. Since monovalent ions act as competitors for divalent metal binding sites (Draper 2004; Kisseleva et al. 2005), reducing the background ionic conditions is expected to reduce both the $K_{1/2}^{Mg}$ of catalysis and folding, which therefore could enable more accurate measurements of metal dependent folding by shifting the saturation of the folding transitions to below 100mM Mg^{2+}. **Figure 3.3** shows the Mg^{2+} dependent catalytic activity of the WT HHRz (dashed line) and fluorescence quenching of the four 2AP mutants described above (solid lines) in 20 mM Na^{+}. We find that in the lower monovalent ionic background, the $K_{1/2}^{Mg}$ for catalysis is reduced to ~20mM (**Figure 3.3, Table 3.2**). Additionally, the k_{max} of cleavage is greatly affected by the concentration of Na^{+}. Whereas cleavage rates approach >200 min^{-1} in 100 mM Na^{+}(Canny et al. 2004), in background ionic conditions of 20 mM Na^{+} we observe a k_{max} approaching only 4 min^{-1}.

The 2AP7 fluorescence profile in 20mM Na^{+} demonstrates Mg^{2+}-dependent quenching that is similar to the profile of 2AP7 in 100mM Na^{+} (**Figure 3.2**). The data taken in 20 mM Na^{+} fit statistically well to a two state folding model with a $K_{1/2}^{Mg}$ of 130 uM, but as for the case in 100 mM Na^{+}, the two state model does not qualitatively describe the steep metal-dependence of initial quenching, nor the continued quenching at higher Mg^{2+} concentrations (**Figure B4, Appendix B**).When a three state folding model is applied to fit the data obtained in 20 mM Na^{+}, the first quenching phase has a $K_{1/2}^{Mg}$ of 80 uM. Despite the lowered monovalent ionic background, quenching in the second phase does not saturate within the limits of our titration and a $K_{1/2}^{Mg}$ of 1.5 mM is given by non-linear regression analysis. In 20 mM Na^{+}, the profile of the 2AP7 U Loop construct is almost identical to the profile in 100 mM Na^{+} and the initial quench has a higher metal dependence compared to the native loop construct, with a $K_{1/2}^{Mg}$> 8 mM (**Figure 3.2**). Thus, at lower Na^{+} concentrations, the rate and folding profiles of the HHRz are slightly shifted, yet still do not reach saturation by 100mM Mg^{2+}.

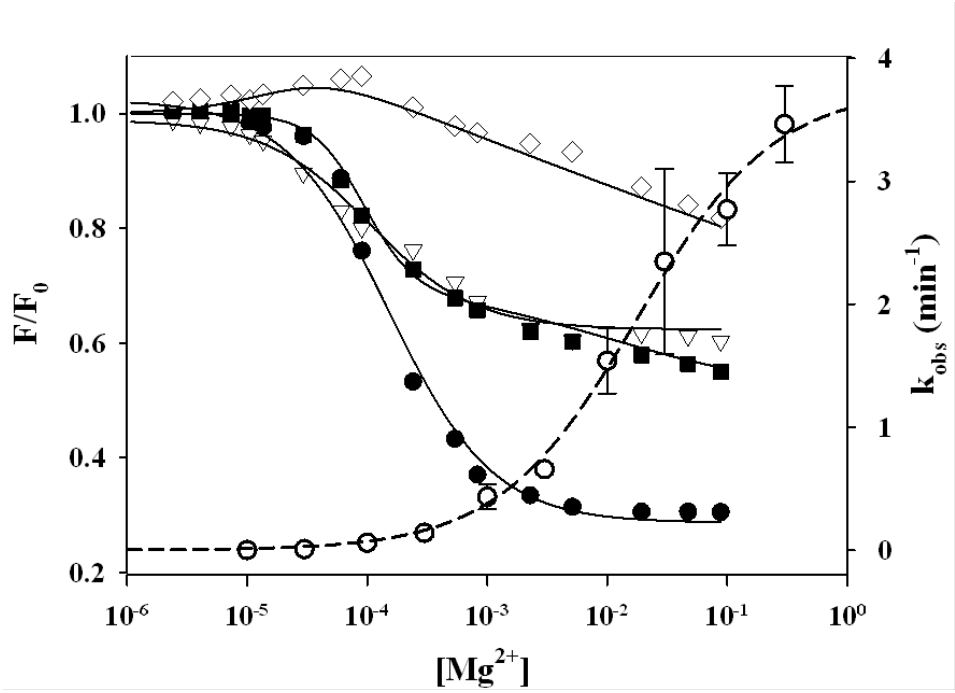

Figure 3.3. Metal dependent folding and catalysis of the HHRz. The HHRz rate (open circles, dashed line) increases at high divalent metal concentrations. Metal dependent folding is monitored by the quenching of 2AP1.1 (black circles), 2AP7 (black squares), 2AP6 (open triangles), and 2AP14 (open diamonds). The solid lines are the non-linear fits of the single presented data set to equation B4 (2AP1.1 and 2AP6) or equation B5 (2AP7 and 2AP14). The metal dependence of HHRz folding is derived from the average parameters of multiple data sets and are given in Table 3.2.

2AP1.1 fluorescence is dependent on global folding

Position 1.1 of the HHRz is not completely conserved in natural HHRz sequences and the only known requirement for this position is that it base-pair with position 2.1 to form the base of helix II. We substituted position 1.1 with 2AP and also position 2.1 with uridine to form an AU-like base pair, and find that these complementary mutations lead to a k_{rel} of 0.55 (**Table 3.1** and **Figure B1, Appendix B**). This mutant HHRz (2AP1.1), therefore, should also report on native folding pathways.

The fluorescence profile of 2AP1.1 shows metal dependent quenching of the fluorophore that, unlike 2AP7, clearly saturates at higher Mg^{2+} concentrations (**Figure 3.3** and **Figure 3.4**). The 2AP1.1 profile was fit to a two-state equation giving a $K_{1/2}^{Mg}$ of

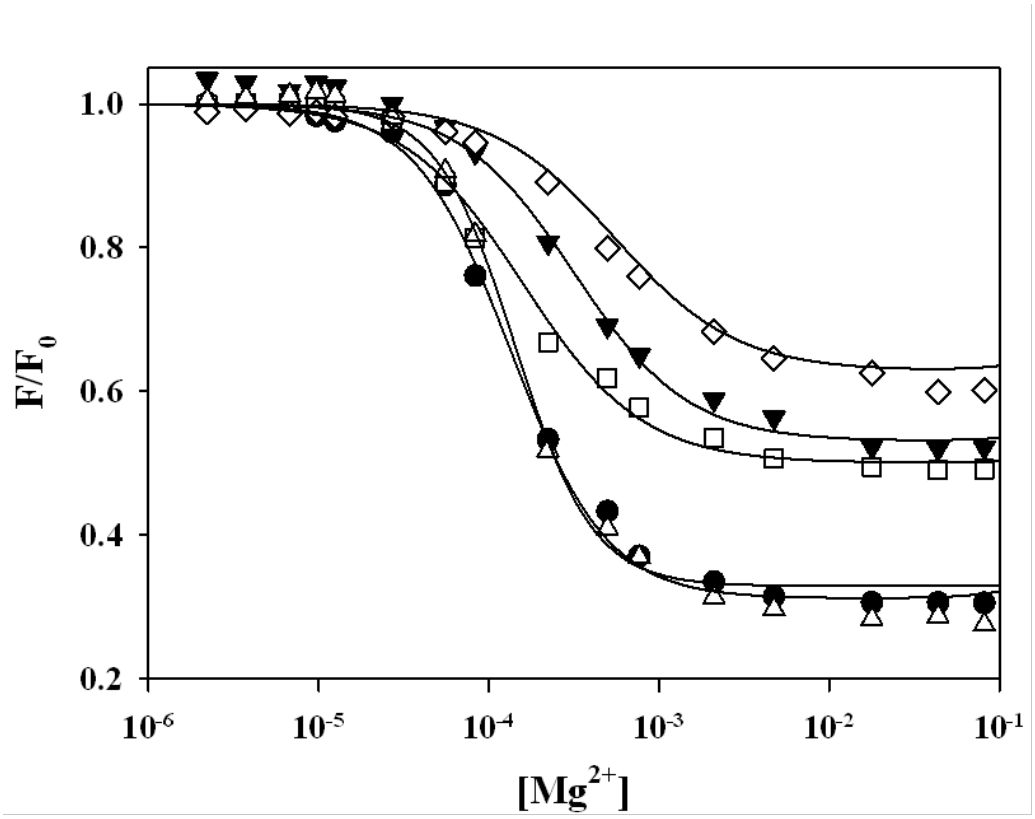

Figure 3.4. Metal-dependent 2AP1.1 fluorescence. Titrations were done in 20mM Na^+, 50mM Tris pH 7.5, at 20° C. 2AP1.1 quenching fits well to a two state model (Scheme B1, Equation B4) in all contexts. Changes in the F/F_0 are most common between the different ribozymes systems: dC17 and WT Loops (black circles), dC17 U Loop (black triangle), 2' –N and WT loops (open square), 2'-N and U Loop (open diamond), and the Pu-14, dC17 mutant. The solid lines are the non-linear fits of the single presented data set to Equation B4. The metal dependence of HHRz folding is derived from the average parameters of multiple data sets and are discussed in the text.

140 uM. The similar $K_{1/2}^{Mg}$ to that obtained for the major transition observed for 2AP7 (80-130uM) suggests that the 2AP1.1 fluorescence quenching results from the same global folding step that also affects the first phase of 2AP7 fluorescence (**Figure 3.3**). Under the initial conditions of the titration (20 mM Na^+), the 2AP1.1-U2.1 base pair is expected to form a base pair as the terminus of Helix I, but may undergo breathing. Quenching of 2AP1.1 fluorescence upon global folding may therefore be due to increased stacking due to stabilization of Helix I. Alternatively or in addition, 2AP1.1 quenching may reflect formation of the uridine turn along with the critical C3-G8 base pair that brings G8 in position to stack with position 1.1.

We also investigated the folding of the 2AP1.1 HHRz in context of the U Loop mutation. Based on 2AP7 fluorescence, the global folding event sensed by 2AP7 is severely inhibited when native loop interactions are disrupted. Therefore, if quenching of 2AP1.1 is dependent on the formation of the Uridine turn, we would expect that 2AP1.1 fluorescence quenching would also have a significantly increased Mg^{2+} requirement in the context of the U loop mutation. **Figure 3.4** shows the Mg^{2+} dependent quenching of the 2AP1.1 U Loop construct compared to the native loop construct. Though this construct shows a higher F/F_0, when the data are fit to the two state folding model the $K_{1/2}^{Mg}$ is only increased ~2 fold to 295 uM. This indicates that despite destabilization of the loop interactions, 2AP1.1 is still sensing a conformational change in low Mg^{2+} concentration. While the observed quenching may be due to increasing stability of Helix I with added Mg^{2+}, that the final state exhibits less fluorescence quenching than with wild type tertiary interactions, could reflect more frequent fluctuations away from base-stacking interactions, leading to less average fluorescence quenching is steady state experiments. Additionally, it is possible that 2AP1.1 fluorescence is influenced by both Helix I stability and interactions from the Uridine turn, and that the lower final F/F_0 is reporting destabilization of the Uridine turn upon interruption of loop-loop interactions.

2AP6 may destabilize core folding

In the crystal structure of the native HHRz, A6 is proposed to make few hydrogen-bonding interactions, none of which are expected to be directly affected by mutation to 2AP (Nelson and Uhlenbeck 2008b). The 2AP6 mutation, however, significantly affects the catalytic rate, with a k_{rel} of 0.008 (**Table 3.1** and **Figure B2, Appendix B**).This mutant, therefore, may have affected the ribozyme in one or more of the ways noted previously.

The low rate constant of the 2AP6 mutation indicates that this mutation severely inhibits ribozyme function. The Mg^{2+} titration of this mutant construct shows fluorescence quenching that is well fit to a two-state model, with $K_{1/2}^{Mg}$ of 100 uM (**Figure 3.3, Table 3.1**). Like 2AP1.1, 2AP6 quenching saturates at higher Mg^{2+} concentrations. The similar $K_{1/2}$ value for quenching of 2AP6 to those of 2AP1.1 and the first phase of 2AP7 suggests that the metal dependent quenching of 2AP6 is also due to

global folding. The low catalytic activity of 2AP6 is not, consequently, easily explained by global structural destabilization of the HHRz. In the native ribozyme crystal structure, A6 is stacked with G5 as part of the uridine turn. Therefore, formation of the uridine turn upon global folding provides one physical explanation for quenching of 2AP6. Given that A6 is positioned on the uridine turn directly 5' to U7, and 2AP7 quenching demonstrates biphasic folding, it is reasonable to expect that 2AP6 quenching would also exhibit a second phase at higher Mg^{2+} concentrations, but this is not observed. It is possible then, that the 2AP6 substitution destabilizes the second metal dependent folding transition, or stabilizes an alternative conformation relative to the folded uridine turn. Further experiments are required to determine if the 2AP6 mutation inhibits catalysis by changing the architecture of the active site and/or if the mutation has directly removed a component of the chemical mechanism.

Mutations at position 14 affect catalysis

Mutation of A14 to G has been found to impair global folding in a trHHRz system (Bassi et al. 1995). Activity measurements with position 14 mutations in the trHHRz indicate that the most important functional group of A14 is N1, which in the crystal structure of the native HHRz hydrogen-bonds with exocyclic amine N2 of G5. Other than this hydrogen-bond, the other interactions of position 14 are predicted to include stacking with neighboring adenine bases. It is expected then, that 2AP substitution in this position would make minimal changes in folding or catalysis as purine stacking and the N1 imine identity are preserved. We find that in the context of the *S. mansoni* HHRz, however, that 2AP14 greatly impairs ribozyme cleavage, with a k_{rel} of only 0.01 (**Table 3.1** and **Figure B2, Appendix B**). The 2AP14 mutant also shows the most dissimilar Mg^{2+} dependent fluorescence profile compared to the other three positions tested (**Figure 3.3**) with first a small increase of fluorescence followed by an unsaturated quenching phase. Due to the catalytic deficiency of this mutant, however, we are unable to determine whether these fluorescence changes are reflecting native ribozyme folding pathways (as observed from position 14) or are due to global destabilization of the HHRz structure.

In order to gain a better understanding of which aspects of the 2AP14 mutant could have caused ribozyme inactivity or potential structural instability, we investigated

the activity and folding of a construct containing only a Purine at this position (Pu14) in the background of the 2AP1.1 substitution. Like 2AP, a purine substitution at position 14 preserves the N1 imine functional group, and removes the exocyclic 6-amine. As opposed to 2AP, a purine substitution does not add steric bulk or an additional hydrogen bond-donor to position 2 of the purine base. Therefore if the altered fluorescence quenching behavior observed in 2AP14 is due to removal of the 6-amino group from A14, then this Pu14-2AP1.1 construct should have a fluorescent profile that is also perturbed relative to the 2AP1.1 construct.

We first tested the catalytic activity of the Pu14-2AP1.1 construct. The Pu14-2AP1.1 double mutant has a k_{rel} of 0.06 (**Table 3.1, Figure B2, Appendix B**), which represents a partial restoration of activity in comparison to the 2AP14 construct (k_{rel} = 0.01) and only a 9-fold reduction in activity compared to the 2AP1.1 mutant background. Despite the reduced activity of the Pu14 construct, the Mg^{2+} dependent fluorescence profile of Pu14-2AP1.1 is nearly identical to the 2AP1.1 profile (**Figure 3.4**). This indicates that the removal of the 6-amino group from A14 does not necessarily globally destabilize the HHRz, as measured by 2AP1.1 fluorescence. Since the inclusion of a 2-amino group at position 14 causes a greater reduction in catalysis than removal of a 6-amino group, it is possible that the added steric bulk at position 2 of the purine ring prevents global or local folding, or the additional hydrogen bond donor at the 2 position stabilizes the formation of a non-native interaction leading to a non-native structure in 2AP14.

The identity of the C17 2'-substitution affects 2AP1.1 fluorescence

The C17 2' hydroxyl, the nucleophile in the HHRz reaction, must be substituted in these and other folding studies in order to block catalysis and measure 2AP fluorescence changes that are due to folding, but not cleavage. A C17 2'deoxy is a commonly used substitution for this purpose and was used in these experiments. The potential importance of the 2' substitution identity on local properties was recently highlighted in metal binding studies of a trHHRz, where it was found that a 2'-NH_2 substitution enables binding of Cd^{2+} to a scissile phosphorothioate, whereas other 2' substitutions did not (Osborne et al. 2009). If a metal dependent structural change of the

HHRz core involves metal coordination near the scissile phosphate, removal of the 2'OH could destabilize this theoretical final state. A 2'–amine substitution more closely mimics a 2'- OH in size and expected sugar pucker (Hruska et al. 1973; Guschlbauer and Jankowski 1980), while still preventing nucleophilic attack. If a metal binds near the 2' functional group in the folding pathways of the native HHRz, the ability of Mg^{2+} to coordinate this position could more readily be observed by mimicking the 2' OH as closely as possible (Frederiksen and Piccirilli 2009).

We tested the effect of a 2' $–NH_2$ nucleophile substitution on the folding of the 2AP1.1 construct (**Figure 3.4**). The general shape of the 2'-NH_2 fluorescence profile is similar to the profile of the dC17 construct, showing an initial quench phase with a $K_{1/2}$ of 170 uM that is comparable to the dC17 $K_{1/2}^{Mg}$ value of 140 uM in 20 mM Na^+. The final quenched fraction (F/F_0) for the C17 2'-NH_2 construct is much less than for dC17, however, and is actually at a similar level to the dC17 2AP1.1 U Loop. The similar $K_{1/2}$ but different ending quench state suggests that the C17 2' $–NH_2$ mutation could change the globally folded state of the HHRz, similar to what is proposed to explain the fluorescence profile of the 2AP1.1 U Loop mutation. We then tested the 2'-NH_2 2AP1.1 construct in the context of the U Loop mutant as well and find that it shows the same relative behavior as the dC17 2AP1.1 U Loop construct (**Figure 3.4**). The $K_{1/2}$ of the first transition increases (540 uM) and the final fluorescence state is less quenched. These results support a model in which the substitution of dC17 with C17 2' $–NH_2$ does not necessarily change the folding pathway of the ribozyme, but instead slightly alters the local environment of 2AP1.1in the HHRz, leading to different amounts of quenching in both pre-folded and globally folded states, yet does not alter the stability of the final state.

A phosphorothioate substitution of the scissile phosphate does not affect core folding

Phosphorothioate substitution and Cd^{2+} rescue studies have demonstrated that there is a ground-state interaction of a metal ion with the pro-R oxygen of the HHRz scissile phosphate (Ward and DeRose 2012). In a crystal structure of the native HHRz, (Martick et al. 2008b), a Mn^{2+} ion coordinates the A9 phosphate, which is 4.3 Å from the scissile phosphate. Although additional metal coordination to the scissile phosphate is not observed by crystallography, MD simulations have modeled the ability of the metal at the

A9 site to form a stable bridging conformation, upon a small change in the electronegativity of the active site (Wang et al. 1999b; Osborne et al. 2005b; Lee et al. 2009). If metal coordination to the scissile phosphate in the HHRz ground-state is accompanied by a conformational change, then substitution with an R_p phosphorothioate could disrupt Mg^{2+} dependent folding, as Mg^{2+} has a decreased affinity for sulfur compared to the native oxygen.

The influence of a phosphorothioate substitution at the scissile phosphate was tested in context of the 2AP7 HHRz in order to monitor the major transition associated with global folding and the second phase that trends with ribozyme activation. Both R_p and S_p stereoisomers of the 2AP7 –dC17 phosphorothioate construct show a two-phase fluorescence profile similar to that for the un-substituted phosphate (**Figure 3.5**). Both the R_p and S_p profiles differ from the phosphate profile, however, in that the $K_{1/2}$ of the first quenching phase increases approximately 2-3 fold to 140 uM and 260 uM, respectively (**Table 3.2**). These data suggest that a phosphorothioate substitution at the scissile phosphate mildly affects the global folding step as measured by 2AP7 fluorescence. The phosphorothioate substitution does not appear to significantly affect the second phase of 2AP7 fluorescence. These data support a model in which the metal-dependent conformational change that leads to activation of the HHRz does not require metal coordination to the scissile phosphate.

Divalent metal identity highlights the second folding phase of the HHRz core

Boots and co-workers (2008) tested the ability of several different metals to both globally fold the HHRz and to support catalysis. Folding $K_{1/2}$ values for Sr^{2+}, Ca^{2+}, Mg^{2+}, or Mn^{2+}, measured by FRET, were found to vary by less than 6-fold. The rate of HHRz cleavage in 1 mM M^{2+}, however, varies by more than 10,000-fold and is roughly correlated with the metal-H_2O pK_a over this series (Boots et al. 2008). While global folding does not appear to be dependent on specific characteristics of these metals, the vast differences in the ability of these metals to stimulate cleavage could be explained by the specific interactions of metal ions in the core of the HHRz. The characteristics of these metals may simply change the affinity of the activating metal for binding the core of the HHRz in a productive coordination mode. For instance, the differences may arise

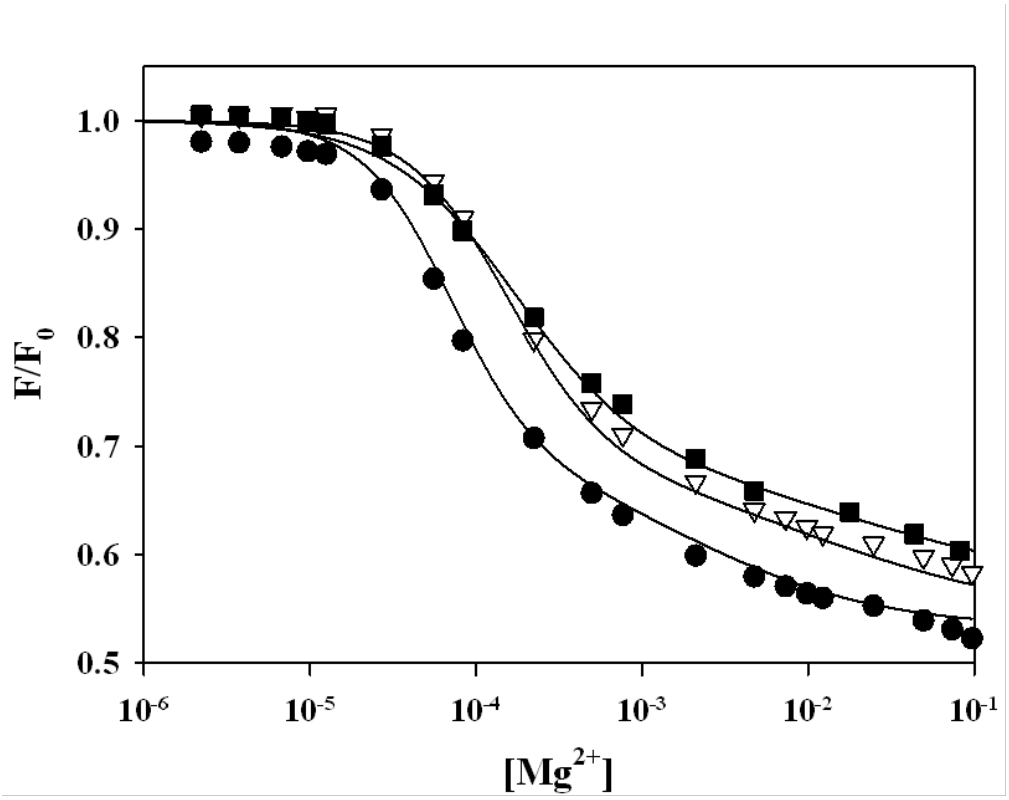

Figure 3.5. Phosphorothioate substitutions do not significantly alter 2AP7 fluorescence. The WT 2AP7 construct (black circles) shows 2 phases of folding. The 2AP7 R_p (open triangles) and S_p (black squares) phosphorothioate constructs show slight destabilization of the initial global folding step, yet do not show altered profiles during the second step of folding. The solid lines are the non-linear fits of the single presented data set to Equation B5. The metal dependence of HHRz folding is derived from the average parameters of multiple data sets and are discussed in the text and presented in Table 3.2. The conditions for these titrations were 20mM Na^+, 50mM Tris pH 7.5, and 20^o C.

from differing affinities of metal ions to the scissile phosphate (Schnabl and Sigel 2010). Alternatively or additionally, the differences in metal ion ionic radius may alter the architecture of the active site, leading to variation in catalytic activation. If there is a specific metal-dependent structural change in the core of the HHRz, then the fluorescence profiles of the 2AP constructs could be affected by metal identity. We therefore compared the abilities of Mg^{2+}, Ca^{2+}, and Sr^{2+} to fold the core of the HHRz using 2AP7 (**Figure 3.6**) as well as 2AP1.1 with the 2'-NH_2 protecting group (**Figure B5, Appendix B**).

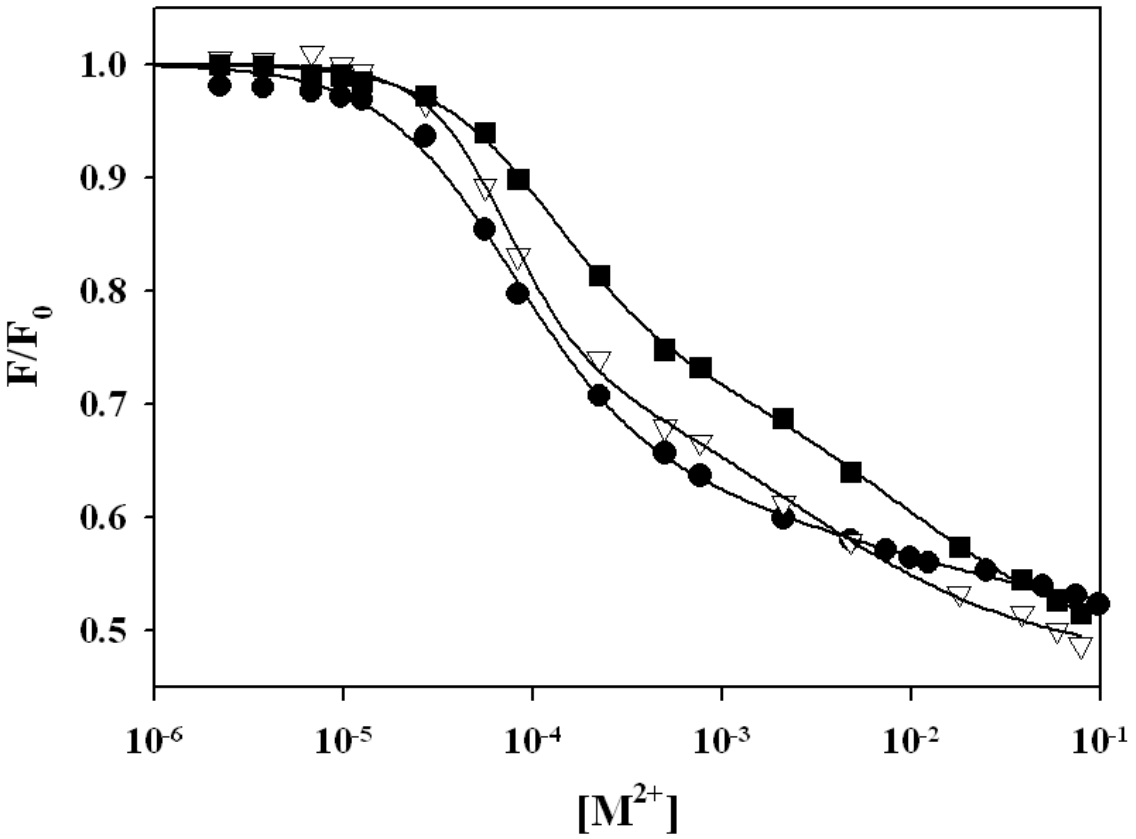

Figure 3.6. 2AP7 titrations in three divalent metal ions. The profile of 2AP7 in Mg^{2+} (black circles) is altered when using Ca^{2+} (open triangles) or Sr^{2+} (black squares). In particular, the shape of the profile during the second folding phase is highlights this phase as being different from the global folding step. The solid lines are the non-linear fits of the single presented data set to Equation B5. The metal dependence of HHRz folding is derived from the average parameters of multiple data sets and are discussed in the text and presented in Table 3.2. The conditions for these titrations were 20mM Na^{+}, 50mM Tris pH 7.5, and 20^{o} C.

As with Mg^{2+}, the 2AP7 titration data for Ca^{2+} and $Sr^{2+}$are best described by a bi-phasic folding model. The Ca^{2+}titration data initially track the Mg^{2+} profile closely, but diverge at ~1 mM Ca^{2+} to approach a lower F_F/F_0 (**Figure 3.6**). The Sr^{2+} titration data do not track the Mg^{2+} profile as closely as the Ca^{2+}, and in the apparent second quenching phase, like Ca^{2+}, decrease more steeply than Mg^{2+} (**Figure 3.6**). Both the Ca^{2+} and Sr^{2+} data show more clearly than the Mg^{2+} data that a bi-phasic folding model describes the quenching of 2AP7 qualitatively better than a single phase model, particularly with respect to the second quenching phase (**Figure B6 and B7, Appendix B**).

Quantitatively, Ca^{2+} folds the core of the ribozyme in the first folding phase with the approximately the same $K_{1/2}$ as Mg^{2+} while Sr^{2+} shows a 3 fold increase in $K_{1/2}$ for the first quenching phase (**Table 3.2**). As the first quenching phase is attributed to the response of 2AP7 upon global folding, these data are in close agreement with the folding studies performed by Boots and co-workers (2008), in which Sr^{2+} had the highest $K_{1/2}$ for stabilizing stem I and II loop interactions. Compared to the Mg^{2+} profile, the altered approach to F_F during the second quenching phase could indicate that metal ion identity affects the architecture of the active site, which is consistent with the differing moderation of catalytic efficiency. In 1mM M^{2+}, Ca^{2+} and Sr^{2+} show 20 and 130 fold decreased HHRz catalysis compared to Mg^{2+}, respectively (Boots et al. 2008). Whereas Mg^{2+} is expected to promote a relatively efficient ribozyme structure, using this interpretation Ca^{2+} and Sr^{2+} would apparently promote a less efficient structure, represented by the different F_F/F_0. An alternative explanation for the varying characteristic of the second folding phase in different metals is to consider that the second phase of quenching is caused not by a structural change, but by a more direct interaction of the fluorophore with metal ions. This alternative explanation is discussed below.

We also tested the effect of metal identity on the fluorescence profile of the 2'-NH_2 protected 2AP1.1 strand. The 2'–NH_2, which more closely mimics the native 2'-OH, could potentially reflect differences in the ability of these metals to fold the core of the ribozyme. The fluorescence profiles of 2AP1.1 in each metal are very similar in that all three profiles approach nearly the same F_F/F_0, with slightly increased $K_{1/2}$ values from Mg^{2+} to Ca^{2+} to Sr^{2+} (**Figure B8, Appendix B**), consistent with the global folding values reported by 2AP7 and FRET (Boots et al.2008). The same trend can be seen in the metal dependent fluorescence profiles of 2AP6, which also is assumed to measure global folding (**Figure B9 Appendix B**).

Control studies support conformation-induced bi-phasic quenching of 2AP7

An alternative explanation for the biphasic quenching of 2AP7is that once the HHRz has globally folded in a low Mg^{2+} concentration, a state is formed in which metal ions act to quench 2-AP directly through one or more of several possible quenching pathways (Lakowicz 2006). Our control studies using 2-aminopurine as a free base

indicate that the three metal ions we tested do not act as general quenchers of 2-AP fluorescence in concentrations up to 100mM M^{2+} (data not shown). Nevertheless, one must also consider that as a polyelectrolyte, an RNA oligomer may more efficiently recruit metal cations to interact with nucleobases, which could cause changes in 2AP fluorescence. In consideration of these possibilities, we also measured the metal dependent fluorescence of the 2AP7 43mer HHRz 'enzyme' strand in the absence of added substrate strand, as well as a control 7mer construct (Appendix B Materials and Methods) to determine the effect of metal ions on2AP7 outside the context of the HHRz.

The 2AP7 43mer and 7mer control constructs both show metal-dependent quenching (**Figure 3.7**) that does not saturate over the range of the M^{2+} titrations. The characteristics of this metal-dependent quenching are very different from that of 2AP7 in the context of the HHRz. The onset of quenching is delayed to higher metal ion concentrations and the slope of the quenching profile is very dissimilar to the 2AP7 HHRz construct. Therefore, the quenching characteristics of the HHRz construct are most likely due to the specific structural changes of the HHRz, as opposed to reflecting a general response of 2AP to metal ions as a component of RNA oligomers.

While the quenching of 2AP in these single strand controls is likely due to increased base stacking of the oligomer as a response to the ionic strength of the solvent, increased interactions between 2AP and solvated metal ions leading to some amount of fluorescence quenching should still be considered as a possible quenching component in the HHRz system. In order to control for these potential "background" or "intrinsic" changes in 2AP photophysics in response to Mg^{2+}, the 2AP7 HHRz data were normalized by plotting the ratio of the HHRz fluorescence to the fluorescence of the control oligomer (**Figure 3.7** open symbols). This type of ratiometric normalization has been used to improve the analysis of 2-aminopurine fluorescence changes in an RNA hairpin model, though the correction was not required for Mg^{2+} dependent fluorescence changes because the control 2AP oligomers used in that study were not responsive to increased Mg^{2+}(Ballin et al. 2007). Normalization of our 2AP7 data using this method leads to bi-phasic fluorescence transitions, in which a quenching phase is followed by an increase in fluorescence. This

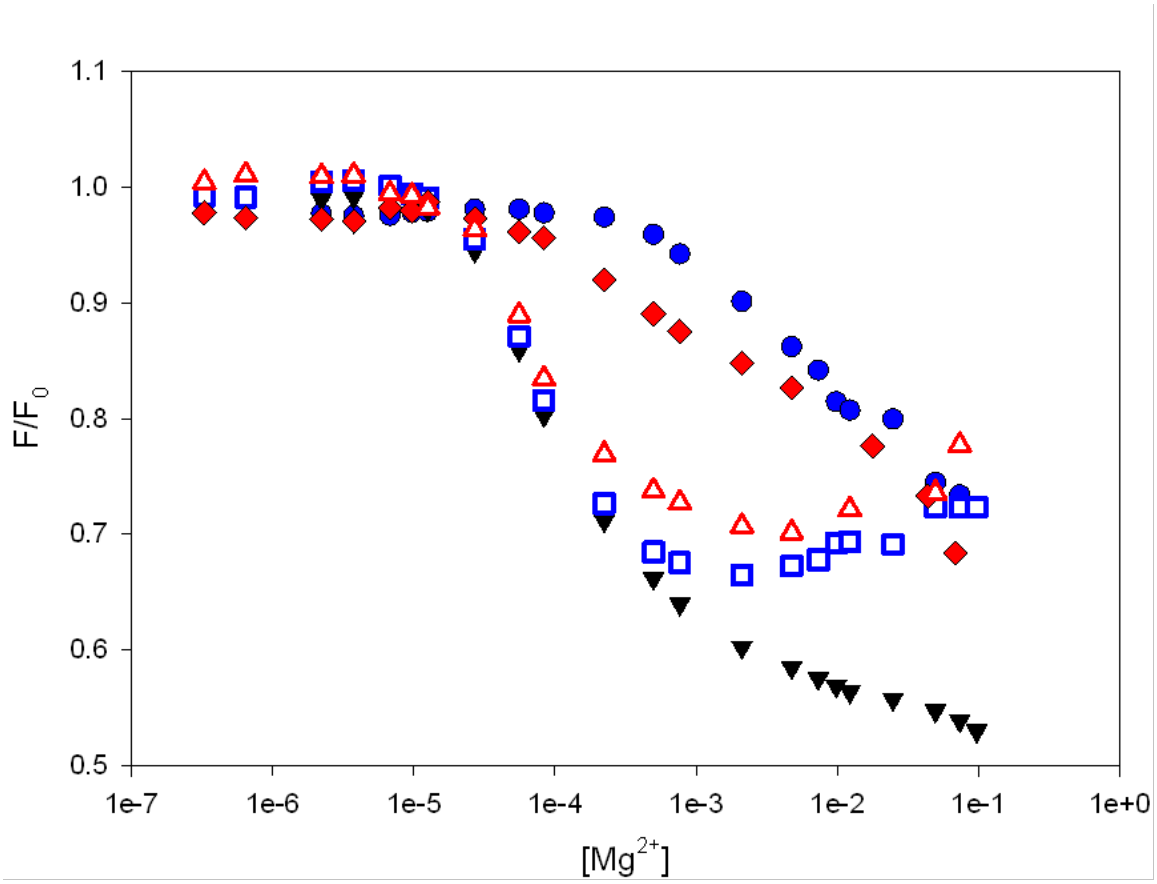

Figure 3.7. Control studies of 2AP7 titrations. The 43mer HHRz enzyme strand (red diamonds) and the 7mer control (blue circles) were titrated as single strand oligomers in 20 mM Na^+, 50mM Tris ph7.5 at 20° C. Both constructs show metal dependent fluorescence quenching. However the profiles are very different than titrations of the complete 2AP7 HHRz system (black triangles). To control for this potential "background quenching", the 2AP7 HHRz data are divided by the fluorescence profile of the enzyme strand and 7mer control oligomers (open red triangles and open blue squares, respectively). Using these controls, the 2AP7 data now show a second folding phase leading to increased fluorescence.

analysis, therefore, still supports the bi-phasic folding model for 2AP7. This normalization also presents an alternative physical model for HHRz folding, in which global folding causes stacking of 2AP7, and a metal-dependent second phase correlated with catalytic activation of the ribozyme consequently weakens base stacking interactions with position 7.

Another possible explanation for the continued quenching of 2AP7 is that the core of the ribozyme, as a three helix junction, presents a considerably concentrated negative electrostatic environment that when formed, may be particularly efficient at recruiting

metal ions that might affect 2AP7 fluorescence. As this explanation is specific for the core of the HHRz, but does not rely on conformational changes to explain quenching, there is no obvious control to correct for this type of background quenching. However, if this scenario does explain the second phase of quenching, one might have also expected continued metal-dependent quenching with the other 2AP substitutions we used in the core. While 2AP14 quenching was not saturated by 100mM Mg^{2+}, which we argue is explained by an inability for this mutant to globally fold the ribozyme, both 2AP1.1 and 2AP6 show saturation of fluorescence quenching under conditions that we argue represent the globally folded HHRz. Regardless of this analysis, further experiments are required to absolutely determine if and how "background" fluorescence changes might be pertinent to 2AP7 fluorescence.

Discussion

Given the wide range of conformational space that a particular RNA motif might sample, it is of great interest to understand the factors that direct an RNA sequence to a particular functional conformation. Divalent metal ions play significant role in the stabilization of RNA conformations, both through general charge shielding, and direct and indirect coordination. For the folding of smaller RNA motifs, such as the HHRz, a general model of metal-dependent folding can be applied consisting of global collapse to a near native state followed by a second phase in which a compact native structure is increasingly populated (Woodson 2010).Studies on native HHRz constructs with tertiary interactions between stems I and II indicate that divalent cations have separate influences on global folding and local activation, wherein low concentrations of Mg^{2+} and other divalent metals satisfy a nonspecific requirement for global folding, and a lower affinity metal requirement leads to catalytic activation of the HHRz (Canny et al. 2004; Kim et al. 2005; Boots et al. 2008). The low affinity metal interaction may directly participate in the mechanism of endonucleolytic cleavage; for example, a metal ion is predicted to coordinate the pro-R oxygen of the scissile phosphate (Wang et al. 1999b; Osborne et al. 2005b; Ward and DeRose 2012). Another, non-exclusive possibility is that the most active conformation of the ribozyme is only very transiently populated, and that under high concentrations of Mg^{2+}a greater fraction of HHRz molecules access this

conformation, thereby leading to increasingly higher rates of catalysis. This latter possibility is supported by trFRET and smFRET studies of native HHRz constructs that show an increase in the number of conformational states under activating metal ion conditions (McDowell et al. 2010).

Here, we use the fluorescent base analog 2-aminopurine to report on conformational changes of the core of the HHRz. The results of our ensemble steady-state 2AP folding studies show that the core of the HHRz goes through two metal dependent folding transitions. The measured metal dependence of the folding transitions presented here are consistent with a model in which a low concentration of M^{2+} ions stabilize a globally folded HHRz, which is sensed by multiple 2AP probes in the core of the HHRz. Global folding is then followed by a structural change in the core of the ribozyme, which is correlated with the considerable catalytic activation of the HHRz in Mg^{2+} concentrations greater than 1mM. Interestingly, the second transition is only observed via a fluorescent probe at position 7, indicating that the second transition involves changes in interactions within the uridine turn of the HHRz core. Metal-dependent structural changes of the uridine turn have previously been linked to activation in trHHRz systems (Hammann et al. 2001; Edwards and Sigurdsson 2005).

The exact nature of how metal ions act to stabilize the folded core of the ribozyme remains unknown. The only specific metal ion site that has been characterized in the HHRz involves the A9/G10.1 pocket of the active site. Crystal structures of the HHRz have modeled a metal ion bound by N7 of G10.1 and the pro-R phosphate oxygen of A9 in the core of the ribozyme. Additionally, metal coordination to the pro-R oxygen of the scissile phosphate is required for efficient catalysis. The A9/G10 metal ion is predicted to fulfill this role by coordinating both the A9 and scissile phosphate in order to activate catalysis (Wang et al. 1999a; Ward and DeRose 2012). One model to explain how metal-dependent folding is correlated with the metal dependence of catalytic activation is that the ground-state coordination of the catalytically relevant metal ion stabilizes the active conformation of the ribozyme. However, de-stabilization of this interaction by phosphorothioate substitution did not significantly alter the second folding phase of the HHRz (**Figure 3.5**), indicating that this metal coordination event is not required for the conformational change. Therefore, an alternative model for metal ion induced folding of

the core would involve the population of a second, as yet uncharacterized metal ion site and/or a non-specific requirement for high cation concentrations to enable a second conformational change in the HHRz core. The population of this folded state would then simply enable the metal ion to coordinate the pro-R oxygen.

A general dependence on high cation concentration for folding the core of the HHRz is supported by the finding that Ca^{2+} and Sr^{2+}, which are both poor activators of HHRz catalysis, still enable the second conformational change to occur (**Figure 3.6**). However, the altered profile of the second folding phase may indicate these ions have a different affinity for the second site, and or induce a distinct architecture of the active site. Therefore, the observed differences in the ability of these metal ions to activate catalysis (Boots et al. 2008) is likely explained by differences in the coordination properties of the metal ion that populates the A9/scissile phosphate position and not by the general ability to stabilize a second conformational change.

While this paper was in review, Buskiewicz and Burke (2012) published the results of steady-state and time-resolved fluorescence studies of the HHRz using the fluorescent base analog pyrollocytosine (PC). PC substitutions were made at position 1.9 (within the interacting loop I), 1.1 at the base of stem I, and positions 3 and 7 located in the uridine turn. Steady-state measurements of metal-dependent fluorescence changes for probes in both peripheral loop I (PC1.9) and at position 7 (PC7) in the core have similar Mg^{2+}-dependencies, with values that are close to those assigned here for the 'global folding' transition. In their study, however, stem and core folding are differentiated by time-dependent experiments showing that the rate of core folding (as followed at PC7) has a 10-fold weaker Mg^{2+}-dependence than the Mg^{2+} dependence global folding. These data are interpreted to mean that global and core folding are separable events, and that the faster rate of global folding provides an initial population of intermediates from which the core subsequently organizes.

Unlike the 2AP7 data presented here, the steady-state fluorescence amplitude changes of PC7 did not show any additional metal dependent fluorescence features at the higher concentrations of Mg^{2+} that would be associated with increasing ribozyme activity, indicating that PC7 does not detect a second conformational change correlated with metal-dependent catalytic activation (Buskiewicz and Burke 2012). That the

fluorescence transitions of PC7 and 2AP7 are different does not necessarily mean that the observations by Buskiewicz and Burk (2012) are contradictory to our 2AP7 data, as the photophysical properties of these two base analogs are different (Hardman and Thompson 2006; Hardman et al. 2008). The differing photophysical properties of these probes could enable 2AP7 to sense two conformational changes in the HHRz core, while PC7 fluorescence could be insensitive to the conformational change. In fact, the very nature of the fluorescence changes for these two probes is different as PC7 shows an increase in fluorescence upon folding, while 2AP7 shows fluorescence quenching. These dissimilar observations actually highlight the utility of using several types of experimental probes in order to achieve the most thorough analysis of a particular system.

The steady state 2AP data presented herewith in show that the core of the HHRz is affected by distal tertiary interactions that influence both the $K_{1/2}$ of metal-dependent folding, as well as the architecture of the globally folded state. Inherent within the biphasic model of HHRz folding and activation is the concept that under physiological ionic conditions, global HHRz folding is supported but an energetic barrier persists in forming the most active conformation of the HHRz core. It is surprising that such a barrier persists even in the presence of tertiary interactions that are presumably evolved to enhance activity and therefore promote on-path structural changes. An energetic barrier for stabilizing the most active conformation of the ribozyme may be a non-issue *in vivo*, however, as transient population of the active state could be sufficient to achieve a k_{obs} that is appropriate for the *in vivo* functions of this ribozyme. Additionally, the HHRz may also be required to perform the reverse reaction (strand ligation), and therefore transient access to the active state may allow for a tunable balance between cleavage and ligation. Fluorescent base analogs provide a window through which local environmental perturbations of the HHRz core can be observed that have not been detected by "global" folding studies. These steady state fluorescence experiments establish the potential of the 2AP1.1 and 2AP7 systems for use in more detailed, time-resolved and single molecule fluorescence studies, which could aid in determining the factors that lead to the structural dynamics and catalytic activation of the HHRz three helix junction.

Summary and bridge to Chapter IV

In chapter II, we confirmed metal coordination to the scissile phosphate of the HHRz. X-ray crystal structures and computational modeling have led to the hypothesis that the 2'OH of G8 acts as the general acid, however in Chapters II & III we provided evidence that a metal-dependent conformational change may re-arrange the active site. Such a re-arrangement could place a catalytic metal ion in position to act in one of several roles to aid in general acid catalysis. In Chapter IV, we investigate the effect of metal ions on general acid catalysis of the HHRz.

CHAPTER IV

METAL-DEPENDENT GENERAL ACID CATALYSIS OF THE HAMMERHEAD RIBOZYME

Overview

This chapter describes our investigation into the mechanism of general acid catalysis of the HHRz cleavage reaction. Several lines of evidence had previously pointed to a role for metal ions in the mechanism of general acid catalysis, including a strong correlation between metal ion Lewis acidity and the HHRz rate. However, complete pH-rate dependent profiles of the HHRz in several metals that would more thoroughly investigate this correlation had yet to be published. Here, we present pH-rate profiles in several metal ions with the observation that while metal ions affect the pH profile, this effect does not follow a trend based on a single physical metal ion-characteristic. Instead, the metal ions are grouped into Group II alkaline earth metal affectors, and transition metal affectors. We hypothesize that these differences are based on coordination preferences of metal ions in the active site. This project was conceived of and designed by Dr. DeRose and myself. The pH-rate profiles were determined by Dan Morris, Matthew Hendrix, and Greg Solis under my and Dr. DeRose's mentorship. As members of the Hammerhead sub-group of the DeRose Lab, Dan, Matt, and Adam Unger participated in group discussions which led to our experimental strategies. I have co-written a manuscript with Dr. DeRose for this work, which we plan to submit to *Biochemistry*.

Introduction

The Hammerhead ribozyme (HHRz) is a member of a class of ribozymes that perform site-specific cleavage of a phosphodiester bond using general acid-base catalysis. This ribozyme class includes the HHRz, Hairpin, HDV, VS, and GlmS S ribozymes. Cleavage takes place by a reversible transesterification reaction, and is initiated by in-line attack of a 2'-O on the 3' –phosphorous, resulting in a 5'-O leaving group and a 2'-3' cyclic phosphate. Despite sharing a common reaction, these ribozymes are structurally

diverse and current research shows that a variety of catalytic strategies are used by each ribozyme (DeRose 2002; Fedor 2009). Of particular interest is the source of general acid and general base contributions to these reactions. For this class of ribozymes, several lines of evidence indicate that nucleobase functional groups play mechanistic roles in proton transfer (for review see (Fedor 2009)). The ability of these ribozymes to use seemingly ill-suited nucleobase functional groups for roles as acids and bases is of particular interest in the ribozyme field and a subject of much debate. The catalytic rates of the HHRz, HDV, and VS ribozymes also depend on the identity of divalent metal ions, possibly due to roles in general acid-base catalysis. The molecular details of how ribozymes utilize metal ions and RNA functional groups in their catalytic mechanisms are still incompletely understood.

In the HHRz, the N1 position of G12 is proposed as a general base, based on mechanistic studies and proximity in crystal structures (for review (Cochrane and Strobel 2008)). A metal ion is known to coordinate the scissile phosphate, acting to stabilize the transition state as well as other potential roles ((Ward and DeRose 2012) and for review see (Nelson and Uhlenbeck 2008a)). The molecular identity of the general acid is still in question. The highly conserved nucleotide G8 was implicated in general acid catalysis of the HHRz based on pH-rate profile analysis with different G8/G12 substitutions (Han and Burke 2005). However, crystal structures of the native ribozyme indicate that the G8 nucleobase functional groups are not well positioned to act as a general acid (Martick and Scott 2006; Chi et al. 2008). Instead, X-ray crystallography structures show that the 2' -OH of G8 is positioned to donate a hydrogen bond to the leaving group, and therefore the 2'-OH is proposed to act as the general acid in the HHRz. Removal of this functional group by mutation severely inhibits catalysis, demonstrating the relevance of this position to HHRz function (Thomas and Perrin 2009). In combination with mutations, 3'-phosphorothiolate substitution studies suggest a role for the G8 2'-OH in general acid catalysis, either as a component of general acid placement or as the general acid itself (Velikyan et al. 2001; Thomas and Perrin 2009). However, the ability of this entity to function as a general acid poses serious questions. A particular question concerns the potential of a functional group with a pK_a of 12-15 to act as an effective acid (Velikyan et al. 2001; Acharya et al. 2003). In general, the pK_as of nucleobase functional groups in the

active site of ribozymes are thought to be shifted 2-3 units in order to perform effectively as acids and bases (for review see (Fedor 2009)). The HHRz would be the only known ribozyme to use a 2'-OH as a general acid, however, representing a pK_a decrease of 4-7 units assuming a target pK_a range of <8 (Bevilacqua 2003). In order to shift pK_as toward neutrality, ribozymes can use a variety of strategies. For instance, the active sites of ribozymes have altered electrostatic environments which affect acid-base properties. Another possibility is the stabilization of a nucleobase tautomer to encourage the active protonation state of a functional group. Interactions with the target functional groups either through hydrogen bonding or metal coordination can also be used to shift the pK_as. The HHRz is known to use divalent metals in catalysis, vida infra, and there is a distinct possibility for a multifunctional role for metal ions through participation in the general acid component of catalysis.

There are several lines of experimental evidence that suggest a role for metal ions in participating in general acid catalysis of the HHRz. For instance, just the proximity of the leaving group 5' –O to the metal ion known to coordinate the scissile phosphate makes a metal-associated water molecule a strong candidate for the general acid (Martick and Scott 2006; Chi et al. 2008). Alternatively, a metal ion could coordinate and stabilize developing charge on the leaving group. Direct coordination to the leaving group, however, is unlikely a significant contribution to catalysis based on phosphorothiolate substitutions (Thomas and Perrin 2009). Molecular simulations also support a role for metal ions in affecting general acid catalysis. Using a model in which a single metal ion is coordinating both the A9 and scissile phosphates in the transition state, Lee and co-workers demonstrate that the metal ion may also develop strong interactions with the G8 2' –OH in the late transition state (Lee et al. 2008). In further support of the influence of a metal ion on catalysis, it was found that at 1mM M^{2+}, there is a 10000 fold difference in the ability of different metal ions to activate the HHRz for catalysis (Roychowdhury-Saha and Burke 2006; Boots et al. 2008). The dependence of rate on metal identity demonstrates a strong positive correlation with the decrease in M-OH_2 pK_a, suggesting models in which the metal ion is either required in transferring a proton to the leaving group or re-protonating the GA through a proton shuttle mechanism. Since the pK_a of the M-OH is related to the Lewis acidity of the metal ion, the rate difference among different

metal ions also supports a model in which a metal ion directly coordinates an RNA functional group in order to perturb the pK_a of this group toward neutrality in acting as the general acid. If this were the case, one might expect greater shifts in the pK_a of the general acid toward neutrality as the Lewis acidity character increases through the metal ion series. The correlation observed by Boots and co workers (2008), while better than alternatives such as ionic radius or 'hardness,' does not follow the pK_a trend perfectly, perhaps due to compounding factors such as differences in the affinity of metal ion for the active site or differences in the inherent rate (k_1 of **Scheme 4.1**) in the presence of different metals. These compounding factors also prevent metal ion-rate correlations at single pHs from being fool proof determinants of metal ion involvement in ribozyme acid-base catalysis.

Scheme 4.1. HHRz general acid-base catalysis

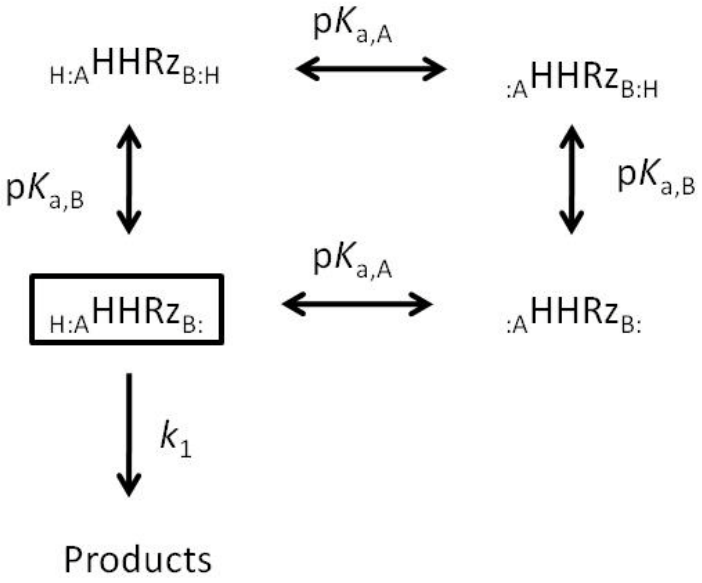

To gain a clearer understanding of how and if a particular component of the ribozyme active site affects general acid-base catalysis, a pH-rate profile can be experimentally determined and fit to estimate the pK_a values of the functional groups involved (for review see (Bevilacqua 2003)). The observed rate, k_{obs}, is dependent on the intrinsic rate of catalysis (k_1) and the fraction of the ribozyme in which the acid is protonated and the base is deprotonated (**Scheme 4.1**). The fraction of ribozyme in the

active state is therefore dependent on the Brønsted properties of both the general acid and base, as only a ribozyme with both a protonated acid and a deprotonated base would be catalytically active. Alteration of the general acid pK_a by mutation or substitution would then predictably shift the pH dependence to reflect the difference in the active population profile, as the point at which the acid becomes significantly deprotonated is expected to shift in proportion to the change in pK_a of the affected functional group. The pH dependent rate profile of the HHRz in several different ionic conditions indicates that at pH $\geq$ 8, the HHRz rate begins to level off and in some conditions decreases, indicating that a protonated group essential for catalysis begins to become significantly deactivated at high pH (Canny et al. 2004; Han and Burke 2005; Roychowdhury-Saha and Burke 2006; Thomas and Perrin 2008). This effect could due to deprotonation of the general acid, though under some conditions it could represent alkaline denaturation of the active site (Buskiewicz and Burke 2012).

The role of metal ions in general acid catalysis can be investigated by creating a series of pH dependent rate profiles for the HHRz in the presence of different activating metals. If a metal ion provides the general acid via its associated water molecule or coordinates the RNA functional group acting as the general acid, one would expect characteristic shifts in the pH-rate profiles that correlate with the Lewis acidity or metal-aqua pK_a of the different metal ions. In support of the role of metal ions affecting the pK_a of the general acid, the pH dependent rate profiles of two different HHRz constructs have been reported to show shifted profiles in Cd^{2+} compared to the profile in Mg^{2+}, which correlates well with the changes in M-OH_2 pK_a between the two metal ions (Roychowdhury-Saha and Burke 2006; Thomas and Perrin 2009). In the study of a *S. mansoni*-derived HHRz, removal of the 2'-O led to a less dramatic shift in pK_a upon metal ion substitution. These results caused the authors to hypothesize that in the WT ribozyme a metal ion directly coordinates the 2'-OH, leading to a large shift in the pK_a of that group (Thomas and Perrin 2009). In this model, when the 2'-O is removed a metal-associated water molecule, with a higher pK_a than the metal-bound 2' -OH, plays the role of the general acid. Surprisingly, with the RzB HHRz, the expected shift in pH profile was not observed in studies using Mn^{2+} as the activating ion, despite a significant decrease in the pK_a of Mn-OH_2 compared to that of Mg-OH_2 (Roychowdhury-Saha and

Burke 2006). The lack of the expected shift in the pH profile in the case of Mn^{2+} could be due to an indirect correlation between metal acidity and the ability to shift the general acid pK_a in the context of this ribozyme. Additionally, collecting data effectively above pH 8.5 is difficult due to compounding factors such as non-specific cleavage of RNA, metal solubility issues, and the potential for alkaline denaturation.

In order to gain a more thorough understanding of the effect of metal ions on general acid catalysis in the HHRz, we determined the pH dependent rate profile of the S. mansoni HHRz in a series of transition metal and Group II ions. We find that transition metal ions, with metal-aqua pK_a's lower than for Mg^{2+}, distinctly shift the ribozyme profile indicating their role in changing the pK_a of the general acid. However, there is no direct correlation between metal-aqua pK_a and the calculated general acid pK_a. Instead, the resulting profiles show clustering based on the whether the metal is a group II ion or transition metal. This trend is also observed using the RzB hammerhead construct, extending previous reports that the RzB and *S. mansoni* HHRzs operate with similar mechanisms despite the highly different catalytic potential reported for these two HHRz constructs. We also investigated the effect of mutations affecting the pK_a of the imine nitrogen (N1) of position A6, which in the crystal structure of a native HHRz is relatively close to the 5'-O leaving group and has previously been shown to be important for catalysis (Ward and DeRose 2012 in review). Together our results support a role for metal ions in general acid catalysis that is most likely as a Lewis acid affecting the pK_a of the 2' -OH of G8. Additionally, our results suggest a mechanistic role for position A6 in general acid catalysis.

Results and Discussion

Dependence of the HHRz rate on pH in varying metal ions

In 1mM M^{2+}, the HHRz exhibits a rate dependence that correlates with the pK_a of the metal–bound water (Boots et al. 2008). However, this analysis does not directly investigate the effect of the metal-aqua pK_a on the acid-base components of catalysis due to compounding factors such as potential differences in metal affinity for the active site residues, and/or the effect of metal identity on the intrinsic rate of catalysis (k_1) due to characteristics aside from Lewis acidity. For instance, metal ions are known to coordinate

phosphate oxygen with differing apparent affinities based on several factors, including electronic properties of the metal and the identity of other ligands in the coordination sphere (Schnabl and Sigel 2010). The characteristics of the metal-phosphate coordination could therefore alter transition state stabilization, leading to differences in the intrinsic rate of catalysis. Additionally, as the metal-scissile phosphate coordination event has been shown to form in the ground-state of the ribozyme (Ward and DeRose 2012), the size and geometry of the metal coordination sphere may alter the inline attack angle of the 2'-O nucleophile or orientation of other groups, again thereby altering the transition state energy. In order to more carefully examine the linkage between metal ion Lewis acidity and metal-water pK_a, one must determine the pH dependence of rate in the presence of different metals.

We determined the pH dependence of the MSL HHRz rate using Sr^{2+}, Ca^{2+}, Mg^{2+}, Mn^{2+}, Cd^{2+}, and Zn^{2+} as the activating divalent metal ions (Figure 4.1 and 4.2). There are several factors to consider when performing this type of experiment in order to obtain the most complete data set. Transition metals, particularly Cd and Zn, have highly reduced solubility at high pH. For this reason we chose relatively low metal concentrations, so that at peak pH values, the data were not limited by transition metal ion solubility. We performed metal titrations to determine a concentration of metal ions which would ensure that small changes in solubility or metal affinity did not artificially decrease the observed rate (data not shown). Additionally, we tested the effect of buffer identity on rate in order to avoid changes in metal ion concentration from metal-buffer interactions (data not shown). It was found that the most consistent rate profiles used MOPS for pH 6-8, with a near continuous transition using TRIS at pH >8 for the Group II metals. Due to metal ion solubility issues and inconsistencies between rates in different buffers, data for transition metals in pH >8 are not reported.

The pH rate profile of native HHRz constructs in Mg^{2+} has been determined under a variety of conditions (Canny et al. 2004; Roychowdhury-Saha and Burke 2006; Thomas and Perrin 2008). The general trend for these profiles is that there is a log-linear dependence from pH 6-8 followed by leveling off of the profile and slight decreases in rate at or above pH 8.The general shape of the *S mansoni* HHRz pH-rate profile is not significantly affected by lowering the Mg^{2+} concentration to 15uM Mg, as we see the

same general profile as has been previously reported in 1mM (**Figure 4.1**). At pH > 8, the profile strays from a log-linear dependence and begins to level off potentially due to deprotonation of the general acid. The rate profiles of the HHRz in the other Group II metals, Sr^{2+}, and Ca^{2+}, are very similar to the profile in Mg^{2+}, with a log linear dependence up to pH 8 followed by leveling off of the profile. The pH-rate profiles of the three tested transition metals (Mn^{2+}, Cd^{2+}, and Zn^{2+}), show profiles that stray from log linear behavior between pH 7 and 7.5, suggesting the deprotonation event leading to rate limitations has shifted to a lower pH in the presence of these metal ions. While a previous study indicated that the pH-rate profile in Mn^{2+} was similar to that of Mg^{2+} (Roychowdhurdy-Saha and Burke 2006), we find the opposite trend, in that the Mn^{2+} profile is more similar to Cd^{2+} than Mg^{2+}. Our Mn^{2+} data, however, are limited to pH <8 in order to avoid potential solubility problems, while Roychowdhurdy-Saha and Burke (2006) extended their data up to pH 8.5 in 1mM Mn^{2+}.

Metal ions perturb the pK_a of the general acid

The pH-rate data were fit to a general acid/base catalysis model to generate two pK_a values representing protonatable groups affecting HHRz catalysis (**Table 4.1**). Though there is inherent ambiguity in the assignment of these pK_a s to either the general base or general acid based purely on this type of experiment (Bevilacqua 2003), there are several studies that suggest the N1 of G12 plays the role of the general base (Han and Burke 2005; Chi et al. 2008; Thomas and Perrin 2008). Additionally, pH-rate profiles in Mg^{2+} show that the pK_a of the base is estimated at 8-8.4 (Canny et al. 2004; Roychowdhury-Saha and Burke 2006; Thomas and Perrin 2009). Therefore the pK_a closest to 8 is commonly considered to represent the pK_a of the general base. For this reasoning to be accurate for a range of metal ions, we also must assume that changing the identity of the metal ion used for activating catalysis has no effect on the identity and/or pK_a of the general base. To our knowledge, there have been no studies that directly investigate the effect of metal ions on general base catalysis in native HHRz's. It is generally assumed, based on crystallographic and computer models, that the metal ion

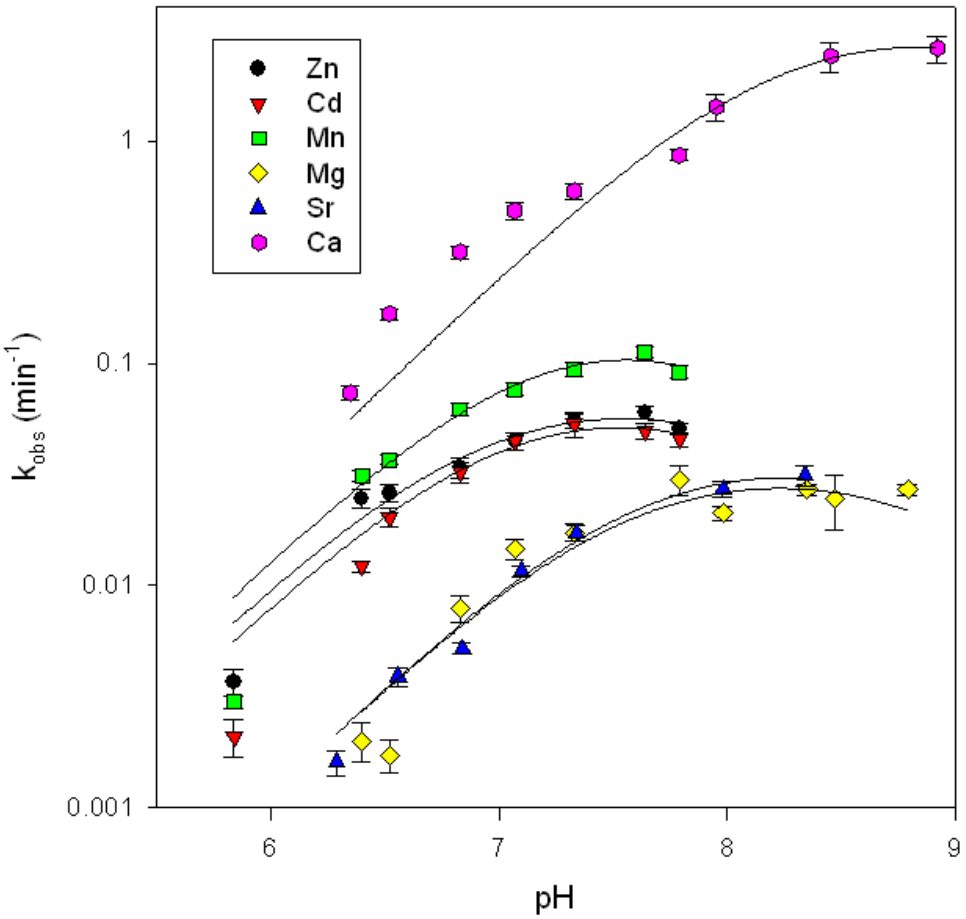

Figure 4.1 The pH-rate dependence of the HHRz in different metal ions. The rate of the HHRz was determined in 2.5 mM MES, 50 mM buffer (MOPS pH 5-8, Tris pH 8-9), and 47.5 mM Na^+ at 20 ^oC. The final pH was determined by scaled up blank control experiments. The rate profiles of the HHRz in 15uM Zn^{2+} (black circles), 15uM Cd^{2+} (red triangles), 15uM Mn^{2+} (green squares), 15uM Mg^{2+} (yellow diamonds), 100uM Sr^{2+} (blue triangles), and 1mM Ca^{2+} (pink circles), were fit (solid lines) using non-linear regressions of the data to Equation C1 as discussed in the Materials and Methods section (Appendix C).

that coordinates the pro-R oxygen of the scissile phosphate does not include direct interactions with the presumed general base (Lee et al. 2008). As the electrostatic environment of the active site can be changed based on the presence of metal ions, however, it is possible that there are indirect effects on the general base pK_a. As an initial model, we assign the pK_a value closest to 8 as the general base and assume that the second value is reporting the pK_a of the general acid.

Table 4.1. The pK_a values determined from the pH-rate profile data from Figure 4.1 and assigned to the general acid and base of the HHRz as described in the text

Metal	pK_a of M-OH_2	pK_a general acid	pK_a general base
Zn^{2+}	8.9	6.9 ± 0.2	8.2 ± 0.4
Cd^{2+}	10.1	7.0 ± 0.2	8.1 ± 0.4
Mn^{2+}	10.6	7.2 ± 0.3	7.9 ± 0.4
Mg^{2+}	11.4	8.9 ± 0.4	7.5 ± 0.3
Ca^{2+}	12.7	≥ 9.5	8.2 ± 0.2
Sr^{2+}	13.2	≥ 9.5	7.5 ± 0.1

Our results confirm previous observations that metal ions affect the pK_a of the general acid of the HHRz (Roychowdhury-Saha and Burke 2006; Thomas and Perrin 2009). However, there is only a very weak correlation between metal aqua pK_a and the pK_a of the general acid (**Figure 4.2**). While the calculated general acid pK_a's do decrease slightly for the series between Mg^{2+} and Zn^{2+}, the differences are within error. In fact, no strong correlation exists between the observed pK_a of the general acid and several other quantifiable traits of metal ions, including the ionic radius, hydration energy, absolute hardness, and absolute electronegativity (as compiled by Feig and Uhlenbeck 1999). Instead, the most apparent trend between different metal ions is grouping based on whether the metal ion is a group II metal, or a transition metal, which is also apparent based on the shift of the pH-rate profiles. For the group II metal ions, the pK_a is estimated to be >9, while for the transition metals, an apparent pK_a of ~7 is reported. Therefore, the values assigned as the general acid pK_as are not well described by a model in which the water ligand of a metal ion plays the role of a general acid.

The RzB HHRz system shows similar metal-dependent pH rate profiles

While the core of the HHRz is highly conserved, the unpaired motifs in helices I and II are highly variable (De la Pena et al. 2003). The variability of sequences outside the core leads to HHRz systems with differential kinetic properties and metal ion

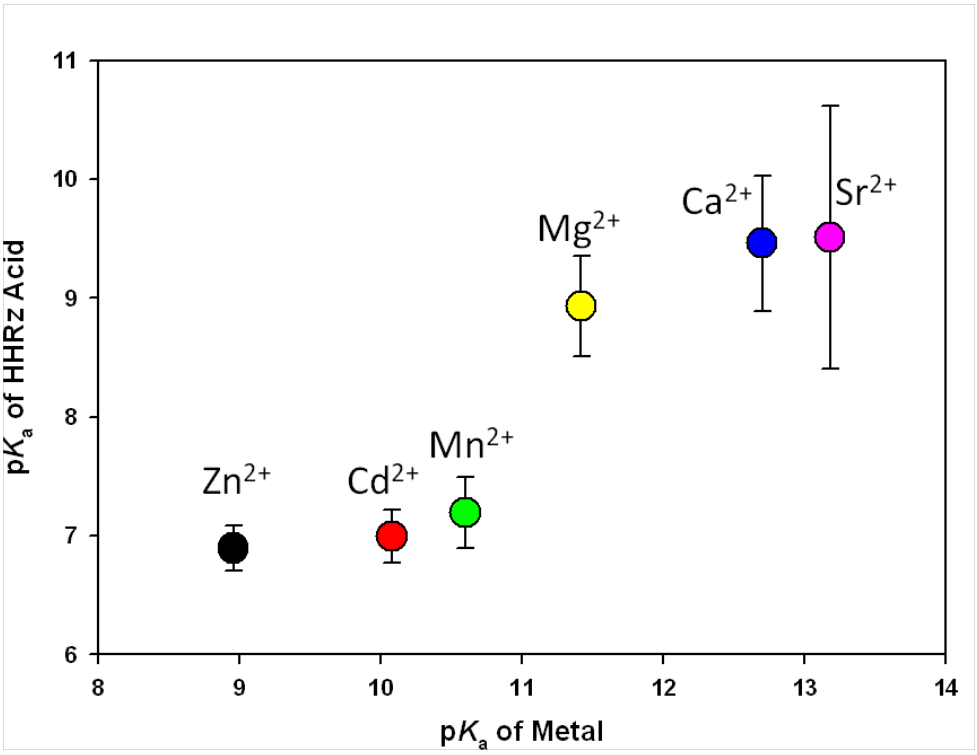

Figure 4.2. A plot of the HHRz general acid pK_a as a function of the metal-bound water pK_a. The values of the general acid pK_a are derived from Figure 4.1 as described in the text and the error bars are derived from the non-linear regression analysis. The pK_a values of the metal-aqua species are from (Feig and Uhlenbeck 1999).

requirements (Saksmerprome et al. 2004; Shepotinovskaya and Uhlenbeck 2008). The RzB HHRz, for example, was derived from the peach latent mosaic virus HHrz and has been shown to achieve unprecedented rates of catalysis at low divalent metal ion concentrations. Additionally, the comparison of metal-dependent pH-rate profiles of the RzB in 1mM Cd^{2+} and Mg^{2+} at 37 ^{o}C also suggested a role for metal ions in general acid catalysis. In order to ensure that our determination of the pH-rate dependence of the MSL1L2 ribozyme in low metal ion conditions was a robust analysis of the general HHRz mechanism, and not specific to this particular system, we produced pH-rate profiles for the RzB in Mg^{2+} and Zn^{2+} in our background conditions (**Figure 4.3**) The RzB data are similarly clustered with the group II and transition metal ions and support the generality of this analysis. These data show that despite differences in the sensitivity to metal ions, the general acid component of these two different HHRz systems are both affected by metal ion identity.

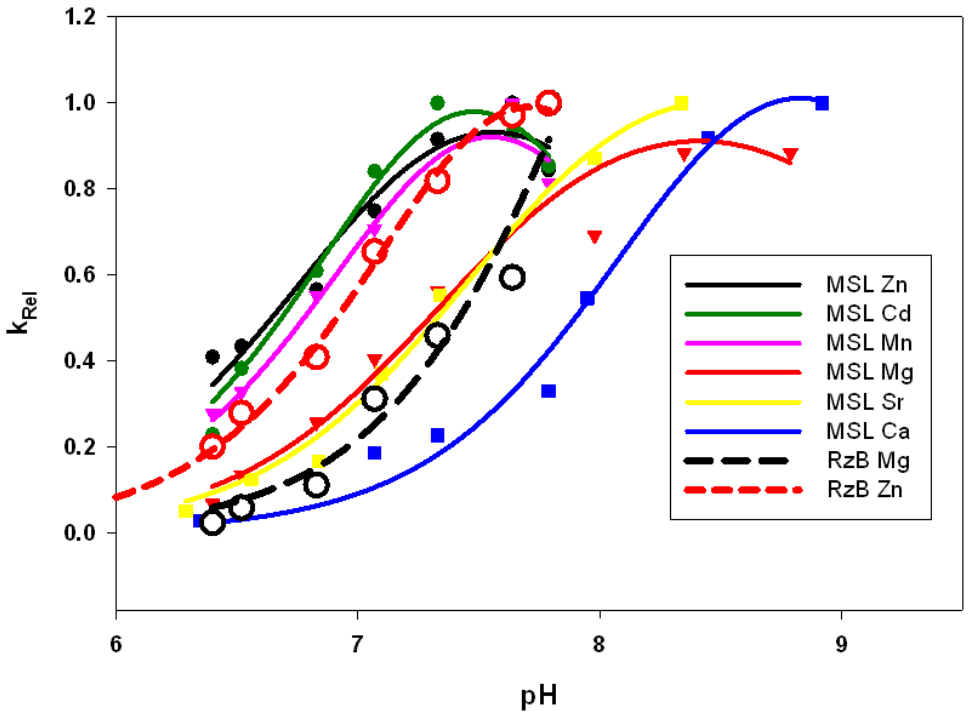

Figure 4.3. The pH-rate profiles of two HHRz constructs. The MSL1L2 is plotted with solid symbols and lines and RzB with open symbols and dashed lines. The relative rates are plotted to emphasize that the metal ion groups provide similar pH profile curves, with the transition metals showing profiles shifted to lower pH values.

Is the shift in the pH-rate profile due to alkaline denaturation?

At pH>8, the slope of the pH-rate profiles of native HHRzs indicate that a deprotonation event is becoming increasingly significant in determining the rate limiting step. While some research groups attribute this pH sensitivity to deprotonation of the general acid, others have suggested that alkaline denaturation causes this characteristic decrease in the rate, as the active site may increasingly become de-stabilized. Recently, experimental evidence to support this hypothesis was provided via folding studies of the HHRz using pyrrolo-C substitutions in the core of the S mansoni HHRz. In these experiments, the rate of folding was measured by monitoring the change in pyrrollo-C fluorescence upon addition of 10mM Mg^{2+}. At pH 8, the rate of folding approached the

rate of catalysis, suggesting that under certain conditions, folding of the HHRz core into the active site may become rate limiting.

Alkaline denaturation is not likely to have caused the characteristic decrease in rate seen in our experiments. Based on the data of Burke and coworkers, the maximum rate of folding for this ribozyme in 10mM Mg^{2+} is ~2000 min^{-1}, and occurs at pH ~7. By pH 8.5 the folding rate has decreased by ~20 fold to 120 min^{-1}. The rate of cleavage under the same ionic conditions rises from ~20 min^{-1} at pH 7, to ~120 min^{-1} at pH 8.5. Therefore, under these particular conditions, the ribozyme may indeed be limited by the rate of folding at high pH. However, under non-saturating metal ion conditions, such as the conditions in which we performed our titrations, this should not be the case. At Mg^{2+} concentrations less than 1mM, the rate of folding at pH 7 reported by Burke and coworkers is still >1000 min^{-1}. If the shape of the pH dependent folding rate profile is not affected by changing the metal ion concentration or metal identity, then the rate of folding at pH 8.5 would be expected to decrease 20-fold, to approximately 50 min^{-1}. Therefore, at high pH, where the rate of folding most closely approaches the rate of cleavage, folding is still ~500 fold faster than the rates of cleavage we measured at low metal ion concentrations. This analysis indicates that folding should not be the rate limiting step in any of our experiments. By ensuring that the conditions in which we monitor the rate limiting step involves the chemistry of cleavage and not folding, we therefore conclude that the loss of activity comes from deprotonation of the general acid and not alkaline denaturation.

Substitutions of the A6 position affect HHRz catalysis

The HHRz crystal structure shows the 2-OH of G8 as the only functional group within hydrogen bonding distance to the 5' leaving group of the scissile phosphate. However, as we have demonstrated in Chapters II and III, a crystal structure does not necessarily represent the most active conformation of the HHRz in solution, and therefore small conformational changes could re-arrange the active site of the HHRz. With this conformational flexibility in mind, reviewing the HHRz crystal structure indicates that the N1 functional group of position A6, if protonated, could act as the HHRz general acid. The pK_a of the N1 of adenosine in model systems is 3.5, but could be shifted in the

context of the HHRz active site. The utilization of a protonated Adenosine is similar to mechanistic models of the Hairpin ribozyme (for review see (Fedor 2009)).

To investigate possible roles of the A6 position in HHRz general acid catalysis, we substituted the A6 position with nucleobase analogs that shift the pK_a of the N1 position. With a pK_a of 8.7, inosine would be expected to have a dramatic effect on HHRz pH-rate profiles, while 2-aminopurine (pK_a 3.8) might be expected to appear similar to the wild type A6 profile (pK_a values from (Han and Burke 2005)) . The pH-rate profiles of the A6, 2AP6, and I6 HHRz systems in 1mM Mg^{2+} are shown in **Figure 4.4**. Both the 2AP6 and I6 mutants show reduced catalytic rates (~1/100 and 1/10 at pH 7, respectively) and have pH-rate profiles significantly different from the HHRz rate profile. While the I6 profile shows the expected shift indicating a general acid with a much higher pK_a, the 2AP6 pH-rate profile is similarly shifted.

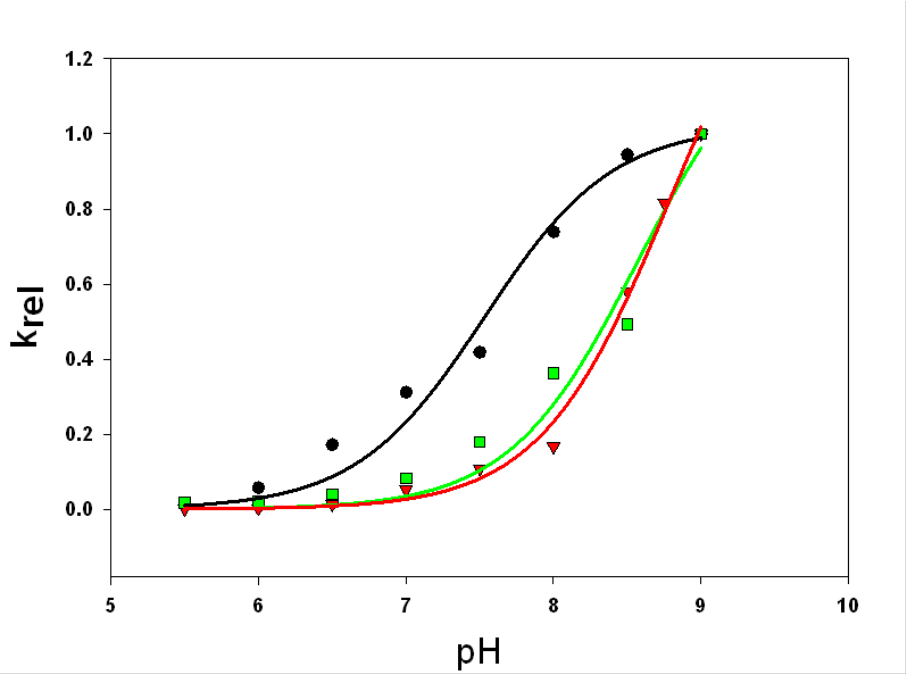

Figure 4.4. The pH rate profile of A6 mutants. Experiments were performed in 1mM Mg^{2+}, 100mM Na^{+}, 50mM Buffer (MES pH 5.5-6, MOPS pH 6.5-7, HEPES pH 7, TRIS pH 8-8.5, CHES pH 9 and additional 2.5mM MES), at 20 ^{o}C. Both the 2AP6 (red) and I6 (green) show shifts in the profile to higher pH values compared to the wild type A6 profile (black). The max rate at pH9 for the A6, I6, and 2AP6 are 6.1, 6.5, and 1.2 min^{-1}, respectively. The data are fit to a equation C1, with the general base pK_a set at 8, yielding general acid pK_a's > 9.

The unexpected shift in the 2AP6 profile does not support a model in which the N1 of position 6 acts a general acid. However both of these mutants may have changed the participants in the HHRz mechanism. Relatively conservative mutants have the potential to disrupt the HHRz by removing components important to the chemical mechanism or through affecting the conformation of the active site. Therefore, it is possible that while the I6 mutation may have affected the pK_a of the general acid, the added steric bulk of the 2AP6 mutant might have re-organized the core of the HHRz. Without further structural analysis of the 2AP6 and I6 mutants, we cannot conclude that this position is directly involved in the chemical mechanism of the HHRz.

Summary and Conclusion

The pH-rate profile of the Hammerhead ribozyme strays from log-linear dependence at high pH, indicating that the protonation state of a functional group has become rate limiting. We find that pH rate profiles in different metal ions indicate that the transition metals alter the profile in comparison to group II metals. These pH-rate profiles can be fit to a general acid-base model to generate two pK_as. Structural and experimental data informed the decision to assign the pK_a closest to 8 as the general base. Based on this assignment, transition metals shift the pK_a of the general acid ~2 units lower than when in the presence of group II metals.

Previous computational and biochemical studies have supported a model for HHRz general acid catalysis in which a catalytically important metal ion coordinates the 2'OH of G8, which would shift its pK_a toward neutrality (Roychowdhury-Saha and Burke 2006; Lee et al. 2008; Thomas and Perrin 2009). Under this model, one might expect that there would be a direct dependence of the pK_a shift of the general acid on metal ion Lewis acidity. Instead of this dependence, however, we find that transition metals and group II ions act as two separate classes in affecting general acid pK_a. This observation may indicate that Lewis acid character is not the only factor in determining the ability of metal coordination to shift the pK_a of functional groups. Alternatively, these data could

indicate that the type of metal coordination is dependent on metal identity i.e. that while group II metals may interact with the 2'OH via outer sphere interactions that only slightly shift the pK_a of the 2'-OH, transition metals may prefer inner sphere coordination, providing more significant shift in pK_a.

Our pH-rate data are complementary to the observed cleavage rates of the HHRz in 1mM M^{2+} and pH 7 reported by Boots and co-workers (2008). In their study, the rates of cleavage using transition metals were very similar to each other and exceeded the rates of group II metals by at least an order of magnitude. Such a significant difference in rate could be attributed to the fact that in transition metals the peak rate of the HHRz occurs closer to pH 7, while in the group II metals the rate peaks at a much higher pH. The concept that metal ions differentially coordinate the general acid could also help explain the correlations presented by Boots and co-workers (2008). In their data, a linear correlation is observed between the metal-aqua pK_a value for Group II metal ions, but the transition metal ions did not show this correlation. When the data were analyzed in terms of absolute hardness of the metal ions, however, the opposite case was true. Whereas group II metals did not show a correlation, the cleavage rate using transition metal ions is essentially inversely dependent on absolute hardness, in that softer metal ions showed faster rates of cleavage. It should be noted that this discussion is based on the assumption that all divalent ions have similar affinities for the HHRz active site.

If the metal ion types do change the type of coordination between innersphere and outersphere, there is a possibility that the dependence on metal ion characteristics may follow two regimes. For the innersphere coordination regime, there could be a weak dependence on Lewis acidity, leading significant, but nearly identical shifts in the general acid pK_a. For an outersphere coordination regime, in which a metal aqua species may serve as the ultimate proton donor in a proton shuttle mechanism, there may be a different, more direct correlation with metal ion characteristics. While our pH-rate data generally support this hypothesis, the inability to precisely determine the HHRz general acid pK_a with the group II metals makes it difficult to confirm a strong (linear) dependence of metal aqua pK_a and general acid pK_a.

The large shift in the pH-rate dependence between metal ion groupings demonstrates the elasticity of the HHRz active site in regards to the use of metals in the

catalytic mechanism. One issue of debate regarding the HHRz mechanism is the classification of the HHRz as "metal dependent". In physiological conditions, it seems likely that the HHRz would use Mg^{2+} in order to perform catalysis, as it is a biologically relevant and a readily available divalent metal ion. However, in vitro, the HHRz shows appreciable rates of catalysis in monovalent cations alone, suggesting that alternative catalytic mechanisms exist. Here, we have shown that the groupings of divalent metal ions based on characteristic shifts in the pH-rate profile may indicate a new level of complexity in regards to divalent metal-dependent catalytic mechanisms and metal coordination states in the active site of the HHRz. Additionally, our data demonstrate that as an important tool for both structural and biochemical studies, metal substitution strategies must be carefully interpreted due to the potential differences in coordination preferences between metal ion types.

Bridge to Chapter V

Chapter IV established the possible role of a metal ion in resolving HHRz catalysis by affecting the pK_a of the HHRz general acid. The next chapter describes potential interactions of metal ions in affecting the activation of catalysis via establishing ground-state coordination to the scissile phosphate and possible interactions with the 2'-nucleophile. This work, however, is done using NMR studies of a trHHRz as opposed to the native HHRz discussed in the previous chapters.

CHAPTER V

THE IDENTITY OF THE NUCLEOPHILE SUBSTITUTION MAY INFLUENCE METAL INTERACTIONS WITH THE CLEAVAGE SITE OF THE MINIMAL HAMMERHEAD RIBOZYME

Overview

This chapter describes work that was done by Dr. Edith Osborne when the DeRose Lab was located at Texas A&M. Much of this work is described in Edith's Dissertation. The experiments needed complete this project and form it into a publishable unit were completed at the University of Oregon by Max Ruehle. I aided Dr.DeRose in planning which experiments were needed and the interpretation of the results as well as co-writing the manuscript, which was published in *Biochemistry* (Osborne et al. 2009). In this paper, we show that common 2' -OH substitutions used to block ribozyme cleavage may affect the ability of metals to coordinate native ligands. This observation has implications for researchers using these substitutions in spectroscopic and chemical studies of metal-dependent processes in RNA.

Introduction

The Hammerhead ribozyme (HHRz) is a self-cleaving ribozyme that catalyzes the reversible attack of a 2'-OH on the proximal 3' phosphodiester bond, resulting in a 2',3' cyclic phosphate and 5'-OH leaving group. The HHRz consists of 3 base-paired stems with a 3-helix junction of conserved nucleotides forming the active site (Forster and Symons 1987; Uhlenbeck 1987; Haseloff and Gerlach 1988). Originally discovered in viroids and satellite viruses where the HHRz functions in genomic processing during rolling circle replication (Hutchins et al. 1986; Prody et al. 1986; Forster and Symons 1987), the HHRz motif has since been found in a variety of genomes including a recent discovery of a discontinuous HHRz motif in mouse (Blount and Uhlenbeck 2005;

Martick et al. 2008a). The function of the HHRz in higher organisms is currently unknown. One of the earliest-discovered ribozymes, the HHRz has been the subject of many mechanistic studies aimed at understanding the bases for RNA-directed catalysis.

As a negatively charged biopolymer, RNA structure and function depends strongly on cations. The precise contributions of metal ions to ribozyme catalysis are of great interest to the RNA community, and numerous studies have been performed on HHRz constructs to determine the metal requirements of this ribozyme. Many studies have been performed on minimal, or 'truncated' HHRz (mHHRz) domains that contain the conserved core surrounded by three base-paired stems (**Figure 5.1**). Native 'extended' HHRz's (exHHRz) contain additional internal or terminal loops in Stems I and II that mediate tertiary contacts, resulting in a more active ribozyme (Reviewed in (Blount and Uhlenbeck 2005)). Substitution experiments have been used as one approach to discern roles for cations in ribozyme function. Both mHHRz's and exHHRz's have appreciable activity in very high concentrations (1-10 M) of monovalent cations, including NH_4^+, indicating that cation-supported RNA structure and electrostatic neutralization are large contributions to HHRz activity (Curtis and Bartel 2001; O'Rear et al. 2001). However, for both HHRz constructs it has been suggested that a more efficient divalent ion-dependent reaction channel exists in which a coordinated metal ion plays a specific catalytic role (Roychowdhury-Saha and Burke 2007). In the mHHRz, activity in 4 M Na^+ or Li^+ is only 50-fold lower than Mg^{2+}-dependent reaction rates. With the exception of two key phosphorothioate substitutions that are discussed below (Wang et al. 1999a), the monovalent-dependent activity has a similar response to many active-site substitutions. Thus, the contribution of many important groups to catalysis is the same whether catalysis is supported by monovalent or divalent cations. There is, however, an added beneficial interaction that can only be satisfied with divalent ions and an inner-sphere interaction.

In the case of the exHHRz, which can reach $\geq$100-times faster single-turnover rates in Mg^{2+} or other divalent cations than does the mHHRz, activity supported by monovalent cations is lower by 2-3 orders of magnitude than maximum rates with divalent cations (Roychowdhury-Saha and Burke 2007; Boots et al. 2008). Preliminary

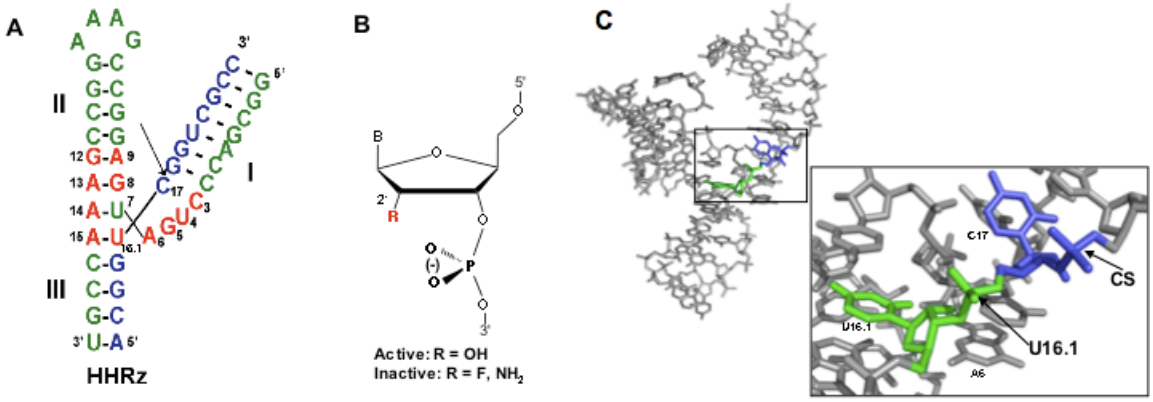

Figure 5.1. Sequence and structure of a trHHRz. (A) Sequence of truncated HHRz (trHHRz) used in this study. Nucleotides in blue identify the substrate strand, and green nucleotides represent the enzyme strand. The conserved core is shown in red, and an arrow identifies the site of cleavage (cleavage site, CS) between nucleotides C17 and G1.1. (B) 2'-nucleophile substitutions used in this study, in combination with phosphorothioate substitutions. (C) X-ray crystal structure of an all-RNA mHHRz (PDB1MME) (Scott et al. 1995) showing location of the phosphodiester groups 3' to C17 (CS) and U16.1 examined in this study using ^{31}P NMR spectroscopy.

phosphorothioate studies also indicate sensitivity to direct metal coordination at specific sites in the exHHRz (Osborne et al. 2005a). While these data indicate that the HHRz is not an obligate metalloenzyme, it is likely that at physiological ionic strengths, HHRz catalysis occurs predominantly via divalent cation-based mechanisms as appreciable rates in their absence are only achieved in >~4 M monovalent ions. In physiological levels of monovalent cations, both types of HHRz constructs are dependent on divalent metal cations for global folding and catalysis, but the onset of activity occurs at lower divalent concentrations for the more stabilized exHHRzs (Blount and Uhlenbeck 2005).

The most likely additional role for divalent cations in HHRz catalysis has been predicted based on thiophosphate interference ('metal-rescue') experiments. In these experiments, a phosphorothioate substitution replaces a non-bridging oxygen with sulfur, resulting in a lower affinity for hard metals such as Mg^{2+}. If the metal-RNA interaction is important for catalysis, the Mg^{2+}-dependent rate is significantly altered upon sulfur

substitution of the putative ligand. The addition of a thiophilic metal such as Cd^{2+} would then be expected to rescue catalysis by coordinating to the sulfur substitute. Working with the mHHRz, Wang and co-workers (Wang et al. 1999a) found that under single turnover conditions and a constant background of 10 mM 'hard' ions (Ca^{2+} or Mg^{2+}) , R_p phosphorothioate substitutions at both the A9 and scissile phosphate positions result in loss of activity that can be substantially rescued by the addition of Cd^{2+}. Moreover, the Cd^{2+}-dependence of activity in constructs containing R_p phosphorothioate substitutions at both of these sites fits best to a model in which a single metal ion bridges between them. This 'bridging metal' model is based on apparent affinities of rescuing metal ions in mHHRz constructs harboring single or double substitutions at the putative metal-binding sites as well as the ability of a single Cd^{2+} equivalent to rescue a dual PS substitution under stoichiometric conditions. Because the apparent affinity of the rescuing metal ion is sensitive to substitutions at the A9 site but not the cleavage site, the model further predicts that a single rescuing metal ion is bound to the A9 phosphate/G10.1 imino N in the ground state of the mHHRz, and that this same metal makes a bridging contact with the scissile phosphate only further along the reaction pathway in the transition state of the reaction, and potentially in an unstable intermediate that is only transiently populated before reaction.

Crystallographic and spectroscopic studies of mHHRz's have consistently identified a metal ion coordinated in the 'A9/G10.1 pocket' consisting of the A9 *pro*-R phosphate oxygen and the N7 imino group of G10.1. In crystal structures of mHHRz's, the active site is somewhat open and the A9 site is located >10Å from the cleavage site scissile phosphate (Blount and Uhlenbeck 2005). In the 'bridging metal' model (Wang et al. 1999a), it is proposed that the mHHRz exists predominantly in this open structure and must undergo a significant conformational change to form a more compact structure representing the catalytically active, and thermodynamically unstable intermediate form of the HHRz that has important functional groups primed catalysis. In the unstable, active-form intermediate, the A9 metal ion is brought into proximity for bridging contact with the scissile phosphate. Potential roles for the critical bridging metal ion include stabilizing the active conformation and/or lowering the free energy of the negatively charged phosphorane transition state (Wang et al. 1999a).

^{31}P NMR spectroscopy in combination with phosphorothioate substitutions can be used as a tool to identify and investigate the properties of potential RNA metal ligands (Pecoraro et al. 1984a; Maderia et al. 2000a; Maderia et al. 2000b; Huppler et al. 2002). A single non-bridging oxygen phosphorothioate substitution results in two ~60 ppm downshifted ^{31}P peaks corresponding to the R_p and S_p stereoisomers of the phosphorothioate (Eckstein 1985; Maderia et al. 2000b). Coordination of Cd^{2+} to sulfur will cause an upfield chemical shift of the relevant stereoisomer peak, allowing for specific identification of metal-RNA interactions (Pecoraro et al. 1984a; Eckstein 1985; Maderia et al. 2000a; Maderia et al. 2000b). Such behavior is found in ^{31}P NMR spectra of an A9 phosphorothioate in the mHHRz (reproduced in **Figure 5.2A**), which confirmed the A9/G10.1 site as a relatively high-affinity metal binding site (Maderia et al. 2000). By contrast, NMR studies to date probing the cleavage site C1.1 phosphorothioate have found little evidence of this site being a metal ligand (Maderia et al. 2000; Suzumura et al. 2002b). For such spectroscopic experiments, the activity of the mHHRz has been blocked by one of a variety of 2' substitutions at the nucleophile. Specifically, previous unsuccessful attempts to observe metal interactions with the mHHRz scissile phosphate by ^{31}P NMR spectroscopy have employed 2'-deoxy and 2'-OMe nucleophile substitutions (Maderia et al. 2000; Suzumura et al. 2002). Overall, results from these previous spectroscopic studies are consistent with the predictions of the 'bridging metal' model: in ground-state mHHRz structures, metal coordination is observed at the A9 site, but not at the cleavage site. In context of the model, spectroscopic evidence for the interaction of a metal ion with the scissile phosphate would be unlikely, as this coordination event is only proposed to happen in either a thermodynamically unstable intermediate or the transition state.

Studies of ribozyme structure generally require repression of catalytic activity, and this is often achieved by substitution of the nucleophile. mHHRz activity can be repressed by 2'-H, -OMe, -F, or -NH_2 nucleophile substitutions (Pieken et al. 1991). Previous NMR studies of metal interactions with the C1.1 phosphate in the mHHRz employed 2'-H and 2'-OMe substitutions to block activity (reproduced in Figure 2A) (Maderia et al. 2000; Suzumura et al. 2002). These studies reported only small

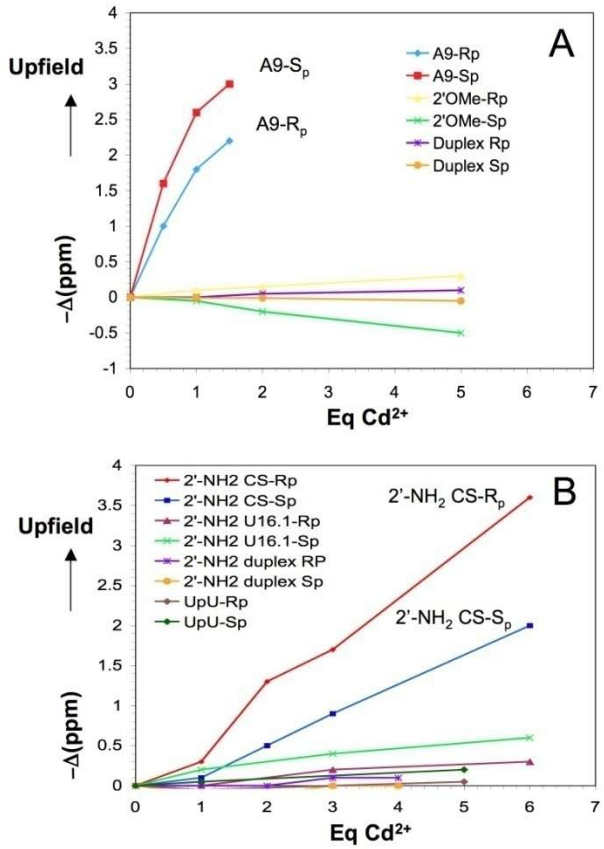

Figure 5.2. Cd^{2+}-induced phosphorothioate ^{31}P chemical shift changes in the mHHRz and control samples. (A) R_p or S_p PS substitutions 5' to A9 (blue, red) or at the cleavage site (CS) with a 2'-OMe nucleophile substitution (yellow, green), and in a control duplex (purple, gold). Data reproduced from Maderia et al. 2000 (Maderia et al. 2000)). (B) R_p or Sp PS substitutions in the HHRz with a 2'-NH_2 substitution (2'NH_2/PS) at the cleavage site (CS, red and blue) or at U16.1 (green and pink). Also shown are data for a control duplex (2'NH_2/PS) (purple and gold), and a dinucleotide $^{am}U_{PS}U$ (brown and green). All RNA concentrations are ~300-500 mM.

chemical shifts upon addition of up to several molar equivalents of Cd^{2+}, indicating that the C1.1 phosphate is a very low-affinity binding site in these substituted constructs and consistent with the model in which a metal interaction with the scissile phosphate does not occur in the dominant ground-state structure. However, an alternative that bears consideration is that a lack of spectroscopic observation of the metal-scissile phosphate interaction could be due to changes in the characteristics of the 2' functional group. The chemical and structural properties of these substitutions differ from those of the natural 2'OH, in particular with respect to potential metal coordination or hydrogen bonding

capabilities that may be required to stabilize metal interactions. For example, although a 2'-OMe substitution is thought to have similar effects on sugar pucker as a 2'-OH (Hruska et al. 1973; Guschlbauer and Jankowski 1980), the 2'-OMe is larger, more hydrophobic and does not participate as strongly in hydrogen bonds or metal ion coordination. Similarly, a 2'-deoxy substituent removes hydrogen-bonding and metal coordination properties at that site.

In this paper we report results of ^{31}P NMR spectroscopy experiments that probe Cd^{2+} interactions with a minimal HHRz construct containing a phosphorothioate substitution at the scissile phosphate in combination with either a 2'-NH_2 or 2'-F substitution in the nucleophile position to block HHRz catalysis. A 2'-F is expected to have a similar atomic radius and electrostatic properties to a 2'-OH and to favor a C3' endo sugar pucker (Guschlbauer and Jankowski 1980), but it is not expected to be available for metal coordination or strong hydrogen bonding (Dunitz and Taylor 1997). By contrast, a 2'-NH_2 substitution is expected to be available for both hydrogen bonding and metal coordination, and favors the 2' endo sugar conformation thought to be required for in-line attack by the nucleophile in the ribozyme reaction (Hruska et al. 1973; Guschlbauer and Jankowski 1980). We find, surprisingly, that the 2'-NH_2 substitution is permissive for metal binding to the mHHRz scissile phosphate, whereas 2'-F substitution does not result in observable metal coordination. Recognizing that close placement of amine and thioate ligands might create an 'artificial' chelate site with inner-sphere Cd^{2+} coordination that would increase apparent affinities significantly above the background level, control studies are presented that monitor metal interactions in constructs in which the 2'-NH_2/PS substitution is placed in a dinucleotide, a duplex, and in the mHHRz at a site adjacent to the cleavage site. The Cd-thiophosphate interaction at the mHHRz cleavage site appears to be $\geq$10-fold stronger than in these control constructs containing the same 2'-NH_2/PS substitution in different contexts. Preliminary results from ^{1}H NMR spectroscopy of a U(2'-NH_2)$_{PS}$U dinucleotide are consistent with a model in which both the phosphate and 2' nucleophile can coordinate a single divalent metal. Taken together, the dependence of metal interactions on 2' nucleophile identity provokes the suggestion that metal coordination to the HHRz scissile phosphate may also involve the 2'-nucleophile position. Integration of these results with the existing 'bridging-metal'

hypothesis is discussed. In general, the results highlight the potential sensitivity of metal ion association with ribozyme active sites upon substitutions within the putative coordination environment.

Results

A 2'-NH_2, but not 2'-F, is permissive for Cd^{2+} coordination to the HHRz scissile phosphorothioate

Previous studies have probed metal interactions with the hammerhead ribozyme cleavage site phosphodiester bond by monitoring the downshifted ^{31}P NMR feature that results from non-bridging phosphorothioate substitution (Maderia et al. 2000; Suzumura et al. 2002). To inhibit activity, either a 2'-H or 2'-OMe substitution of the nucleophile has also been included. Results from these 2'-X/PS (X=H or OMe) have yielded only small ^{31}P chemical shift changes upon addition of Cd^{2+} that are inconsistent with a strong metal site interaction (reproduced in **Figure 5.2A**).

We first extended these studies with a 2'-F substitution at the nucleophile position of the HHRz (**Figure 5.3 and 5.2B**). Like the 2'-H and 2'-OMe substitutions, a 2'-F substitution suppresses activity, enabling NMR experiments that test metal binding to ligands in the active site. The 2'-F is expected to more closely mimic a 2'-OH in size and electrostatics than a 2'-OMe. Upon addition of Cd^{2+} to this 2'-F/PS doubly substituted HHRz, however, no significant changes in the ^{31}P chemical shift were observed for the S_P isomer (**Figure 5.3 and 5.2B**). A slight upfield chemical shift was observed when Cd^{2+} was added to the R_P isomer, as was also observed in an earlier report using the 2'-OMe construct (Maderia et al. 2000). These data indicate that the HHRz with a 2'-F/PS scissile site has only a very weak, yet possibly stereo-specific propensity for metal interactions.

A 2'-NH_2 nucleophile substitution is also expected to suppress catalytic activity of the HHRz. Like a 2'-OH, a 2'-NH_2 is expected to be able to participate in hydrogen bonding and also be an available metal ligand. Additionally, based on studies of uridine mononucleotides, a 2'-NH_2 substitution is expected to favor the 2' endo sugar

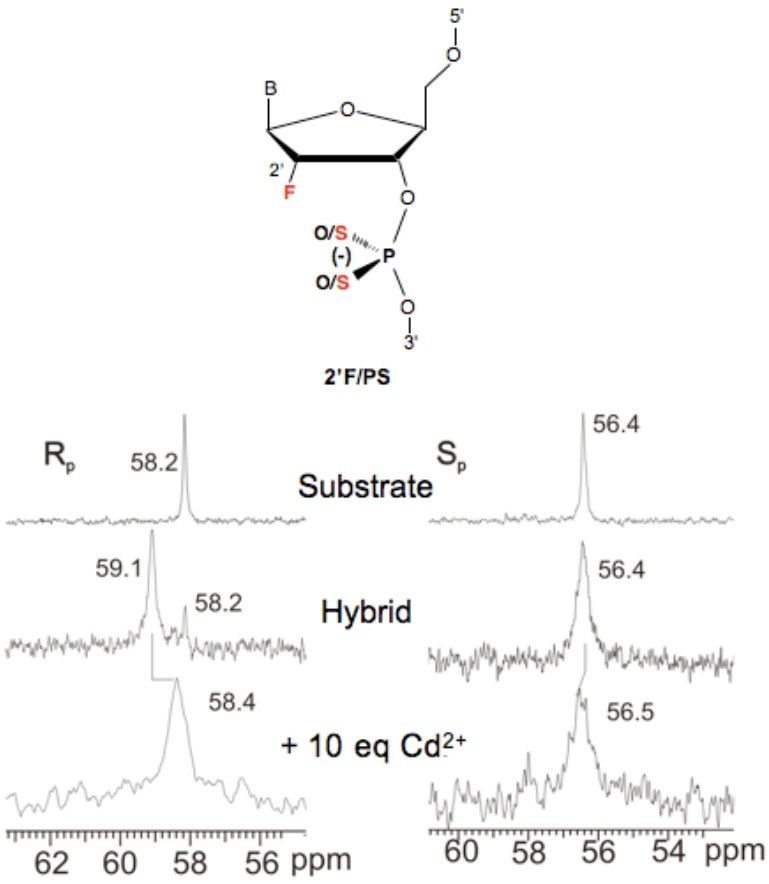

Figure 5.3. ^{31}P NMR spectra of HHRz with a R_p or S_p 2'-F/PS substitution at the cleavage site. Experiments were performed in 5mM HEPES (pH 8.5) and 100 mM Na^+ at 15 °C.

pucker (Hruska et al. 1973; Guschlbauer and Jankowski 1980). The 2' endo conformation, which would favor in-line attack, has been observed for the C1.1 ribose in crystals of an extended HHRz construct thought to most accurately predict the active site (Martick and Scott 2006; Chi et al. 2008; Martick et al. 2008b). Studies of the pK_a of a 2'-NH_2 on various nucleobase analogs indicate that at a pH greater than 7, the amine should be in its unprotonated, neutral state (Verheyden et al. 1971; Hobbs et al. 1973; Aurup et al. 1994; Dai et al. 2007). Single-turnover kinetic studies for both WT and C1.1 2'-NH_2 substituted HHRz constructs, performed in 5 mM HEPES (pH 8.5) and 100 mM Na^+, showed ~1% cleavage over 36 hours in the absence of divalent cations. With addition of divalent metal ions, the 2'-NH_2 HHRz showed only 2% (in 50 mM Mg^{2+}) to

~6% (in 20 mM Cd^{2+} or 20 mM Mn^{2+}) product formation in 36 hours, while the WT HHRz cleaved more than 70% of its substrate under these metal conditions in one hour (Supplementary **Figure D1** Appendix D). Thus, the 2'-NH_2/PS HHRz retains only very weak cleavage ability that would not interfere with an NMR study.

Upon addition of Cd^{2+}, ^{31}P NMR spectra of a racemic mixture of HHRz constructs containing C1.1 2'-NH_2/PS substitutions showed significant upfield chemical shifts (**Figure 5.4 and 5.2B**) of both peaks. This effect was much greater than the shifts observed for the other cleavage site PS constructs with 2'-OMe or 2'-F substitutions (**Figure 5.2B**), suggesting significant metal association with the cleavage site containing the 2'-NH_2/PS substitution. In particular, the furthest downfield peak originating at 58 ppm, which can be assigned to the R_p diastereomer based on previous work (Maderia et al. 2000), moves upfield and merges with the S_p peak in an estimated >3 ppm upfield shift over addition of 6 equivalents of Cd^{2+} (final concentration ~2.2 mM Cd^{2+}/0.1 M NaCl). This result in combination with the previous ^{31}P NMR studies on constructs that lacked a potential metal ligand at the 2' position, and showed little evidence for metal binding, indicates that the 2' position may play a role in metal association with the cleavage site in the mHHRz.

Control studies establish specificity in the HHRz active site Cd^{2+}-phosphorothioate interaction

Both amines and phosphorothioate thio groups are expected to be good ligands for Cd^{2+}, a moderately soft metal ion (Martell and Smith 1971-1974; Martell and Hancock 1996). These two proximal substitutions in the 2'-NH_2/PS constructs may therefore create a non-specific Cd^{2+} binding site that recruits metals that would not otherwise bind to the substituted position. Furthermore, the HHRz active site is located at an RNA three-helix junction, which may increase the effective concentration of metal ions through electrostatic effects (Maderia et al. 2000; Draper 2004; Mohanty et al. 2005; Chu and Herschlag 2008) and therefore enhance an otherwise weak, non-specific interaction. To control for these possibilities, we tested Cd^{2+} association with a dinucleotide model and with two derivatives of the mHHRz containing the NH_2/PS substitutions.

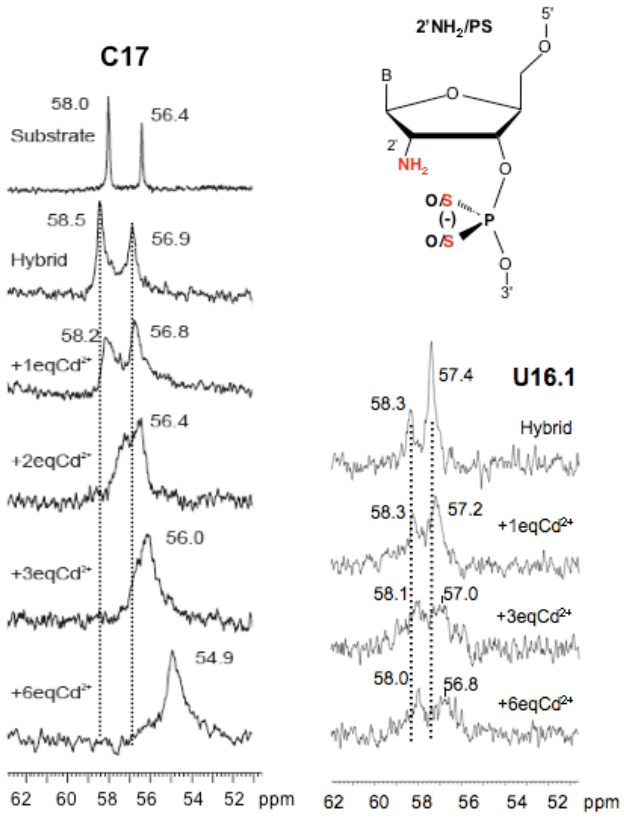

Figure 5.4. ^{31}P NMR of HHRz samples with 2'-NH_2/PS substitution (mixture of PS diastereomers) at the cleavage site (C17, left) or the 5' neighboring position (U16.1, right). Data were obtained at 15^{0}C in 5 mM HEPES (pH 8.5) and 100 mM NaCl with initial RNA concentrations of 450 μM (left) and 440 uM (right).

In order to test the ability of this double substitution to be a general soft metal-binding pocket outside the context of the HHRz, a $^{am}U_{PS}U$ dinucleotide containing the NH_2/PS substituted site was tested for its ability to bind Cd^{2+}. The substituted dinucleotide was separated into its stereoisomers by reverse-phase HPLC. A metal titration showed less than a 0.5 ppm chemical shift change for both isomers through addition of up to 10 equivalents of Cd^{2+} (**Figure D.3 Appendix D**). Addition of 75 molar equivalents of Cd^{2+} still only caused upfield shifts of ~1 ppm. A fit of the titration data to a 1:1 binding model (Equation A.3) indicates a K_d for Cd^{2+} binding to the NH_2/PS site of 22 mM for the S_P isomer and 47 mM for the R_P isomer (0.1 M NaCl) (**Figure D.3 Appendix D**). These low calculated K_D's reflect weak metal binding and reinforce the

conclusion that the double 2'-NH_2/PS substitution alone does not create a high-affinity 'recruiting' metal binding pocket.

Metal ions are known to condense around the dense negative charge of the phosphodiester backbone of an RNA helix (reviewed in (Draper 2004; Chu and Herschlag 2008; DeRose 2008)). An increase of the effective metal concentration near the double 2'-NH_2/PS substitution in any RNA helix could potentially enhance the apparent affinity of this site for Cd^{2+}. We therefore tested an RNA construct composed of the HHRz substrate strand with the cleavage site 2'NH_2/PS substitution in the context of a duplex with its complement strand. This construct showed < 1 ppm upfield chemical shift with addition of up to 5 equivalents of Cd^{2+} for both diastereomers (**Figure D.4 Appendix D**). Similar very weak Cd^{2+}-S interactions were found previously for 2'-H/PS and 2'-OMe/PS substitutions within helices (Maderia et al. 2000). Taken together, these results also reflect a relatively weak Cd^{2+}-sulfur interaction for phosphorothioates outside of the context of the HHRz active site, regardless of the identity of the proximal 2' position.

The increased charge density at the three-helix junction of the HHRz active site could further enhance metal concentrations in that region (Maderia et al. 2000; Draper 2004; Mohanty et al. 2005; Boots et al. 2008; Chu and Herschlag 2008), increasing the propensity for non-specific metal interactions. For this reason, we tested an HHRz construct in which the 2'-NH_2/PS substitution was placed one nucleotide 5' to the scissile phosphate, at position U16.1 (**Figure 5.1**). The mHHRz construct also contained an inhibitory 2'-OMe at the C17 cleavage site. ^{31}P NMR spectra of the mixed diastereomers of this U16.1 2'NH_2/PS mHHRz control construct showed less than a 1ppm change of the phosphorothioate-shifted peaks upon the addition of up to 6 equivalents of Cd^{2+} (**Figure 4**, right). These data indicate that simply positioning a 2'-NH_2 near a phosphorothioate, even at a three-helix junction, does not necessarily create a high affinity metal binding site in the mHHRz. To ensure that the U16.1 double substitution does not significantly alter the local architecture of the mHHRz active site, we tested the activity of a catalytically competent (scissile 2'-OH) mHHRz with the U16.1 2'-NH_2/PS substitution. Previous work has established that the mHHRz activity is tolerant of U16.1 2'-deoxy and

PS substitutions (Kore and Eckstein 1999; Nelson and Uhlenbeck 2008a). The U 16.1 2'-NH_2/PS construct, as a mixture of diastereomers, demonstrated near wild-type catalytic activity (**Figure D5 Appendix D**), indicating that the U16.1 double substitution did not negatively alter the structure of the three-helix junction. These control studies confirm that the observed metal interactions in the double substituted 2'-NH_2/PS HHRz are specific to the scissile phosphate.

Cd^{2+}-NH_2 coordination in the $^{am}U_{PS}U$ dinucleotide model suggested by ^{1}H DQF-COSY spectroscopy

The preceding data indicate that a proximal 2'-functional group that is able to participate in hydrogen bonding and/or metal coordination may be required for a relatively high affinity metal interaction with a phosphorothioate at the mHHRz active site. ^{31}P NMR spectra alone, however, do not confirm that the metal bound to the phosphorothioate sulfur atom is also coordinating the 2' functional group of its 5' ribose. One potential probe for this interaction is the chemical shift of the ribose 2'-H, which is sensitive to the electronegativity of its vicinal 2'- functional group (Guschlbauer and Jankowski 1980). Metal coordination to the 2'- group is expected to change the electrostatic properties of the ligand, and therefore change the chemical shift of the 2'-H (Uesugi et al. 1979; Guschlbauer and Jankowski 1980).

In an initial investigation of metal interaction with the 2' amine in a 2'-NH_2/PS binding site, we used ^{1}H NMR to determine the change in chemical shift of the 2'-H upon the addition of Cd^{2+} in separated isomers of the $^{am}U_{PS}U$ dinucleotide model. Assignments for the 1'-H, 2'-H, and 3'-H ribose protons were based on ^{1}H-^{31}P COSY and DQF-COSY experiments (**Figures 5.5, D.6 and D.7 Appendix D**). For uridine, the previously reported value for the H2' chemical shift with a 2'-OH substituent is 4.34 ppm, and with a 2'-NH_2 is 3.56 ppm (Guschlbauer and Jankowski 1980). Similar values of 4.4 ppm and 3.6 ppm, respectively, were assigned here (**Figure 5.5**). Upon addition of 40 mM Cd^{2+} to either R_p or S_p dinucleotide, shifts are observed in the DQF-COSY H1'-H2' and H2'-H3' cross peaks of the 2'-NH_2 substituted ribose (**Figure 5.5** and supplemental material). Metal coordination to the 2'-NH_2 would result in electron density delocalization away from the H2', and indeed downfield chemical shifts are

observed for ^{1}H resonance from the H1', H2', and the H3' positions upon addition of Cd^{2+}. This result is consistent with previous observations that H2' resonances move downfield as the electronegativity of the other 2' substituents is increased (Guschlbauer and Jankowski 1980). While the ribose ^{1}H chemical shift changes could be due to electron withdrawing influence of metal coordination to the 2'-NH_2, they would also be sensitive to changes in ring conformation (Haasnoot et al. 1980). In both diastereomers of $^{am}U_{PS}U$ in the absence of Cd^{2+}, the $J_{1'2'}$ coupling constant appears to be larger than the $J_{3'4'}$ coupling constant, suggesting that the 2'-NH_2 sugar system has a dominantly C2'-endo sugar conformation (Haasnoot et al. 1980; Kim et al. 1992) and consistent with previous results from NMR studies of uridine mononucleotides (Guschlbauer and Jankowski 1980). Addition of Cd^{2+} does not change the relative $J_{1'2'}$-$J_{3'4'}$ values (**Figure 5.5 and D.7 Appendix D**). Thus, the observed chemical shift changes in the 2'-NH_2 ribose system upon the addition of Cd^{2+} do not appear to be due to a change in the relative sugar conformation populations. In combination with the Cd^{2+}-dependent upfield ^{31}P chemical shift, these ^{1}H NMR data are consistent with Cd^{2+} chelation by both 2'-NH_2 and PS sulfur ligands in the $^{am}U_{PS}U$ dinucleotides. These data further suggest that the ^{31}P chemical shift changes observed upon addition of Cd^{2+} to the mHHRz cleavage site 2'-NH_2/PS construct may also indicate 2'-NH_2 coordination to the metal ion.

Discussion

Potential bidentate 2'-OH/phosphate coordination by divalent metals in the HHRz active site

Repressing activity in ribozymes is a requirement for biophysical studies that are aimed at examining structures occurring prior to the cleavage step. Previous NMR studies of metal interactions with the mHHRz have employed either a 2'-deoxy or a 2'-OMe nucleophile substitution to block activity (Maderia et al. 2000; Suzumura et al. 2002). Metal rescue experiments have identified the *pro*R non-bridging oxygen atoms of both the A9 and scissile phosphates as catalytically important metal ligands in this system, and the bridging-metal hypothesis of Wang and coworkers predicts simultaneous coordination by these ligands in the transition state of the reaction (Wang et al. 1999a). While NMR experiments have confirmed the A9 site to be a high affinity metal

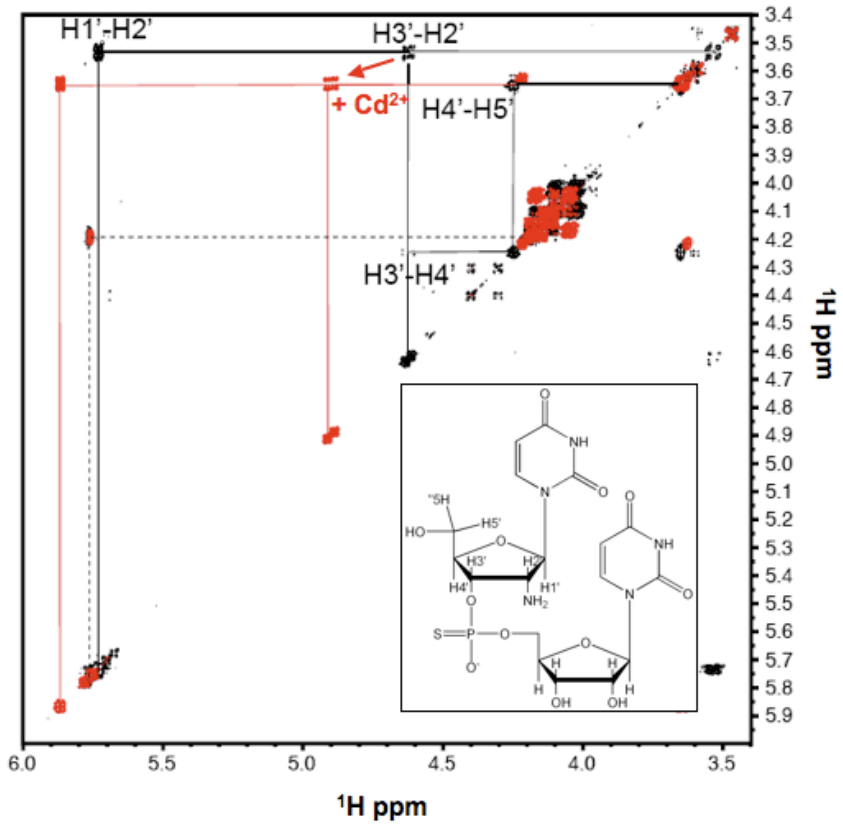

Figure 5.5. DQF-COSY spectra of $^{am}U_{Sp}U$ in absence (black) and presence (red) of 40 mM $CdCl_2$. Data were obtained in D_2O at 10 °C in 10 mM sodium cacodylate (pH 7.4) and 100 mM NaCl. Crosspeak assignments are shown for the 2'NH_2 ribose system (solid lines) and partial assignment for the 2'OH ribose (dotted line).

coordination site, there has been no previous spectroscopic evidence for metal coordination to the scissile phosphate (Maderia et al. 2000; Suzumura et al. 2002). These data are consistent with a model in which the mHHRz maintains predominantly a 'ground-state', open structure with a populated high-affinity A9/G10.1 metal site, and infrequently samples an unstable active structure in which the metal ion may acquire a non-bridging oxygen ligand from the scissile phosphate (Wang et al. 1999a). It is also possible, however, that the cleavage site 2' substitutions used previously to block activity in the spectroscopic studies may also have blocked the ability for a metal to interact with this site.

Any substitution within the active site of the HHRZ may have substantial positive or negative effects on metal coordination. While some substitutions may change the geometry of potential ligands, others may have steric and/or electrostatic effects. Even more problematic would be a substitution that replaces a potential metal ligand for an atom with no metal-binding capabilities. In this study, we continued the spectroscopic investigation of mHHRz scissile phosphate metal coordination by testing the Cd^{2+}-binding abilities of mHHRz cleavage-site phosphorothioates in combination with either a 2'-F or 2'-NH_2 nucleophile substitution. Whereas the 2'-F construct failed to exhibit metal binding to the scissile phosphate, the 2'-NH_2 HHRz demonstrated ^{31}P shifts consistent with innersphere metal ion coordination.

Although a potential nucleophile, the 2'-NH_2-substituted mHHRz shows a loss of divalent metal-dependent catalysis that is not rescued by the addition of the soft metal Cd^{2+}, indicating that these RNA constructs are stable during ^{31}P NMR-detected metal titration experiments. A 2'-NH_2 with an R_p phosphorothioate at the mHHRz cleavage site, however, exhibits up to ~3 ppm upfield changes in chemical shift upon addition of 6 equivalents of Cd^{2+} (**Figure 5.2B and 5.4**). Similar chemical shift changes were previously observed to result from Cd^{2+}-phosphorothioate interactions at the HHRz A9 position (Maderia et al. 2000), a metal-binding site that has also been demonstrated biochemically (Peracchi et al. 1997; Wang et al. 1999a) as well as by crystallography (Scott et al. 1995) and solution EPR experiments (Vogt et al. 2006). The similar magnitude of ^{31}P chemical shift change observed with the 2'-NH_2/PS substitution indicates that this construct has a similar ability to associate with metals at the scissile phosphate, and that the metal coordination and/or hydrogen-bonding properties of the 2'-NH_2 are a contributing factor.

The observation that of the four 2' nucleophile substitutions tested in spectroscopic studies, the 2'-NH_2 is the only functional group that presents an available metal ligand and is the only group resulting in observable metal interactions with the scissile phosphate raises the possibility that metal coordination by the native 2'- OH, or a metal-related hydrogen bonding interaction with this position, is relevant in context of the wild type ribozyme. There are several modes by which a single divalent metal may

interact with the HHRz to promote catalysis (Scheme 5.1), including interactions with both the nucleophile and a non-bridging phosphodiester oxygen atom as shown in model C of Scheme 5.1, and or with the leaving group as shown in model B. The data presented here suggest the interactions in model C, in which a metal ion coordinating the *pro*R oxygen of the scissile phosphate also coordinates to the nucleophilic 2'-OH. Functional and crystallographic evidence for this type of interaction in a ribozyme has been established for the Group I intron (reviewed in (Stahley et al. 2007)). The results of our current experiments do not preclude interaction of an additional metal ion at the mHHRz cleavage site. However, the inability in previous NMR experiments to observe significant metal-phosphorothioate interactions in the absence of a metal-coordinating 2'-nucleophile does indicate that interactions such as in A or B of Scheme 1 do not easily occur in the ground-state of the mHHRz.

While ^{31}P NMR-based results are suggestive of a bidentate metal ion coordination to both nucleophile and scissile phosphate in the mHHRz, further evidence for metal coordination to the 2'-nucleophile would include observation of metal-dependent shifts in signals from that position. Initial evidence for this coordination mode is found in the ^{1}H NMR spectra of the dinucleotide $^{am}U_{PS}U$ model system, obtained in the presence and absence of Cd^{2+}. The upfield shifts of vicinal 2'H protons in **Figure 5.5** are consistent with coordination of the 2'-NH_2 by Cd^{2+} in both stereoisomers of the dinucleotide,

Scheme 5.1. Metal binding modes in a trHHRz

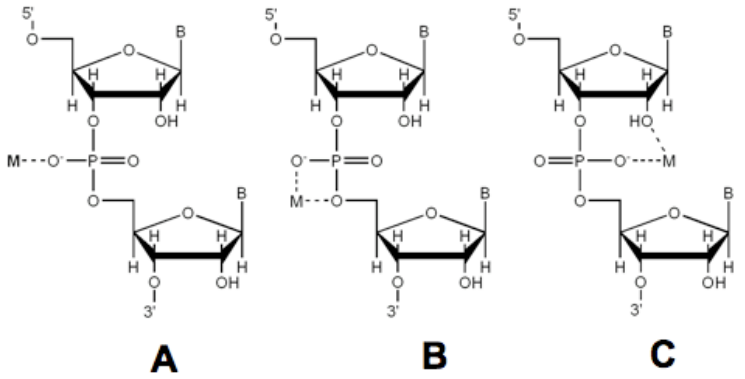

supporting a bidentate metal-binding model. Similar studies probing this interaction in the HHRz are a goal for future experiments.

Cd^{2+} interactions with the mHHRz 2'-NH_2/ PS cleavage site are not due solely to 'recruitment'

As discussed above, substitutions in the active site of a ribozyme can have drastic effects on the ability for a metal to specifically coordinate RNA ligands. These effects can either be prohibitive of a metal coordination event or stabilize a metal coordination that is not representative of the wild type system. In the present ^{31}P NMR studies, a non-bridging phosphate oxygen is substituted with sulfur in order to differentiate the target site from all the other phosphodiester linkages in the RNA construct. This single substitution replaces the relatively hard oxygen atom with a soft metal-coordinating sulfur. For this reason, the common 'hard' divalent ion Mg^{2+} is replaced with 'borderline-soft' (and diamagnetic) Cd^{2+} in our NMR experiments to enable coordination to the substituted site. The other modification to the wild type system in these studies requires 2' substitutions that prevent early steps of the HHRz reaction, allowing observation of an uncleaved HHRz conformation. A 2'NH_2 was the only substitution that supported metal binding at the mHHRz cleavage site, and while this is an interesting result because it has hydrogen-bonding and metal coordination characteristics more similar to hydroxyl than any of the other attempted substitutions, an amine group is also considered a 'soft' ligand that, like sulfur, could enhance Cd^{2+} affinities by orders of magnitude (Martell and Smith 1971-1974; Martell and Hancock 1996). The concern then, is that by placing two soft metal ligands in close proximity, the overall enhancement in metal-binding ability would recruit Cd^{2+} to an otherwise non-native site. This level of artificial enhancement in the Cd^{2+} ion affinities could mean that the metal coordination observed here is a artifact of the construct and not relevant to the wild type reaction.

The potential for metal ion 'recruitment' by the 2'-NH_2/PS site was tested using control constructs containing the 2'-NH_2/PS unit in context of a dinucleotide model, an RNA helix, and a nearby position in the mHHRz. Phosphorothioates embedded within these control constructs all demonstrate very weak interactions with Cd^{2+}, as evidenced by <1 ppm ^{31}P chemical shift changes in up to ~3 mM Cd^{2+} (**Figure 5.2B**), which is a

result that mirrors previous findings for 2'-OMe/PS or 2'-H/PS substitutions embedded in single-strand or duplex RNA strands (Maderia et al. 2000). The observation of >3 ppm ^{31}P chemical shift changes induced by Cd^{2+} when the 2'-NH_2/PS substitution is placed at the mHHRz scissile phosphate is therefore suggestive of a higher-affinity metal-binding pocket that is influenced by its local environment, and not general binding caused solely by the introduction of 2'-NH_2/PS Cd^{2+} ligands.

Relevance of the Cd^{2+}-NH_2/PS active-site metal ion interaction to existing mHHRz activity models

Wang and co-workers established through metal-rescue experiments that a single metal ion is responsible for metal rescue of both the A9 and scissile phosphorothioates despite a measured distance of greater than 10Å between these ligands in structural studies of the mHHRz (Wang et al. 1999a). These and other data lead to a model of the mHHRz reaction in which the ribozyme exists predominantly in an inactive open conformation, and samples an active but thermodynamically unstable closed conformation that brings the two putative metal ligands close enough for a single metal ion to bridge between them. The prediction is that this active conformation, and thus the metal-scissile phosphate interaction, would be difficult to observe spectroscopically due to its thermodynamic instability. Thus, in context of the bridging-metal model, the cleavage-site metal interaction observed in this study is surprising. Three potential explanations for these results are described below.

One possible scenario concerning the significance of these results is that the interaction observed in this study is adventitious and unrelated to mHHRz catalysis. As is common with structured RNAs, both solution and X-ray crystallographic studies of the mHHRz have predicted multiple divalent cation binding sites. It is possible that the interaction observed here with the mHHRz cleavage site is affected by the 2'sugar substituent, but that it does not represent the metal-scissile phosphate interaction that is revealed in mechanistic studies. The fact that the interaction is more easily observed within the mHHRz active site than in the control samples could be ascribed to the electrostatics of the mHHRz active site, which is expected to form a relatively negative electrostatic pocket (Maderia et al. 2000; Mohanty et al. 2005; Chu and Herschlag 2008).

Our attempted control for this situation, the 2'NH_2/PS unit adjacent to the mHHRz cleavage site, could have slightly different geometric and electrostatic properties that influence its ability to coordinate Cd^{2+} relative to the cleavage site position. Even if the metal coordination event observed here is not relevant to mHHRz catalysis, its sensitivity to the 2'-substituent still provides a demonstration of the potential importance of ribose functional group changes on the metal coordination properties of neighboring phosphodiester ligands.

If the metal interaction with the mHHRz cleavage site that is observed in these experiments is indeed related to the functional, bridging metal ion, then its properties are subject to predictions based on the existing model. First, it must be postulated that the 2'-NH_2/PS substitution somehow stabilizes the otherwise thermodynamically unstable 'active' conformation that brings the A9 and cleavage site metal ligands into proximity, allowing sufficient population of the bridging metal site to be observed by NMR. One could argue that simultaneous addition of both the cleavage site 2' amine and the thio ligands have created a Cd^{2+} site with sufficient thermodynamic stability to allow partial population of this bridging state, while at the same time inhibiting the subsequent cleavage step. If these NMR studies are in fact observing the functional bridging metal ion, then the apparent affinity of the metal ion interaction with the cleavage site that is observed by NMR should be sensitive to substitutions at the A9 site. One particular expectation would be that the NMR chemical shift changes should appear at Cd^{2+} concentrations that are expected to fill the A9/G10.1 site. Because of the electrostatic properties of nucleic acids and presence of a charge-shielding counterion atmosphere, as well as possible cation-induced structural changes, metal ion association with RNA is best described in terms of $K_{1/2}$ for the observable rather than K_D for an equilibrium dissociation constant (Draper 2004; Das et al. 2005; DeRose 2008). These NMR experiments were performed by adding equivalents of Cd^{2+} rather than dialyzing to a known equilibrium Cd^{2+} concentration, further complicating interpretation in terms of quantitative affinities since there may be Cd^{2+} association with additional sites on the RNA. This means that the 'free' Cd^{2+} concentration is unknown but is possibly overestimated, leading to an overestimation of apparent $K_{1/2}$ or K_d values. Thus, while these data indicate that a 2'-NH_2 substitution promotes more facile association of Cd^{2+}

with the PS-substituted mHHRz cleavage site than do 2'-X/PS (X=H, OMe, F) substitutions, the data of **Figure 5.2B** cannot be interpreted in terms of thermodynamic affinities for this site. With these caveats in mind, however, one can still compare behavior between similar NMR experiments. It is clear that the Cd^{2+}-thiophosphate interaction with the 2'-NH_2/PS cleavage site (**Figure 5.2B**) requires higher Cd^{2+} concentrations than those needed to fill the mHHRz 2'-OH/PS A9 site (**Figure 5.2A**). At similar RNA concentrations, signal changes from the 2'-NH_2/PS cleavage site are > 3 ppm and not saturated by addition of 6 equivalents, or ~ 2.7 mM Cd^{2+} (0.1 M NaCl), whereas the A9 PS-substituted mHHRz signal is saturating at ~700 uM Cd^{2+} (0.1 M NaCl). A very approximate $\geq$4x ratio of apparent affinities can be estimated from these data, which is broadly consistent with the increase in Cd^{2+} affinity expected upon substitution of the A9 pro-R oxygen for sulfur as measured by Wang and coworkers.[1] These are very qualitative observations, however, and further experiments exploring additional modifications of these sites would be required before a strong link could be drawn between the current experiments and population of the bridging metal site in the mHHRz.

As a final scenario, it is possible that the mHHRz samples in these NMR experiments are not sampling the thermodynamically unstable intermediate that would allow simultaneous metal ion coordination to both the A9 and the scissile phosphate, but that the results are still relevant to the active state of the ribozyme. Even if these experiments are primarily sampling the open ribozyme conformation, the fact that the

---

[1] One estimate of expected affinities comes from the mechanistic studies of Wang and coworkers (*11*), who measure activity-based Cd^{2+} K_d's for the unsubstituted mHHRz A9 site of ~100 μM-280 μM in backgrounds of 10 mM Mg^{2+} or Ca^{2+}, respectively. Their values for the interaction of Cd^{2+} with a A9-R_p phosphorothioate substitution are ~30-70 μM, an increase of 3-4x higher affinity presumably due to the sulfur-Cd^{2+} interaction. Since our NMR studies are performed under different ionic strength, pH, and temperature conditions, we cannot directly compare expected values (and as described in the text, the NMR studies are not performed under conditions allowing for valid $K_{1/2}$ measurements). However, a rough extrapolation might predict a similar difference of 3-4 fold between the Cd^{2+} affinity for the unsubstituted and thio-substituted A9 site. This value is qualitatively consistent with the differences in binding behavior of Figures 5.2A (PS at A9) and 2B (unsubstituted A9).

addition of the 2'-NH_2 ligand makes the scissile phosphorothioate more amenable to metal ion coordination (than when the site includes a 2'-H , F, or OMe) could be an indication of the same propensity in the active conformation of the mHHRz. As is observed here, in the bridging and active conformer an interaction with a 2' ligand may strengthen metal ion association with the cleavage site phosphodiester and thereby stabilize the active conformer and tune reactivity in that state.[2]

While apparently weaker than the high-affinity A9 mHHRz site, the Cd^{2+} interaction with the 2'NH_2/PS cleavage site is still significantly enhanced relative to several control samples. In 0.1 M NaCl, apparent K_d values of 20-50 mM are measured for Cd^{2+} binding to the 2'NH_2/PS unit in the dinucleotide models (**Figure D.3 Appendix D**), at least 10-fold weaker than the interaction with the mHHRz cleavage site. Interestingly, the weak but measurable Cd^{2+} K_d values for the dinucleotide models reflect slightly higher affinity for the S_p thiophosphate, while the S_p stereoisomer of the mHHRz construct had less significant ^{31}P chemical shift changes upon addition of metal (**Figure 5.2B**). This result, in agreement with the stereospecificity found in metal-rescue

---

[2]Comparison with the control constructs indicates a greater propensity towards Cd^{2+} interactions at the mHHRz cleavage site when both 2'NH_2/PS positions are available to interact with the metal ion. It is difficult, however, to relate this observation to quantitative predictions about the 'native' cleavage site state containing Mg^{2+} and potential bidentate 2'OH/PO ligands. Though the Mg^{2+} ion would be presented with two 'hard' ligands, in the case of Mg^{2+} the ion would exchange a high-affinity aqua ligand for the 2'OH, an exchange potentially driven only by the chelate effect. By contrast, the Cd^{2+} ion has a much higher affinity for amine over aqua ligands, which might significantly favor interaction with the 2'NH_2. Still, the fact that addition of a 2'NH_2 was necessary to observe the Cd^{2+} interaction with the mHHRz cleavage site might suggest that in the native state, contribution from the 2' position is also important for this interaction. As suggested by a Reviewer, one such contribution could be deprotonation of the 2'OH along the reaction pathway, increasing negative electrostatic potential and thereby stabilizing the bridging metal ion. Interestingly, MD simulations based on the *Schistosoma* exHHRz crystal structure with Mg^{2+} placed in the A9/G10.1 site, but starting with a deprotonated 2'-O^- nucleophile, have shown much more facile formation of the bridging metal state in comparison with simulations based on the fully protonated nucleophile.

experiments (Ruffner and Uhlenbeck 1990; Slim and Gait 1991; Knoll et al. 1997; Wang et al. 1999a), highlights the potential organization of the mHHRz active site in comparison with the free dinucleotide.

Relationship to current activity models for the extended Hammerhead Ribozyme

Recent research has focused on exHHRz constructs whose extended stems I and II include tertiary contacts that stabilize the formation of the active state. New crystal structures of extended HHRzs exhibit a more compact active site, with many interactions that satisfy predictions from kinetic data obtained with the mHHRz (Martick and Scott 2006; Nelson and Uhlenbeck 2008a). Unlike the case of the mHHRz, and consistent with the predictions of Wang and coworkers (Wang et al. 1999a), in structures of the extended HHRz the A9/G10.1 metal-binding pocket is within a feasible distance to the scissile phosphate to allow a metal ion to bridge the pro-R oxygens. The bridging metal between the two potential pro-R ligands. Mn^{2+} occupies only the A9/G10 pocket in crystallographic studies of a pre-cleaved Schistosome exHHRz with a 2'-OMe substitution at the nucleophile (Chi et al. 2008; Martick et al. 2008b). Based on biochemical predictions and crystallographic contacts, a current acid-base model for HHRz catalysis is proposed that includes activation of the HHRz 2'-nucleophile by deprotonation by the N6 of G12, and protonation of the scissile phosphate leaving group by the 2'-OH of G8 (Han and Burke 2005; Martick and Scott 2006; Martick et al. 2008b; Thomas and Perrin 2008; J.M. and Perrin). In addition to being sensitive to substitutions of G8 and G12, activities of exHHRz's are sensitive to the nature of added divalent cation (Osborne et al. 2005a; Roychowdhury-Saha and Burke 2006), and active-site phosphorothioate inhibition with rescue by Cd^{2+} has been demonstrated in the extended HHRz (Osborne et al. 2005b). Molecular dynamics and biochemical studies have also suggested a metal ion interaction with the 2'-OH of G8, proposed to activate it as the general acid (Lee et al. 2008; Martick et al. 2008b; J.M. and Perrin 2009). Taken together, these observations lead to a current model of combined nucleobase and metal ion contributors to catalysis by the HHRz, with details remaining to be developed.

The experiments reported here could indicate that the 2'-OMe substitution used in crystallographic studies of the exHHRz may inhibit potential metal interactions with the nucleophile. A recent X-ray structure of a slow-cleaving G12A sTRSV exHHRz mutant containing a native 2'-OH nucleophile shows, however, that substitutions at the nucleophile position do not cause gross rearrangements of the catalytic core. The G12A structure does exhibit slight changes in scissile phosphate and nucleophile positions in comparison with the previous Schistosoma structure (Chi et al. 2008). No localized metal ions were reported in the pre-cleaved structure of the G12A exHHRz. In a structure collected post-cleavage, however, densities for two Mg^{2+} ions are reported, one of which is near to the 2'nucleophile (now the cyclic phosphate) and the other of which maintains the A9/G10.1 position. While the appearance of the new metal ion near to the 2' nucleophile in a post-cleavage structure is intriguing, this interaction is not yet predicted from functional data and possibly is relevant only to the cleaved form of the ribozyme or to the crystallographic state.

Summary

The data presented here show that Cd^{2+} interactions with a cleavage-site phosphorothioate in the mHHRz are significantly enhanced by inclusion of a proximal 2'-NH_2 instead of 2'-H, F, or OMe substituents. These results demonstrate an influence of substituents at the 2' nucleophile on metal ion coordination to the scissile phosphate. In the case of the Cd^{2+}-2'-NH_2/PS interaction, the Cd^{2+} is proposed to directly coordinate to the nucleophile position. If present in the active site of the native HHRz, such a bidentate metal-ion coordination would allow metal ions to activate the nucleophile for deprotonation while also coordinating the phosphate, and thereby also aid in transition state stabilization. Other potential avenues by which the 2'-position might influence metal coordination in the HHRz could be via hydrogen-bonding to a metal aqua ligand, or by electrostatics upon deprotonation. Further studies will be required to assess the applicability of these and other metal ion binding modes to activity in the exHHRz.

CHAPTER VI

CONCLUDING REMARKS

Despite extensive study, a detailed description of the HHRz catalytic mechanism has remained elusive. This is in part due to the non-absolute requirement for divalent metal ions and the relatively recent discovery of tertiary stabilization. However, recent structural and biochemical work has begun to fill in the gaps to produce a feasible model of HHRz catalysis in which metal ions and nucleobase functional groups work in concert to perform general acid base catalyzed strand scission.

One of the more challenging aspects of the HHRz mechanism has been determining the extent of metal ion participation in catalysis. The observation that the HHRz globally folds in low M^{2+}concentrations, but is specifically catalytically activated at high M^{2+} suggests that a second metal dependent step activates the HHRz for catalysis (Kim et al. 2005, Boots et al. 2008). The results of our 2-AP work demonstrate that one possible explanation for the high divalent metal ion dependence is that the core of the HHRz undergoes a second conformational change into a relatively unstable conformation. Additionally, the metal ions used in folding experiments hint at the possibility that the metal ion identity may influence the architecture of the active site, such that in ions other than Mg^{2+}, functional groups involved in catalysis could be organized differently, for better or worse.

While the observed second conformational change does not necessarily require a specific metal ion, the identity of the metal ion involved in catalysis is extremely influential on the rate, for several reasons. The metal rescue experiments we performed indicated that the activating metal ion makes a ground state interaction to the scissile phosphate. Therefore, both the affinity of the metal ion and the character of the coordination will affect the energetics of catalytic activation and transition state stabilization. In fact, the rate acceleration of 1mM M^{2+} in the RzB HHRz most closely correlates with the affinity of the metal ion for model phosphate systems (Schnabl and Sigel 2010).

Aside from affecting catalysis through coordination to the scissile phosphate, we have shown that metal ions also participate in general acid catalysis. Our results suggest that metal ions shift the pK_a of the general acid, proposed to be the 2' –OH of G8. Metal ions differentially affect the pH profile, suggesting that the coordination mode is dependent on metal ion identity. For the most physiological relevant metal ion, Mg^{2+}, it is likely that outersphere coordination lowers the pK_a of the general acid and could potentially act as the ultimate proton donor of a proton shuttle mechanism.

Ground-state coordination of the scissile phosphate also indicates that the metal ion may be able to affect catalytic initiation through coordination of the general base or 2' nucleophile. The role of metal ions in general base catalysis has not been explicitly explored in the extended HHRz. However, our NMR studies in a minimal HHRz indicate that an interaction with the 2' functional group may be required for metal coordination to the scissile phosphate in that system. Similar spectroscopic studies of a native HHRz will be required to determine if this observation could be relevant to native HHRz systems.

While questions remain in regards to the details of HHRz catalysis, the work presented in this dissertation aids in explaining the role of metal ions in stimulating HHRz catalysis, and compliments the work of several other research groups. We have demonstrated that at high ionic concentrations, the core of the HHRz may access a relatively unstable conformation with a metal dependence that closely correlates with catalytic activation. Additionally, we show that a metal ion coordinates the scissile phosphate of the HHRz, opening roles for a metal ion in nucleophilic activation. Finally, the metal ion is shown to be important for general acid catalysis via pK_a perturbation by coordination. Therefore, while the HHRz may not be absolutely dependent on metals, it is very likely that the biologically relevant mechanism of the HHRz utilizes metal-mediated catalysis in concert with nucleobase functional groups to achieve strand scission.

APPENDIX A

SUPPORTING INFORMATION FOR CHAPTER II: GROUND-STATE COORDINATION OF A CATALYTIC METAL TO THE SCISSILE PHOSPHATE OF A TERTIARY-STABILIZED HAMMERHEAD RIBOZYME

Materials and Methods

Oligonucleotides

RNA oligomers were purchased from Dharmacon (CO), deprotected according to the manufacturer's instructions, reconstituted in de-ionized and filtered water, and quantified by absorbance at 260nm. The sequences for ribozyme and substrate strands are as follows: Enzyme Strand: 5'-GCAGGUACAUACAGCUGAUGAGUCCCAAAUAGGACGAAACGCG. Substrate Strand:5'- CGCGUC*CUGUAUUCCACUGC. The asterisk denotes the scissile phosphorothioate substitution site.

Reagents

All reagents used were molecular biology grade or better. $CaCl_2 \bullet 2\ H_2O$ was obtained from Sigma Aldrich and $Cd(NO_3)_2 \bullet 4\ H_2O$ from Alfa Aesar.

Separation of phosphorothioate stereoisomers

Phosphorothioate-substituted RNAs consisting of a mixture of the Sp and Rp diastereomers were separated using reverse phase HPLC (Akta purifier; Amersham Biosciences) on a C18 column (Hypersil GOLD, 5um 4.6/250 mm; Thermo Scientific). A stationary phase of 10mM Triethylammonium acetate (TEAA) and a mobile phase of 80% acetonitrile/20% 10mM TEAA were used. A multi-step gradient was used which provided baseline separation of two major peaks.

The configurations of the separated stereoisomers were determined using stereospecific digestion by phosphodiesterase I (Slim and Gait, 1991). This treatment leaves an undigested dinucleotide in the S_p fraction which is identified using HPLC separation, while the R_p fractions are completely digested into single nucleotides.

Digestion mixtures contained 2.5nmol RNA, 10mMTris pH 8, 10mM $MgCl_2$, 0.1 unit of snake venom phosphodiesterase I (Sigma Aldrich), and 1 unit of calf intestine alkaline phosphatase (USB). Reactions were incubated at 37 C for one hour. A dinucleotide peak was observed only in fractions from the second peak, identifying this peak as the S_p distereomer fraction.

HHRz Cleavage Assays

Catalytic activities of the HHRz were determined by using the 43nt enzyme strand (ES) and 5'-^{32}P- labeled 20nt substrate strand (S). Substrate strands were radioactively labeled (5' -^{32}P) using γ- ^{32}P-ATP and polynucleotide kinase (New England Biolabs). Labeled RNA was purified by PAGE, eluted in 100mMacetic acid pH 4.0 with TEMED, and desalted by EtOH precipitation and run through a G-25 column. Enzyme strand at 3uM was mixed with trace labeled substrate, in the presence of 2x Na^+ and 100 mM Bis-tris Propanediol buffer pH 6.5. The complex was annealed by heating to 90 C for 2 minutes, cooling to 4 C for 20 minutes, and equilibrating at 20 C for 10 minutes. Reactions were initiated by the addition of an equal volume of 2x [Ca^{2+}] and 2x [Cd^{2+}] to the annealed RNA. Final conditions were 1.5uM ES, trace S*, 1x Na, 50mM buffer, 1x Ca^{2+} and 1x Cd^{2+}. Time points were quenched by the addition of 166 mM EDTA in 66% formamide with trace amounts of xylenecyanol and bromophenol blue. Cleavage products were separated by dPAGE, then quantified using storage phosphor screens (Kodak) and imaging by Imagequant. A zero time point correction was used to account for background cleavage during the annealing steps.

We assume a model in which the rate in Ca^{2+} represents the folded, but non-activated HHRz and the addition of Cd^{2+} activates the ribozyme (Scheme A.1).

Scheme A.1.

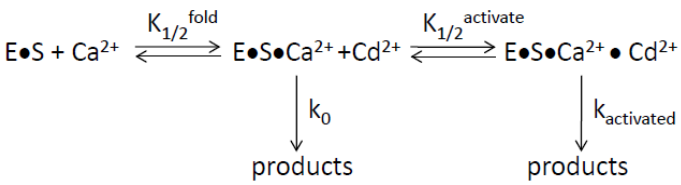

Rate constants were determined by fitting the corrected fraction cleaved versus time to either a monophasic (Equation A.1) or biphasic (Equation A.2) model

$$y(t) = A(1 - e^{-k_{obs}t}) \qquad \text{(A.1)}$$

$$y(t) = A(1 - e^{-k_{obs1}t}) + B(1 - e^{-k_{obs2}t}) \qquad \text{(A.2)}$$

where A and B represent the extents of cleavage and k_{obs1} and k_{obs2} are observed rate constants (Kim et al. 2005; Osborne et al. 2005a). Most fits of 'native' HHRz kinetic data are best described by a model of two non-interacting populations, with the faster phase corresponding to the majority population and a slow phase of <0.01 min^{-1}. In the case of the R_p-S substitution, Equation A.1 fit the very slow rates in 0 to ~10^{-6} M [Cd^{2+}], and Equation A.2 was used when the fitting parameters indicated ~50% for the second population and significantly improved values of R^2. The Cd^{2+} dependence of the rate constant for the fastest population was fit to a binding equation (A.3),

$$y = y0 + \frac{k_{max}x^n}{K_{1/2}^n + x^n} \qquad \text{(A.3)}$$

where k_0 is set as the rate in only Na^+ and Ca^{2+}, k_{max} is the predicted maximum rate of cleavage at saturating Cd^{2+}, and n is the cooperativity coefficient. Nonlinear regression fits were performed using SigmaPlot 11 (Systat Software, Inc.).

APPENDIX B

SUPPORTING INFORMATION FOR CHAPTER III: METAL DEPENDENT STRUCTURAL TRANSITIONS MEASURED BY 2-AMINOPURINE IN THE THREE HELIX JUNCTION OF THE HAMMERHEAD RIBOZYME

Materials and Methods

Oligonucleotides

RNA sequences (**Figure 5.1A**), with indicated substituted oligonucleotides, and a 7mer 2AP7 control strand (UGA-2AP-AAG) were purchased from Dharmacon, de-protected according to the manufacturer's instructions, and stored at -30 C in H_2O. The 2' group of the substrate C17 position was substituted with either 2'-deoxy or 2' -NH_2 to prevent cleavage during fluorescence titrations. Strand length homogeneity was checked by denaturing PAGE. Stock concentrations were determined by UV absorbance at 260nm.

HPLC Separation of Phosphorothioate Diastereomers

Phosphorothioate-substituted RNAs consisting of a mixture of the Sp and Rp diastereomers were separated using reverse phase HPLC (Akta purifier; Amersham Biosciences) on a C18 column (Hypersil GOLD, 5um 4.6/250 mm; Thermo Scientific) with a stationary phase of 10mM TEAA and a mobile phase of 80% Acetonitrile 20% 10mM TEAA. A multi-step gradient was used which provided baseline separation of two major peaks. The Rp stereoisomer elutes off the column first (Wang et al. 1999b; Maderia et al. 2000; Frederiksen and Piccirilli 2009).Similar fractions were combined following reducing fraction volumes by low-heat speed-vacuum concentration and purified by ethanol precipitation, reconstituted in H_2O and quantified by UV absorbance at 260nm.

Chemicals

All chemicals used were molecular biology grade or better. Metal salts were analytical grade or better. $MgCl_2 \bullet 6H_2O$ and $SrCl_2 \bullet 6H_2O$ were purchased from Mallinckrodt, and $CaCl_2 \bullet 2H_2O$ and NaClfrom Sigma-Aldrich.

HHRz Cleavage Assays

Activities of the HHRz and mutants were determined by using the 43nt enzyme strand (ES) and 5'-^{32}P- labeled 20nt substrate strand (S). Substrate strands were radioactively labeled (5' -^{32}P) using γ- ^{32}P-ATP and polynucleotide kinase (New England Biolabs). Labeled RNA was purified by PAGE, eluted in 100mM Acetic Acid pH 4.0 with TEMED, and desalted by EtOH precipitation and run through a G-25 column. Enzyme strand at 3uM was mixed with trace labeled substrate, in the presence of 200mM Na^+ and 100mM buffer. The complex was annealed by heating to 90 C for 2 minutes, cooling to 4 C for 20 minutes, and equilibrating at 20 C for 10 minutes. Reactions were initiated by the addition of an equal volume of 2x [Mg^{2+}] to the annealed RNA. Final conditions were 1.5uM ES, trace S*, 100mM Na, 50mM buffer, and 1x Mg^{2+}. Time points were quenched by the addition of 233uM EDTA in 66% formamide with trace amounts of xylene cyanol and bromophenol blue. Cleavage products were separated by dPAGE and the quantified using storage phosphor screens (Kodak) and imaging by Imagequant. A zero time point correction was used to account for background cleavage during the annealing steps. Rate constants were determined by fitting the corrected fraction cleaved versus time to either a monophasic fit (Equation A.1) , or when appropriate, a bi-phasic fit (equation A.2), where A and B represent the extents of cleavage and k_{obs1} and k_{obs2} are observed rate constants(Kim et al. 2005; Osborne et al. 2005a). For k_{rel} calculations, the faster of the two rates were compared when applicable. Due to the limitations of hand quench kinetic experiments, rates above 5 min^{-1} are not reported and excluded in Mg^{2+}dependent fits . The Mg^{2+} dependence of the fast rate was fit to a binding equation (A.3), where y0 is set as the rate in the absence of Mg^{2+}, k_{max} is the predicted maximum rate of cleavage at saturating Mg^{2+}, and n is the cooperativity coefficient. Nonlinear regression fits were performed using SigmaPlot 11 (Systat Software, Inc.).

Steady State Fluorescent Measurements of 2AP Constructs

Samples for fluorescence titrations were prepared by annealing 2' – cleavage protected 20nt HHRz substrate strand with the corresponding 43nt enzyme strand at 90 C for 2 minutes, 4 C for 20 minutes and equilibrated at 20 C for 10 minutes in 20mM or 100mM Na, 50 mM Tris pH7.5. The strand containing the 2AP substitution is considered the signal strand, which was kept at 1/10 the concentration of the non-signal strand. For a typical experiment, the starting conditions were ~1 uM signal strand. Fluorescence measurements were taken on a Jobin-Yvon Fluoromax spectrophotometer equipped with a temperature-controlled cell holder set at 20 C. Samples were excited at 305nm and steady state fluorescence intensity was recorded at 370nm. Metal titrations were done using aliquots of increasing metal concentrations in identical Na^+ and buffer conditions as the sample. Due to experimental limitations involving light scatter, data were not collected at metal ion concentrations above 100mM M^{2+}. The emission values were corrected against a blank containing non-fluorescent RNA in Na^+ and buffer titrated with M^{2+}. After subtracting the blank values, the emission values were corrected for dilution of the signal. Each folding experiment was repeated at least 3 times. The reproducibility of F_F/F_0 was found to vary by up to 10% between RNA preparations, while experiments from a given RNA preparation varied by only ~3%.

The M^{2+} induced folding of the HHRz were interpreted in terms of either a 2-state (1 transition) or 3-state (2 transitions) model (cf. Rueda and co-workers (Rueda et al. 2003)), depending on the position of the 2AP probe within the HHRz. In the two-state folding scheme (B.1), the probe reports on a single transition from an unfolded (U) to a folded state (F) with an apparent metal ion dissociation constant (K) that we describe as a $K_{1/2}$ of folding and a cooperativity co-efficient (n).

$$(E \cdot S)_U \overset{M^{2+}}{\longleftrightarrow} (E \cdot S)_F \qquad \text{(B.1)}$$

The observed fluorescence is treated as a weighted fluorescence contribution from each state so that

$$F_{obs} = \alpha_U F_U + \alpha_F F_F \qquad \text{(B.1)}$$

where α_i is defined as

$$\alpha_U = \frac{K^n}{K^n + x^n} \qquad \text{(B.2)}$$

$$\alpha_F = \frac{x^n}{K^n + x^n} \qquad \text{(B.3)}$$

therefore, F_{obs} is expressed as a function of M^{2+} (x), the $K_{1/2}$, and a cooperativity coefficient (n)

$$\frac{F_{obs}}{F_0} = \frac{K^n + \frac{F_F}{F_0} x^n}{K^n + x^n} \qquad \text{(B.4)}$$

where $F_U = F_0$.

In some cases, the relative fluorescence values were plotted against M^{2+} and the data were fit as a three state model with an added transition from the folded state to the "active state", which has a separate $K_{1/2}$ (K_2) and cooperativity co-efficient (n_2).

$$(E \cdot S)_U \overset{M^{2+}}{\longleftrightarrow} (E \cdot S)_F \overset{M^{2+}}{\longleftrightarrow} (E \cdot S)_A \qquad \text{(B.2)}$$

For this scheme the data are fit to the equation

$$\frac{F_{obs}}{F_0} = \frac{K_1^{n_1} K_2^{n_2} + \frac{F_F}{F_0} K_2^{n_2} x^{n_1} + \frac{F_A}{F_0} x^{n_1 + n_2}}{K_1^{n_1} K_2^{n_2} + K_2^{n_2} x^{n_1} + x^{n_1 + n_2}} \qquad \text{(B.5)}$$

Non linear regressions were performed using SigmaPlot 11 (Systat). When either phase of the titration data was not saturated, constraints were applied to F_i/F_0 to qualitatively reflect the titration data. Data fit to equation B.5 did not always produce statistically significant results, which we attribute to the inability to reach saturating conditions for the final folded state. Therefore, reported F_i/F_0 and K_i values can be interpreted to represent upper or lower bounds.

Table B1. Parameters for the fits of HHRz construct activity as shown in Fig B1 and B2.

HHRz	% Fast Pop	Fast Rate (min^{-1})	% Slow Pop	Slow Rate (min^{-1})	k_{rel}
WT pH7	48	2.7 ± 0.5	21	0.06 ±0.02	-
2AP1.1	36	1.5 ± 0.2	32	0.01 ± 0.002	0.55
2AP7	39	1.2 ± 0.2	30	0.03 ± 0.01	0.44
WT pH6.5	33	1.2 ± 0.1	34	0.04 ± 0.005	-
2AP6	43	0.009 ± 0.001	-	-	0.008
2AP14	34	0.017 ± 0.003	-	-	0.01
2AP1.1/Pu14	38	0.084 ± 0.003	-	-	0.06

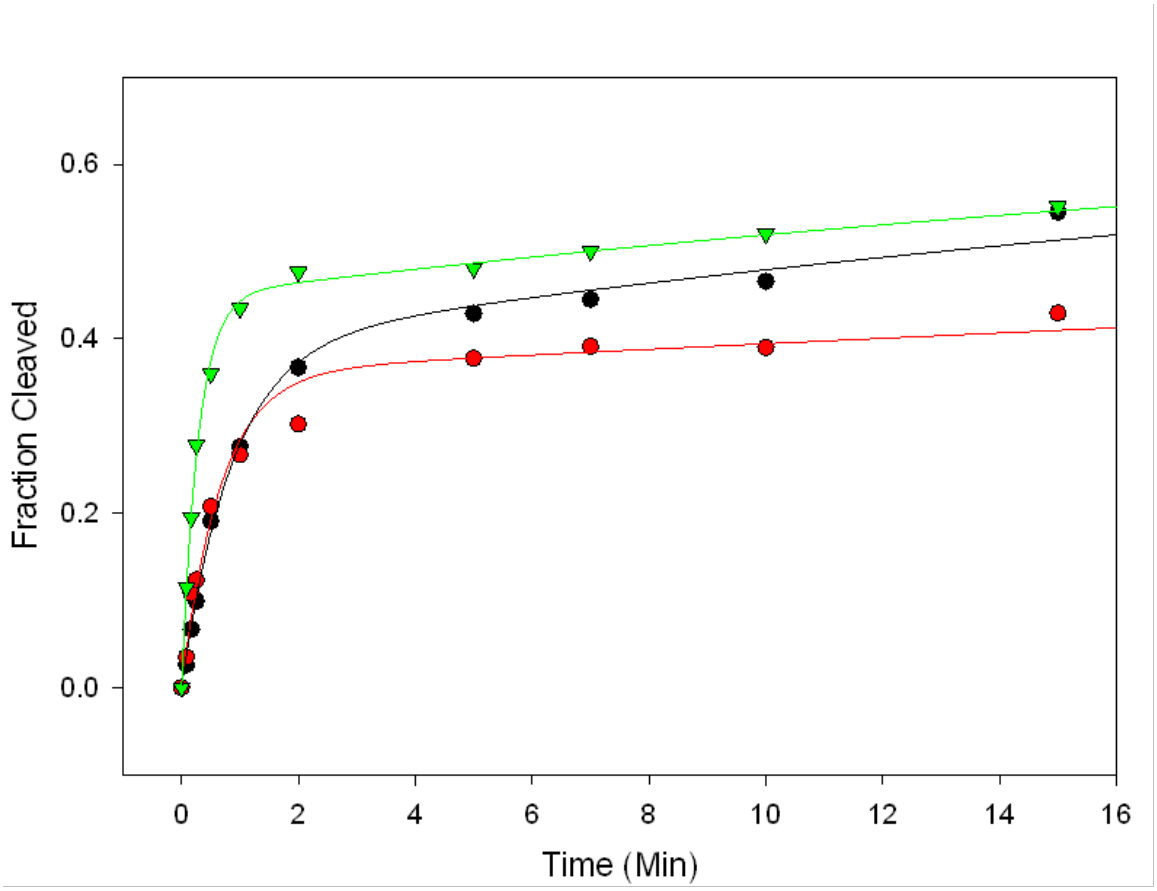

Figure B1. 2AP1.1 and 2AP7 catalysis. Cleavage of WT (green), 2AP1.1 (red) 2AP7 (black) HHRz constructs in 1mM Mg^{2+}, 100mM Na^{+}, 50mM MOPS pH 7.0, 20 ^{o}C. Fitting parameters in Table S1.

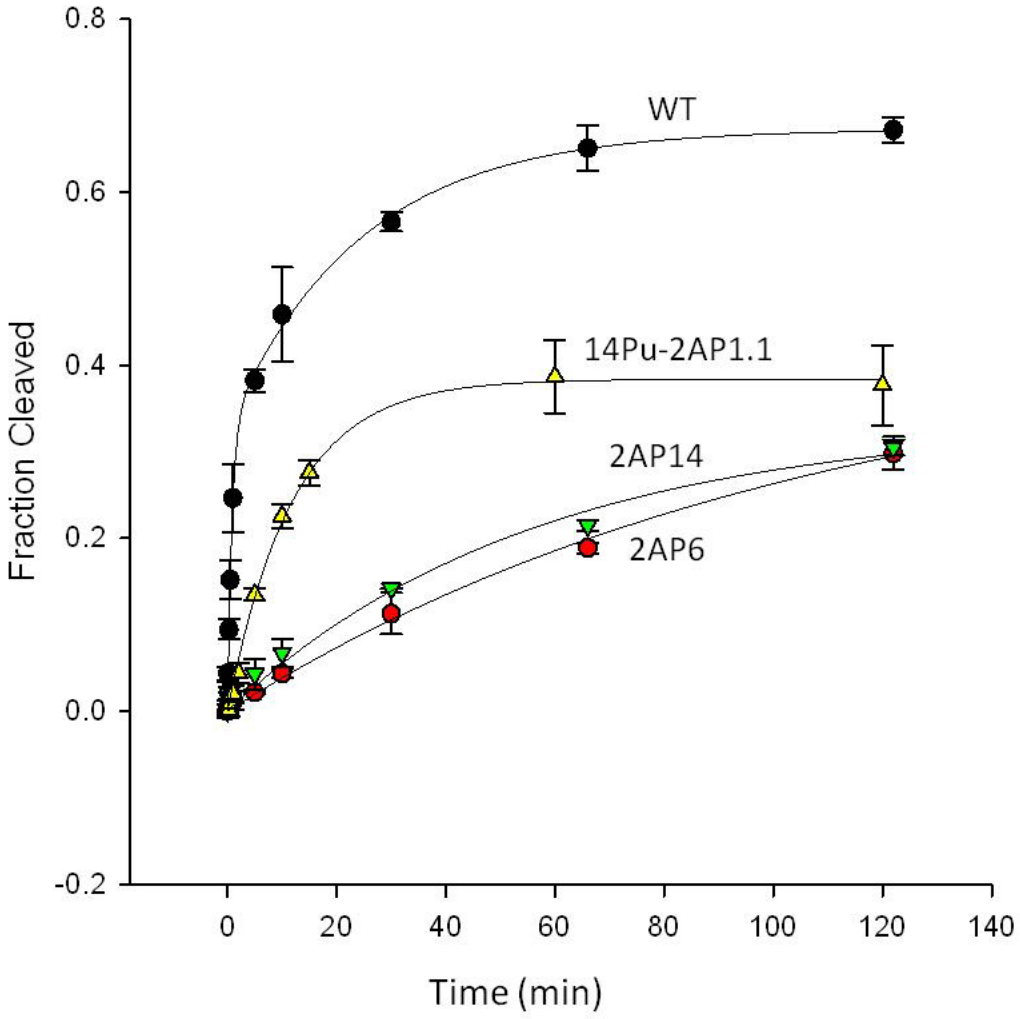

Figure B2. 2AP6, 2AP14, and 14Pu-2AP1.1 catalysis. Cleavage of WT (black), 14Pu-2AP1.1 (yellow), 2AP14 (green), and 2AP6 (red) HHRz constructs in 1mM Mg^{2+}, 100mM Na^{+}, 50mM BisTrisProp pH 6.5, 20 ^{o}C. Fitting parameters in Table B1

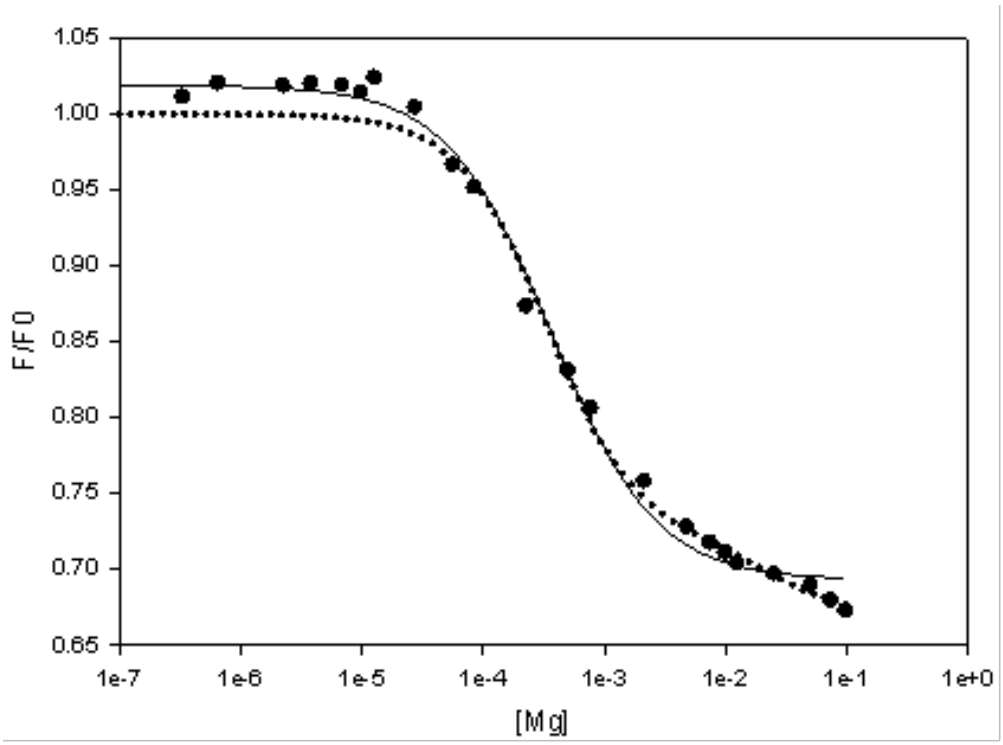

Figure B3. 2AP7 in 100mM Na data do not fit well to a 2-state folding model. The regression analysis using this model (solid line) do not fit the continuing quenching of the data at high metal concentrations. A three-state model describes the data better (dotted line).

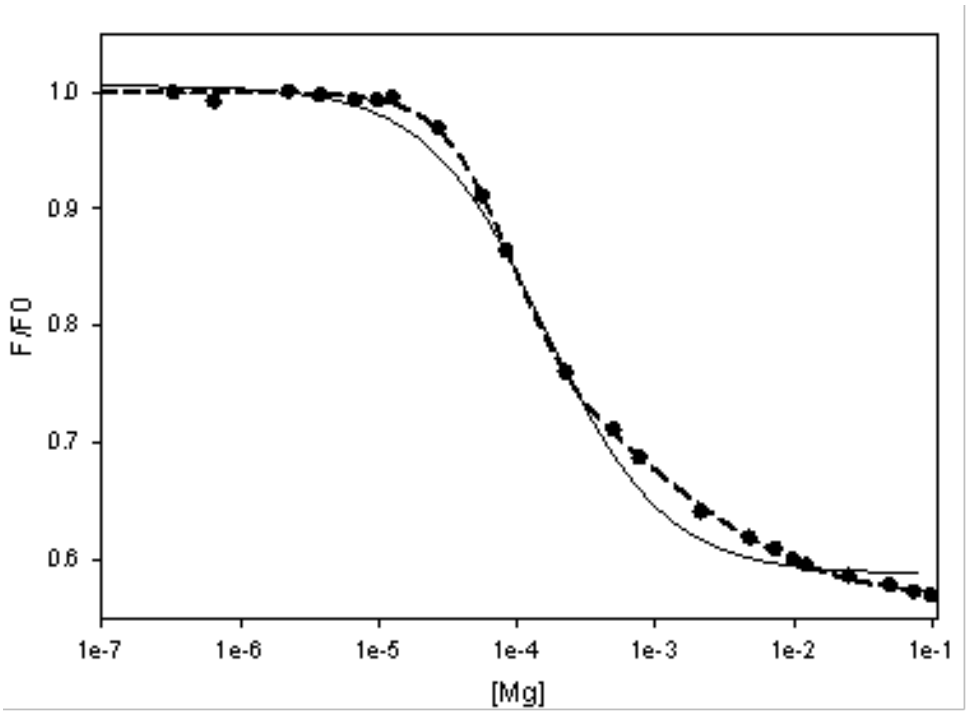

Figure B4. 2AP7 in 20 mM Na^+ data do not fit well to a 2-state folding model. The regression analysis using this model (solid line) do not fit the continuing quenching of the data at high metal concentrations. A three-state model describes the data better (dotted line).

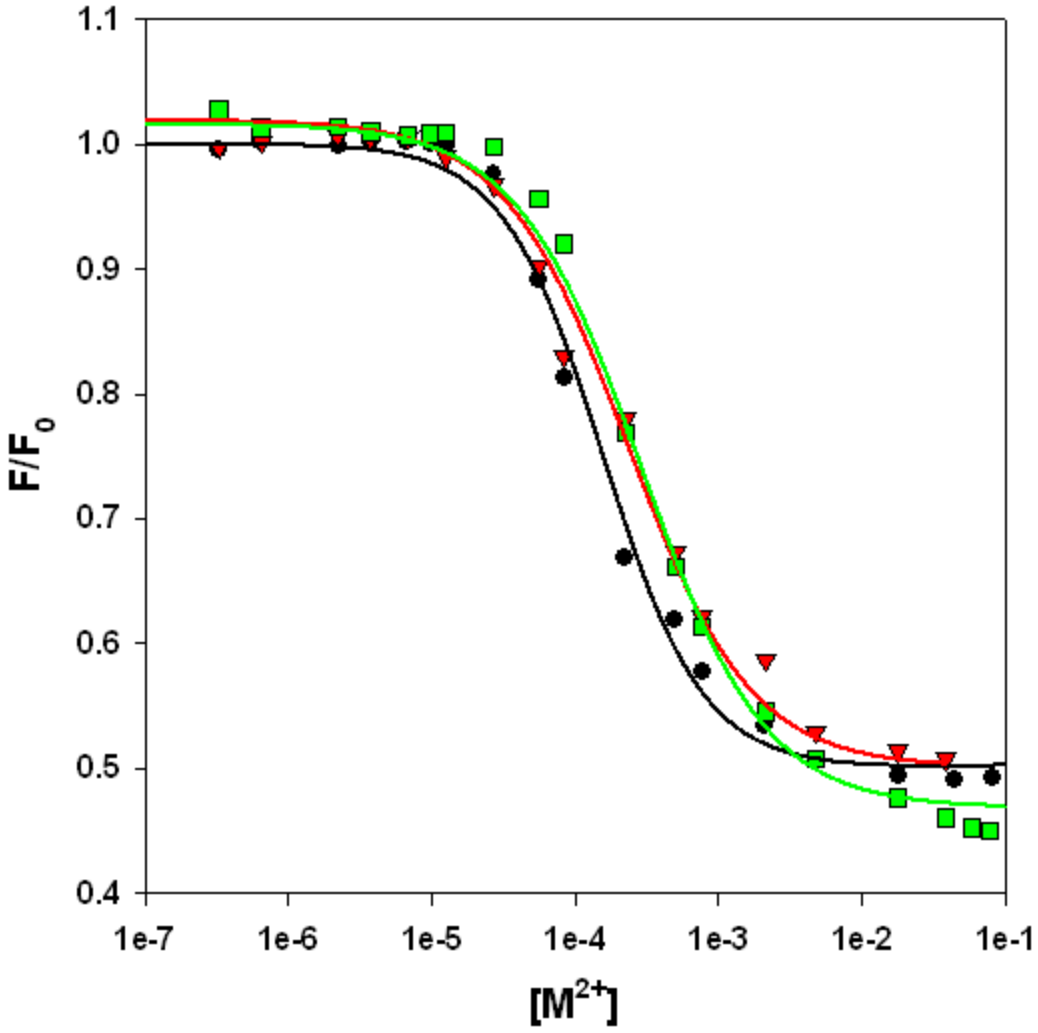

Figure B5. 2AP1.1 fluorescence titrations in different metals. Mg^{2+} (black), Ca^{2+} (red) and Sr^{2+} (green) in 20mM Na^{+} ph 7.5 20 ^{o}C.

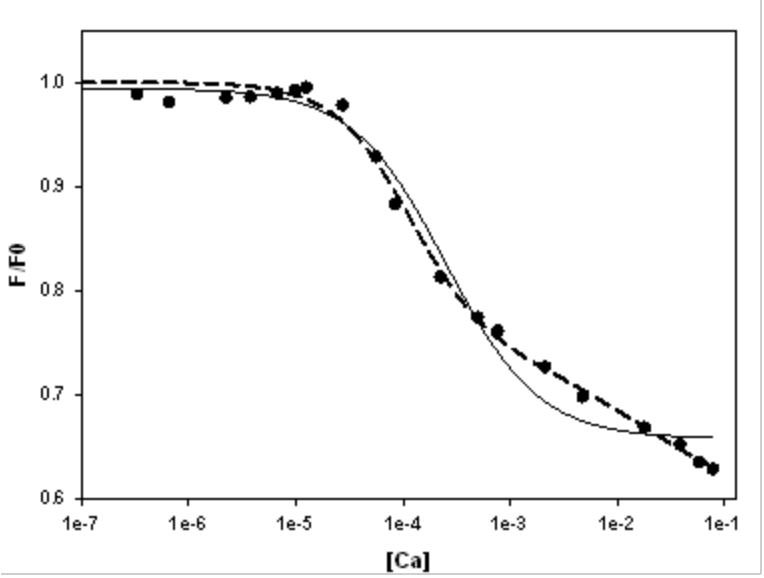

Figure B6. 2AP7 Ca^{2+} titration data do not fit well to a 2-state folding model. The data do not fit well to equation B4 (solid line) at high metal concentrations. A three-state model describes the data better (dotted line).

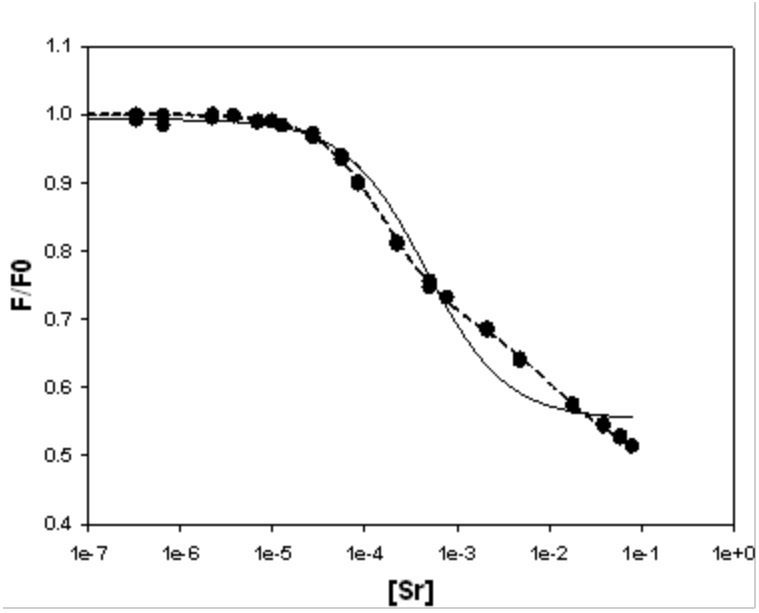

Figure B7. 2AP7 Sr^{2+} titration data do not fit well to a 2-state folding model. The data do not fit well to equation B4 (solid line) at high metal concentrations. A three-state model describes the data better (dotted line).

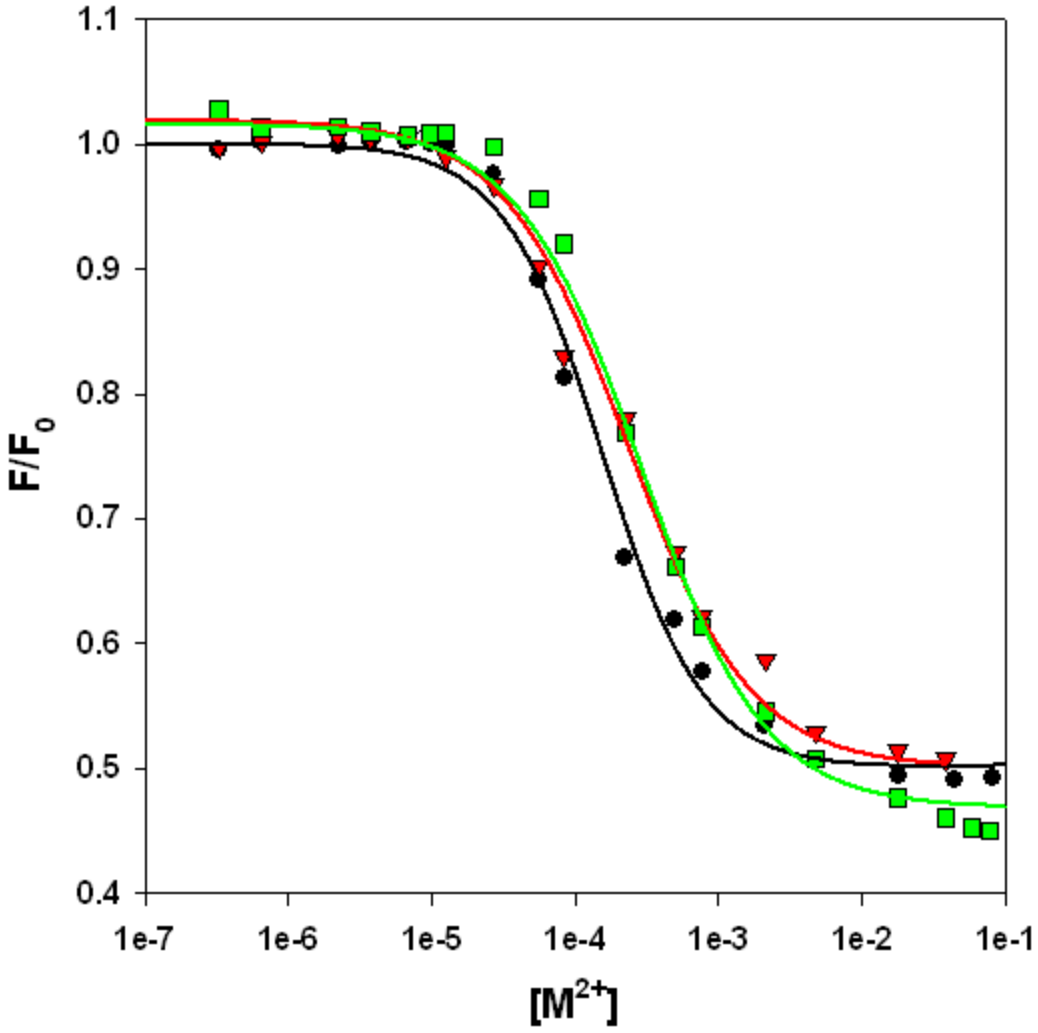

Figure B8. 2AP1.1 titrations in different metals. Mg^{2+} (black), Ca^{2+}(red), and Sr^{2+} (green) all fold the HHRz similarly, with slightly increasing $K_{1/2}$ values for global folding.

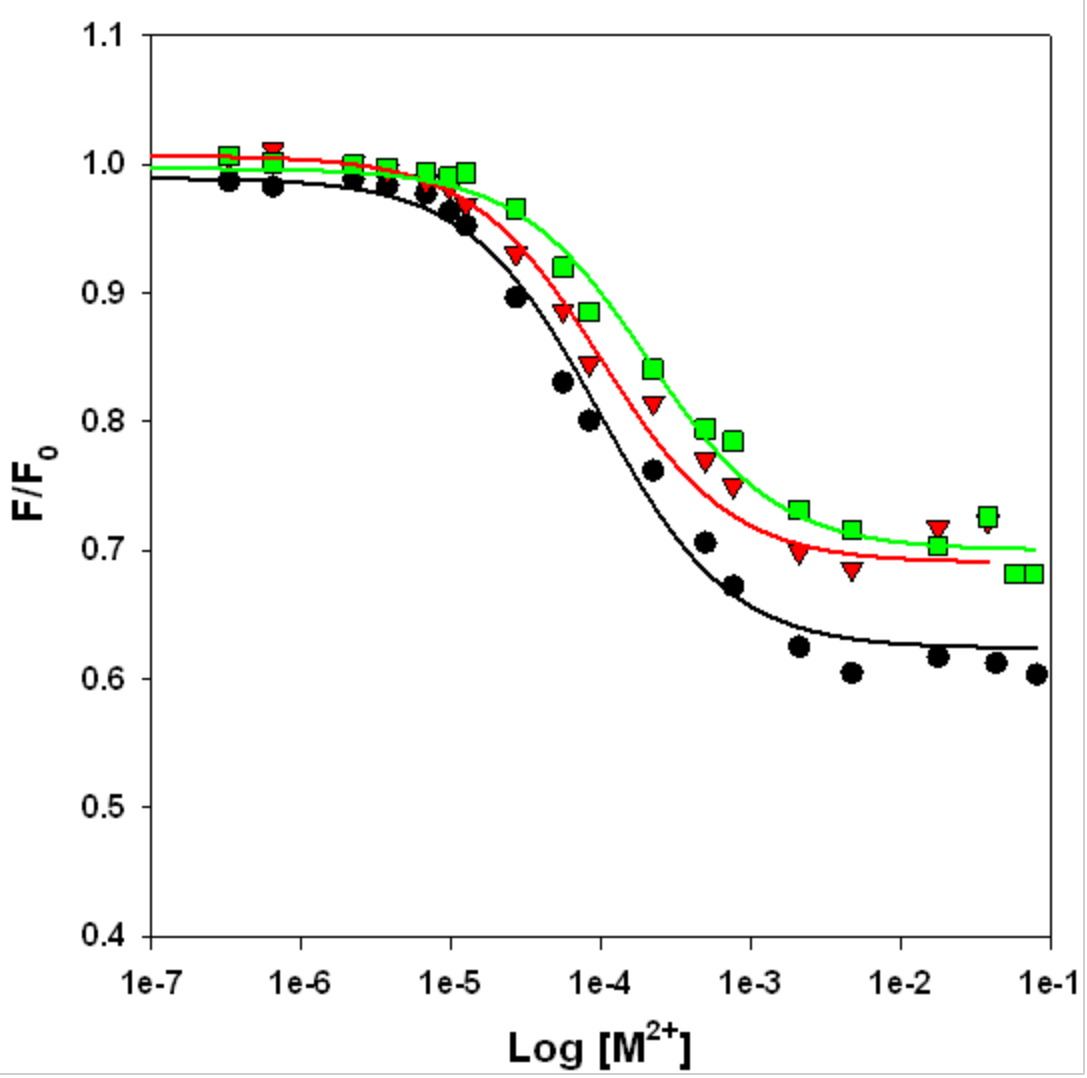

Figure B9. 2AP6 titrations in different metals. Mg^{2+} (black), Ca^{2+}(red), and Sr^{2+} (green) all fold the HHRz similarly, with slightly increasing $K_{1/2}$ values for global folding and slightly altered final quenching.

APPENDIX C

SUPPORTING INFORMATION FOR CHAPTER IV: METAL-DEPENDENT GENERAL ACID CATALYSIS OF THE HAMMERHEAD RIBOZYME

Materials and Methods

Reagents

All Oligonucleotides were ordered from Dharmacon (CO) and de-protected as per the manufacturer's instructions. Reconstituted RNA concentrations were determined by UV absorbance at 260 nm using the reported extinction co-efficients.

The sequences for S mansoni ribozyme MSL1L2 enzyme and substrate strands are as follows:

Enzyme Strand: 5'-GCAGGUACAUACAGCUG(A)UGAGUCCCAAAUAGGACG AAACGCG.

Substrate Strand: 5'-CGCGUCCUGUAUUCCACUGC.

The sequences of the RzB strands are enzyme from (Roychowdhury-Saha and Burke 2006):

Enzyme Strand: 5' GGG ACU UAA GCC CAC UGA UGA GUC GCU GGG AUG CGA CGA AAC GCC C.

Substrate strand: GGG CGU CUG GGC AGU CCC

The parentheses denote position A6, which was substituted with either a 2-aminopurine or Inosine in the appropriate experiments. Buffers and metal hydrate salts were molecular biology grade or better.

HHRz Cleavage Assays.

Catalytic activities of the HHRz were determined by using the enzyme strand (ES) and 5'-^{32}P labeled substrate strand (S). Substrate strands were radioactively labeled (5' -^{32}P) using γ- ^{32}P-ATP and polynucleotide kinase (New England Biolabs). Labeled RNA was purified by PAGE, eluted in 100mM acetic acid pH 4.0 with TEMED, and desalted by EtOH precipitation and run through a G-25 column. The enzyme strand at

3uM was mixed with trace labeled substrate, in the presence of 5mM MES at pH 5.5 and 20mM NaCl. The complex was annealed by heating to 90 C for 2 minutes, cooling to 4 C for 20 minutes, and equilibrating at 20 C for 10 minutes. Cleavage reactions were initiated by adding an equal volume of 2x M^{2+} buffered near the target pH, and a concentration of NaCl so that the final reaction conditions were 1.5 uM ES, trace labeled S, 1x M^{2+}, 2.5mM MES pH 5.5, 50 mM buffer near the target pH, and 47.5 mM Na^{+}, 20 C. The final pH reported was determined by measuring the pH of a scaled up reaction mixture lacking RNA. The metal ion concentration was selected to maximize the pH range at which rates could be determined by manual mixing, while also avoiding metal solubility issues at high pH. For the pH dependence of WT ribozymes in different metals, MOPS buffer was used for pH 6-8, and TRIS buffer was used for pH >8. Fresh buffered metal solutions were prepared for each day. For the comparison of WT, 2AP6, and I6 pH profiles, the final reaction conditions were 1mM Mg^{2+}, 100mM Na^{+}, 50mM Buffer (MES pH 5.5-6, MOPS pH 6.5-7, HEPES pH 7, TRIS pH 8-8.5, CHES pH 9), with the additional 2.5mM MES pH from annealing. After initiation with M^{2+}, time points were quenched by the addition of 166 mM EDTA in 66% formamide with trace amounts of xylene cyanol and bromophenol blue. Cleavage products were separated by dPAGE, then quantified using storage phosphor screens (Kodak) and imaging by Imagequant (Molecular Dynamics). A zero time point correction was used to account for background cleavage during the annealing steps.

Rate constants were determined by fitting the corrected fraction cleaved versus time to either a monophasic (Equation A.1) or biphasic (Equation A.2) model in Sigmaplot 11 (Systat), where A and B represent the extents of cleavage and k_1 and k_2 are the observed rate constants of population A and population B (Kim et al. 2005; Osborne et al. 2005). When a bi-phasic model was used, the fast rate was used for further analysis. The pH dependent rate profiles were fit in Sigmaplot to equation (C.1) based on relationships discussed in the text and described elsewhere (Bevilacqua 2003)

$$k_{obs} = k_{max}/(1 + 10^{pK_1 - pH} + 10^{pH - pK_2} + 10^{pK_1 - pK_2}) \qquad \text{(C.1)}$$

APPENDIX D
SUPPORTING INFORMATION FOR CHAPTER V: THE IDENTITY OF THE NUCLEOPHILE SUBSTITUTION MAY INFLUENCE METAL INTERACTIONS WITH THE CLEAVAGE SITE OF THE MINIMAL HAMMERHEAD RIBOZYME

Materials and Methods

Oligonucleotides.

Hammerhead ribozyme RNA oligomers shown in Figure 1 with their respective modifications were purchased from Dharmacon (CO) and deprotected according to manufacturer's instructions. Deprotected RNA was purified by denaturing gel electrophoresis on 20%/7 M urea polyacrylamide gels and electroeluted from the gel slice. Eluted RNA was dialyzed against 5 mM triethanolamine (TEA; pH 7.0), 100 mM Na^+, for at least 48 hours with several reservoir changes, concentrated (Centricon-3, Millipore), ethanol precipitated, and resuspended into buffer to form a stock solution. Substrate strand RNA with a 2' substituent at the U16.1 nucleotide was deprotected used without further purification. Oligonucleotide concentration was determined by UV absorbance at 260 nm and extinction coefficients provided by the manufacturer. Control RNA duplexes consisting of the HHRz substrate strand with a phosphorothioate substitution indicated by an asterisk (5' ACGCUC*GCUCGCG 3') and its unmodified complement were also obtained from Dharmacon, as were $^{am}U_{PS}U$ dinucleotides.

Separation of phosphorothioate isomers.

Phosphorothioate-substituted RNA consisting of a mixture of phosphorothioate diastereomers, R_p and S_p, were separated using reverse phase HPLC (Akta Purifier, Amersham Biosciences) on a C18 column (5μ 6.3/250, Amersham Biosciences) fitted with a guard column (Upchurch, Oak Harbor, WA) (Slim and Gait 1991; Maderia et al. 2000). For oligomers, a stationary phase of 0.1 M ammonium acetate and a mobile phase

of 80% acetonitrile/20% 0.1 ammonium acetate was used. For the separation of the dinucleotide diastereomers, a more volatile buffer system composed of a 10 mM triethylammonium acetate stationary phase and a mobile phase of 70% acetonitrile/30% triethylammonium acetate, was employed that allowed for removal of the buffer by lyophilization or rotoevaporation. All buffers were filtered using a 20 μM filter flask and degassed by bubbling through helium for 30 minutes before use. Gradients were adjusting based on the size of RNA, with larger RNAs typically requiring a more shallow gradient.

The configurations of separated phosphorothioate diastereomers were determined by digestion with phosphodiesterase I (*Crotalus adamanteus* venom, USB) (Slim and Gait 1991). While the R_p phosphorothioate linkage is cleaved, the uncleaved S_p phosphorothiaote linkage results in a dinucleotide which can be indentified using HPLC separation. Typical digestion mixtures contained 4.0 nmoles of RNA, 0.1 M Tris (pH 8.5), 0.3 mM dithiothreitol (DTT), 0.3 mM $MgCl_2$, 0.1 units of snake venom, and 8 units of calf alkaline phosphatase (USB). Reactions were incubated at 37 °C for 8 hours.

NMR spectroscopy.

All NMR samples were placed in Shigemi D_2O matched quartz tubes (Shigemi Inc., Allison Park, PA). All samples contained at least 400 μM RNA in a volume of 200 μL. ^{31}P NMR spectra of the substrate strand containing a phosphorothioate at the cleavage site were collected first, and then a 1:1 substrate to enzyme hybrid was formed by heating the sample to 90 °C for 90 seconds followed by bench cooling. Cd^{2+} was then added to the sample. Experiments were performed in 5mM HEPES (pH 8.5) and 100mM Na^+. This pH was chosen to ensure deprotonation of 2'-NH_2 substitutions. ^{31}P NMR experiments were performed at 15 °C unless otherwise indicated.

For metal cation titrations, a metal stock solution was made in deionized H_2O or D_2O, and the appropriate volume was added directly to the NMR sample tube. Control experiments indicated no change in pH in the buffer systems employed. In order to prevent nonspecific degradation of the RNA in the presence of metals, no additional heating steps were used. $MgCl_2$ and $MnCl_2$ metal stocks were purchased from Sigma. $CdCl_2$ and $Cd(NO_3)_2$ were purchased from Alfa Aesar. All were 99.9%+ purity.

^{1}H-decoupled ^{31}P NMR spectra were recorded at 202 MHz on a Varian Unity Spectrometer with a 5 mM broadband probe. A pulse sequence of a 500 ms delay, 30º pulse, followed immediately by an acquisition of 0.4 seconds was used. At least 10,000 transients (approximately 8 hours) were collected for each sample. Unless otherwise noted, samples were suspended in a buffer of 5 mM HEPES (pH 8.5) and 100 mM NaCl. An external reference solution of trimethyl phosphate (TMP) or phosphoric acid was used. Where appropriate, the equilibrium dissociation constant (K_d) of the metal-RNA interaction and the total shift for a fully bound RNA-M^{2+} complex ($[\Delta]_T$) was found by fitting to a 1:1 binding model (Equation D.1) (Gonzalez and Tinoco 1999).

$$\Delta_{obs} = \frac{[\Delta]_T}{2 \bullet [MC]_T} \bullet [(M + [MC]_T + K_d) - \sqrt{(M + [MC]_T + K_d)^2 - (4 \bullet M \bullet [MC]_T}] \quad (D.1)$$

$[MC]_T$ and M are the total concentration of model compound/RNA and added metal, respectively, and Δ_{obs} is the observed change in chemical shift for each data point.

^{1}H NMR spectroscopy was performed on a Varian Inova 500-MHz spectrometer equipped with triple-axis gradient probes. ^{1}H samples were run in 10 mM sodium cacodylate buffer (pH 7.4) and 100 mM NaCl. 5,5-Dimethylsilapentanesulfonate (DSS) with a chemical shift of 0 ppm was used as an internal reference. Use of cacodylate buffers results in a residual methyl proton resonance at 3.8 ppm (Roberts 1993). Double-quantum filtered (DQF) homonuclear ^{1}H-^{1}H correlated spectroscopy (COSY) and ^{1}H-^{31}P-COSY experiments were performed on RNA samples that had been exchanged in D_2O by lyophilization or vacuum drying the sample, adding D_2O, and repeating multiple times. NMR spectra were processed using NMRpipe software and VarianNMR software and visualized using nmrDraw and Inkscape (Delaglio et al. 1995).

Hammerhead ribozyme kinetics.

Cleavage activity of the trHHRz WT and variant with a C17 2'-NH_2/PS (cleavage site) substitution were measured at indicated single timepoints under the conditions of the NMR experiment (~400 μM enzyme and substrate strands, 5 mM Hepes pH 8.5, 100 mM NaCl) except at 24 ^{0}C. Kinetics of the trHHRz WT and variant with a U16.1 2'-NH_2/PS substitution were measured in single-turnover conditions (10:1 enzyme:substrate) in 25 mM MOPS pH 7.0, 100 mM NaCl, 1.5 μM enzyme and 0.15 μM substrate plus trace

amount of ^{32}P-labeled substrate, and the indicated divalent metal ion concentrations at 20 ^{0}C. Data are plotted as (fraction cleaved, f) vs. time, and fit to a single-exponential rate expression (Equation A.1

In order to ensure that the ^{31}P NMR chemical shift change of the phosphorothioate peak seen in the hammerhead construct with a phosphorothioate at the cleavage site and a 2'-NH_2 at the nucleophile position is not due to the creation of an artificial site in the HHRz, control studies of an RNA duplex containing a 2'-NH_2 and a phosphorothioate were performed (**Figure D.1 and D.2**). Some degradation, indicated by the presence of a cyclic phosphate peak at 20 ppm, was observed in these samples. The study was performed on separated phosphorothioate diastereomers. A less than 1 ppm upfield chemical shift with addition of up to 5 equivalents of Cd^{2+} was observed, suggesting a weak Cd^{2+}-sulfur interaction. Thus, simply positioning a 2'-NH_2 near a phosphorothioate in a duplex does not create a strong metal binding site.

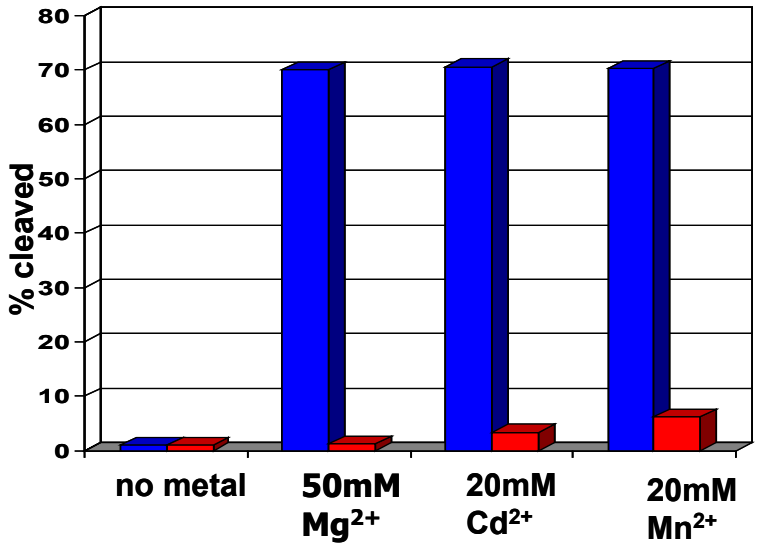

Figure D1. Activity of a HHRz with a 2'-NH_2 substitution at the nucleophile position. The reaction products of a 3 μM 1:1 enzyme:5'-^{32}P-labelled substrate complex was analyzed using a phosphoimaging analysis. Percent cleavage of a WT HHRz (red) after 1 hour and a 2'-NH_2 substituted HHRz (blue) after 36 hours incubation in 5 mM HEPES (pH 8.5) and 100 mM Na^+ in the absence of divalent cations, 50 mM Mg^{2+}, 20 mM Cd^{2+}, or 20 mM Mn^{2+}.

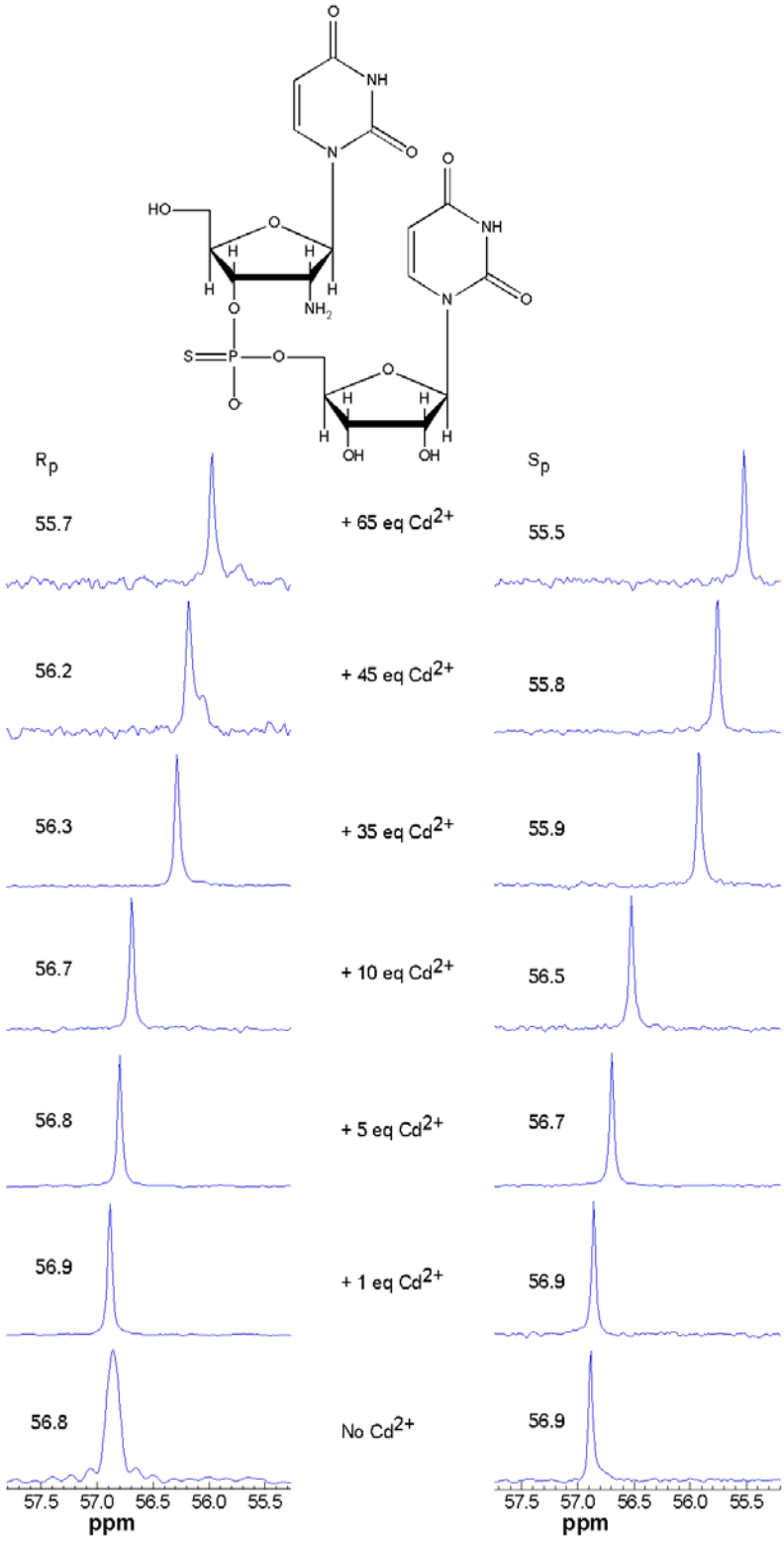

Figure D2. ^{31}P NMR of $^{am}U_{PS}U$ Cd^{2+} Titration. Experiment was performed on 400 μM separated diastereomers at 15 °C in 5 mM HEPES (pH 8) and 100mM Na^{+}.

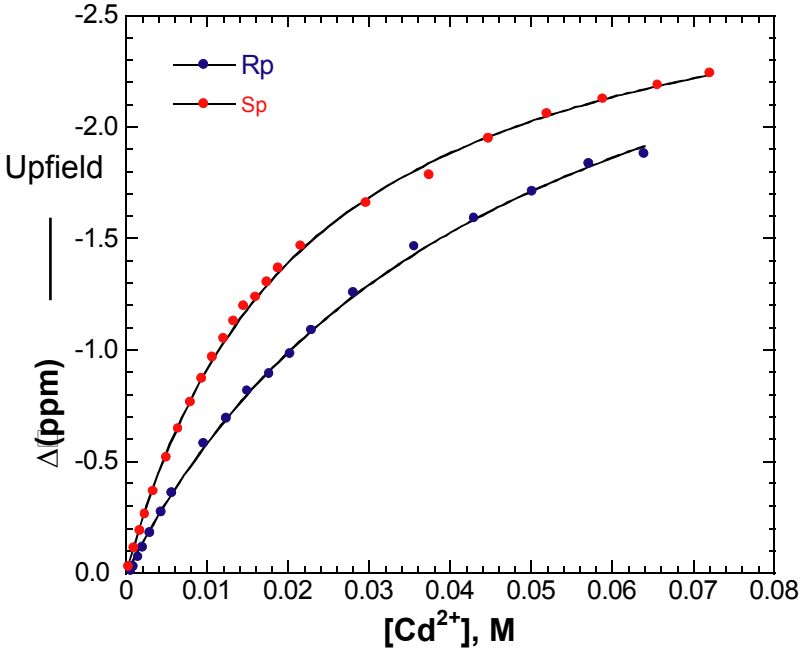

Figure D3. Fit of ^{31}P NMR of $^{am}U_{PS}U$ Cd^{2+} Titration. R_p (blue) and S_p (red) change in chemical shift with added Cd^{2+} fit to Equation 1. For R_p, K_d = 46.9 mM and S_p, K_d = 21.6 mM. Sample conditions were 15 °C in 5 mM HEPES (pH 8.0) and 100 mM Na^+.

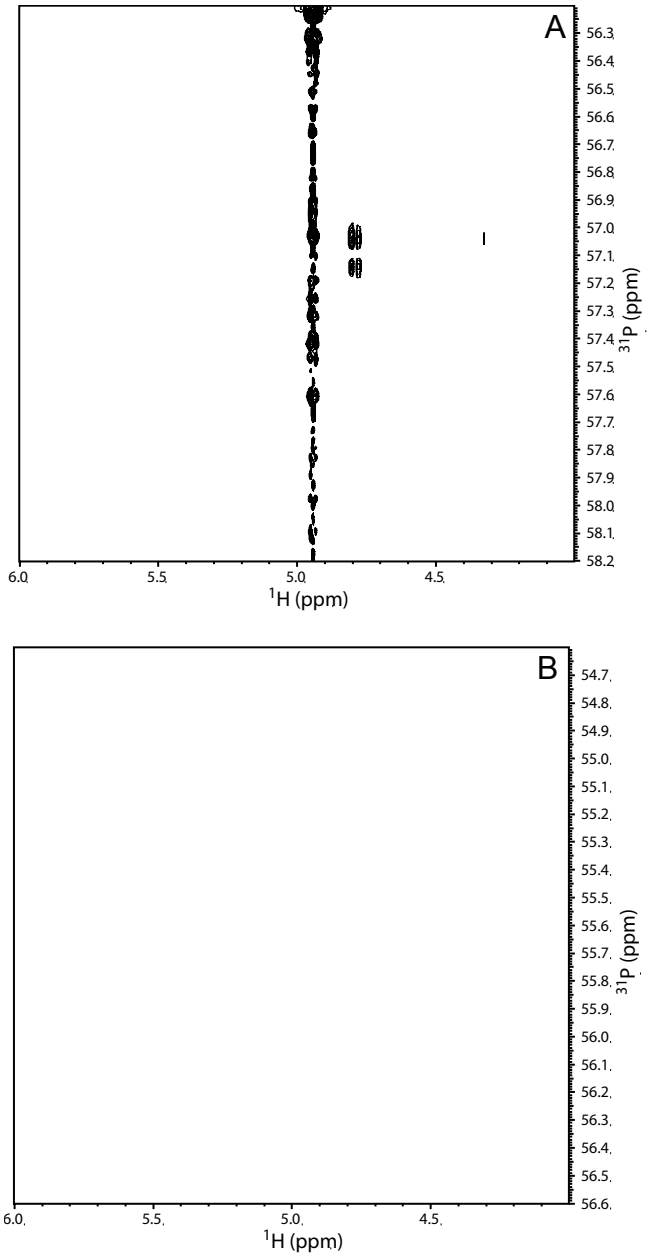

Figure D4. ^{1}H-^{31}P-COSY of U-2'-NH_2-R_p-U. Experiment was run in D_2O at 10 °C in 10 mM phosphate buffer (pH 7.0) and 100 mM NaCl in the (A) absence and (B) the presence of 40 mM Cd^{2+}. The spectra show the crosspeak between the H3' of the 2'-NH_2 ribose and the phosphorothioate phosphorus.

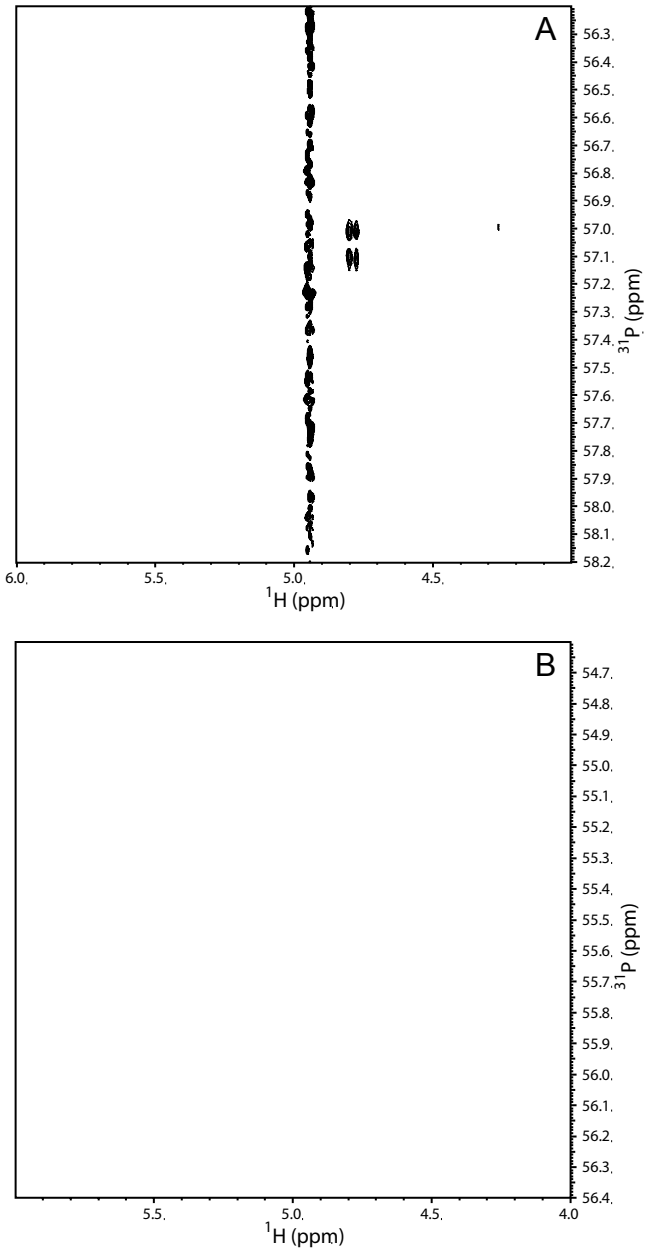

Figure D5. ^{1}H-^{31}P-COSY of U-2'-NH_2-S_p-U. Experiment was run in D_2O at 10 °C in 10 mM phosphate buffer (pH 7.0) and 100 mM NaCl in the (A) absence and (B) the presence of 40 mM Cd^{2+}. The spectra show the crosspeak between the H3' of the 2'-NH_2 ribose and the phosphorothioate phosphorus.

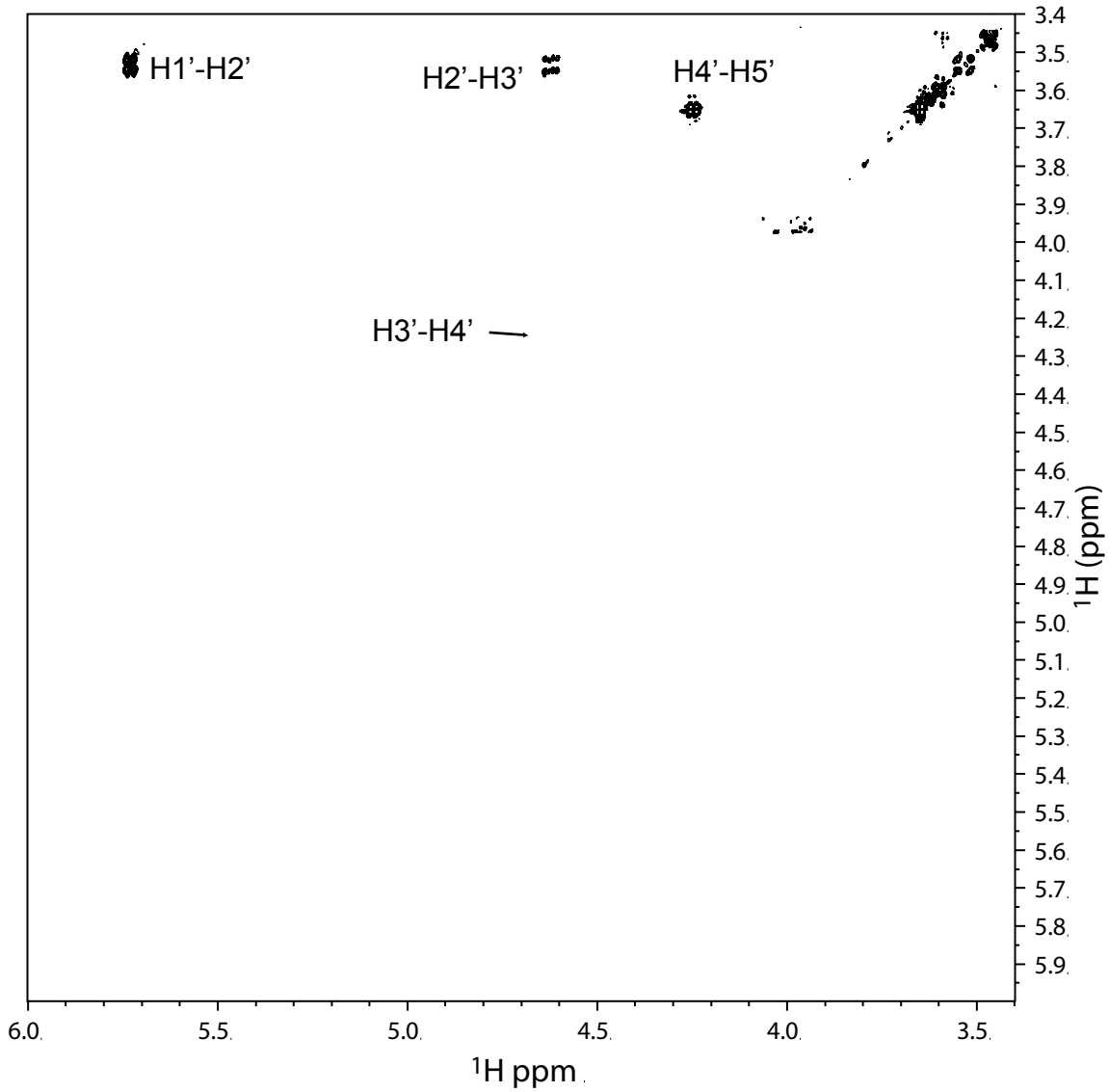

Figure D6. DQF-COSY spectra of $^{am}U_{Sp}U$. Experiment was run in D_2O at 10 °C in 10 mM sodium cacodylate (pH 7.4) and 100 mM NaCl in the absence (black) and presence (red) of 40 mM $CdCl_2$.

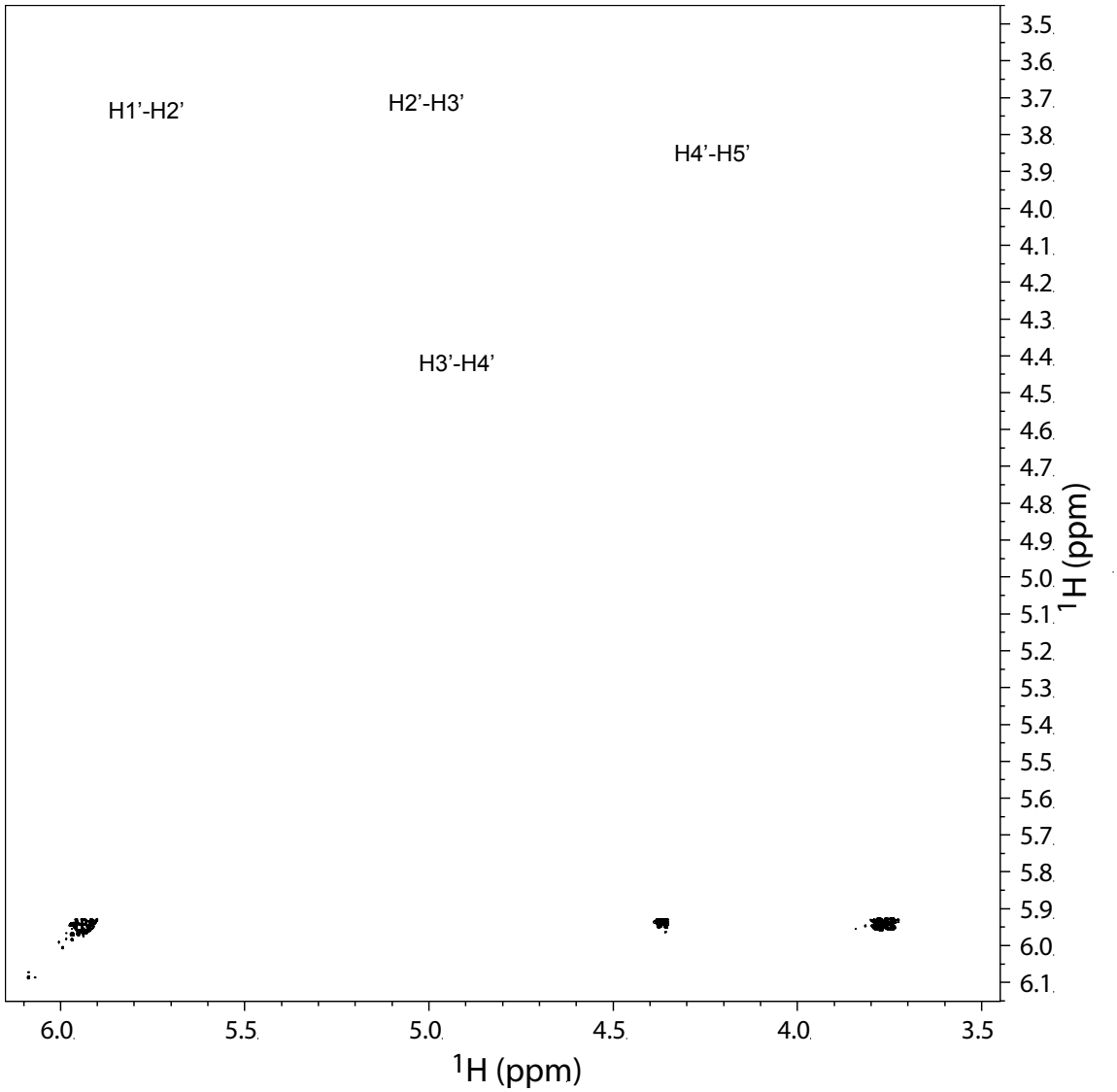

Figure D7. DQF-COSY spectra of $^{am}U_{Rp}U$. Experiment was run in D_2O at 10 °C in 10 mM sodium cacodylate (pH 7.4) and 100 mM NaCl in the absence (black) and presence (red) of 40 mM $CdCl_2$.

REFERENCES CITED

Acharya, S., Foldesi, A., and Chattopadhyaya, J. 2003. The pK(a) of the internucleotidic 2'-hydroxyl group in diribonucleoside (3'-->5') monophosphates. *J Org Chem* **68**(5): 1906-1910.

Aurup, H., Tuschl, T., Benseler, F., Ludwig, J., and Eckstein, F. 1994. Oligonucleotide duplexes containing 2'-amino-2'-deoxycytidines: thermal stability and chemical reactivity. *Nucleic Acids Res* **22**(1): 20-24.

Ballin, J.D., Bharill, S., Fialcowitz-White, E.J., Gryczynski, I., Gryczynski, Z., and Wilson, G.M. 2007. Site-specific variations in RNA folding thermodynamics visualized by 2-aminopurine fluorescence. *Biochemistry* **46**(49): 13948-13960.

Bassi, G.S., Mollegaard, N.E., Murchie, A.I.H., Vonkitzing, E., and Lilley, D.M.J. 1995. Ionic Interactions and the Global Conformations of the Hammerhead Ribozyme. *Nature Structural Biology* **2**(1): 45-55.

Bevilacqua, P.C. 2003. Mechanistic considerations for general acid-base catalysis by RNA: revisiting the mechanism of the hairpin ribozyme. *Biochemistry* **42**(8): 2259-2265.

Blount, K.E. and Uhlenbeck, O.C. 2005. The structure-function dilemma of the hammer head ribozyme. *Annual Review of Biophysics and Biomolecular Structure* **34**: 415-440.

Boots, J.L., Canny, M.D., Azimi, E., and Pardi, A. 2008. Metal ion specificities for folding and cleavage activity in the Schistosoma hammerhead ribozyme. *RNA* **14**(10): 2212-2222.

Buskiewicz, I.A. and Burke, J.M. 2012. Folding of the hammerhead ribozyme: Pyrrolo-cytosine fluorescence separates core folding from global folding and reveals a pH-dependent conformational change. *Rna-a Publication of the Rna Society* **18**(3): 434-448.

Buzayan, J.M., Gerlach, W.L., and Bruening, G. 1986. Satellite tobacco ringspot virus RNA: A subset of the RNA sequence is sufficient for autolytic processing. *Proc Natl Acad Sci U S A* **83**(23): 8859-8862.

Canny, M.D., Jucker, F.M., Kellogg, E., Khvorova, A., Jayasena, S.D., and Pardi, A. 2004. Fast cleavage kinetics of a natural hammerhead ribozyme. *Journal of the American Chemical Society* **126**(35): 10848-10849.

Chi, Y.I., Martick, M., Lares, M., Kim, R., Scott, W.G., and Kim, S.H. 2008. Capturing hammerhead ribozyme structures in action by modulating general base catalysis. *PLoS Biol* **6**(9): e234.

Chu, V.B. and Herschlag, D. 2008. Unwinding RNA's secrets: advances in the biology, physics, and modeling of complex RNAs. *Curr Opin Struct Biol* **18**(3): 305-314.

Cochrane, J.C. and Strobel, S.A. 2008. Catalytic strategies of self-cleaving ribozymes. *Accounts of Chemical Research* **41**(8): 1027-1035.

Curtis, E.A. and Bartel, D.P. 2001. The hammerhead cleavage reaction in monovalent cations. *RNA* **7**(4): 546-552.

Dai, Q., Lea, C.R., Lu, J., and Piccirilli, J.A. 2007. Syntheses of (2 ')3 '-N-15-Amino-(2 ')3 '-deoxyguanosine and determination of their pK(a) values by N-15 NMR spectroscopy. *Org Lett* **9**(16): 3057-3060.

Das, R., Travers, K.J., Bai, Y., and Herschlag, D. 2005. Determining the Mg2+ stoichiometry for folding an RNA metal ion core. *J Am Chem Soc* **127**(23): 8272-8273.

De la Pena, M., Gago, S., and Flores, R. 2003. Peripheral regions of natural hammerhead ribozymes greatly increase their self-cleavage activity. *EMBO J* **22**(20): 5561-5570.

de la Pena, M. and Garcia-Robles, I. 2010. Ubiquitous presence of the hammerhead ribozyme motif along the tree of life. *Rna-a Publication of the Rna Society* **16**(10): 1943-1950.

Delaglio, F., Grzesiek, S., Vuister, G.W., Zhu, G., Pfeifer, J., and Bax, A. 1995. NMRPipe: a multidimensional spectral processing system based on UNIX pipes. *J Biomol NMR* **6**(3): 277-293.

DeRose, V.J. 2002. Two decades of RNA catalysis. *Chem Biol* **9**(9): 961-969.

-. 2008. Characterization of nucleic acid metal ion binding by spectroscopic techniques. In *Nucleic Acid-Metal Ion Interactions*, (ed. N.V. Hud), pp. 154-175. Royal Society of Chemistry, Cambridge.

Draper, D.E. 2004. A guide to ions and RNA structure. *RNA* **10**(3): 335-343.

Dufour, D., de la Pena, M., Gago, S., Flores, R., and Gallego, J. 2009. Structure-function analysis of the ribozymes of chrysanthemum chlorotic mottle viroid: a loop-loop interaction motif conserved in most natural hammerheads. *Nucleic Acids Res* **37**(2): 368-381.

Dunitz, J. and Taylor, R. 1997. Organic fluorine hardly ever accepts hydrogen bonds. *Chem Eur J* **3**: 89-98.

Edwards, T.E. and Sigurdsson, S.T. 2005. EPR spectroscopic analysis of U7 hammerhead ribozyme dynamics during metal ion induced folding. *Biochemistry* **44**(38): 12870-12878.

Epstein, L.M. and Gall, J.G. 1987. Self-Cleaving Transcripts of Satellite DNA from the Newt. *Cell* **48**(3): 535-543.

Erat, M.C. and Roland, K.O. 2011. Metal Ions in Life Sciences. **9** 37-100.

Fedor, M.J. 2009. Comparative enzymology and structural biology of RNA self-cleavage. *Annu Rev Biophys* **38**: 271-299.

Fedor, M.J. and Williamson, J.R. 2005. The catalytic diversity of RNAS. *Nature Reviews Molecular Cell Biology* **6**(5): 399-412.

Feig, A.L. and Uhlenbeck, O. 1999. The role of metal ions in RNA biochemistry. In *The RNA World*, (ed. R.F.G.e. al.), pp. 287-319. Cold Spring HArbor Labratory Press, Cold Spring Harbor, NY.

Ferbeyre, G., Smith, J.M., and Cedergren, R. 1998. Schistosome satellite DNA encodes active hammerhead ribozymes. *Molecular and Cellular Biology* **18**(7): 3880-3888.

Flores, R., Hernandez, C., de Alba, A.E.M., Daros, J.A., and Di Serio, F. 2005. Viroids and viroid-host interactions. *Annual Review of Phytopathology* **43**: 117-139.

Forconi, M. and Herschlag, D. 2009. Use of phosphorothioates to identify sites of metal-ion binding in RNA. *Methods Enzymol* **468**: 311-333.

Forster, A.C. and Symons, R.H. 1987. Self-cleavage of virusoid RNA is performed by the proposed 55-nucleotide active site. *Cell* **50**(1): 9-16.

Frederiksen, J.K. and Piccirilli, J.A. 2009. Identification of catalytic metal ion ligands in ribozymes. *Methods* **49**(2): 148-166.

Gesteland, R.F., Cech, T., and Atkins, J.F. 2006. *The RNA world : the nature of modern RNA suggests a prebiotic RNA world*. Cold Spring Harbor Laboratory Press, Cold Spring Harbor, N.Y.

Gonzalez, R.L., Jr. and Tinoco, I., Jr. 1999. Solution structure and thermodynamics of a divalent metal ion binding site in an RNA pseudoknot. *J Mol Biol* **289**(5): 1267-1282.

Guerrier-Takada, C., Gardiner, K., Marsh, T., Pace, N., and Altman, S. 1983. The Rna Moiety of Ribonuclease-P Is the Catalytic Subunit of the Enzyme. *Cell* **35**(3): 849-857.

Guschlbauer, W. and Jankowski, K. 1980. Nucleoside conformation is determined by the electronegativity of the sugar substituent. *Nucleic Acids Res* **8**(6): 1421-1433.

Haasnoot, C.A.G., Deleeuw, F.A.A.M., and Altona, C. 1980. The Relationship between Proton-Proton Nmr Coupling-Constants and Substituent Electronegativities .1. An Empirical Generalization of the Karplus Equation. *Tetrahedron* **36**(19): 2783-2792.

Hall, K.B. 2009. 2-Aminopurine as a Probe of Rna Conformational Transitions. *Methods in Enzymology, Vol 469: Biophysical, Chemical, and Functional Probes of Rna Structure, Interactions and Folding, Pt B* **469**: 269-285.

Hammann, C., Luptak, A., Perreault, J., and de la Pena, M. 2012. The ubiquitous hammerhead ribozyme. *RNA* **18**(5): 871-885.

Hammann, C., Norman, D.G., and Lilley, D.M. 2001. Dissection of the ion-induced folding of the hammerhead ribozyme using 19F NMR. *Proc Natl Acad Sci U S A* **98**(10): 5503-5508.

Han, J. and Burke, J.M. 2005. Model for general acid-base catalysis by the hammerhead ribozyme: pH-activity relationships of G8 and G12 variants at the putative active site. *Biochemistry* **44**(21): 7864-7870.

Hardman, S.J., Botchway, S.W., and Thompson, K.C. 2008. Evidence for a nonbase stacking effect for the environment-sensitive fluorescent base pyrrolocytosine--comparison with 2-aminopurine. *Photochem Photobiol* **84**(6): 1473-1479.

Hardman, S.J. and Thompson, K.C. 2006. Influence of base stacking and hydrogen bonding on the fluorescence of 2-aminopurine and pyrrolocytosine in nucleic acids. *Biochemistry* **45**(30): 9145-9155.

Haseloff, J. and Gerlach, W.L. 1988. Simple RNA enzymes with new and highly specific endoribonuclease activities. *Nature* **334**(6183): 585-591.

Hobbs, J., Sternbach, H., Sprinzl, M., and Eckstein, F. 1973. Polynucleotides containing 2'-amino-2'-deoxyribose and 2'-azido-2'-deoxyribose. *Biochemistry* **12**: 5138-5145.

Horton, T.E., Clardy, D.R., and DeRose, V.J. 1998. Electron paramagnetic resonance spectroscopic measurement of Mn2+ binding affinities to the hammerhead ribozyme and correlation with cleavage activity. *Biochemistry* **37**(51): 18094-18101.

Hruska, F.E., Mak, A., Singh, H., and Shugar, D. 1973. Proton magnetic-resonance study of effect of 2'-O-methylation on ribonucleoside conformation. *Can J Chem* **51**(7): 1099-1106.

Hunsicker, L.M. and DeRose, V.J. 2000. Activities and relative affinities of divalent metals in unmodified and phosphorothioate-substituted hammerhead ribozymes. *J Inorg Biochem* **80**(3-4): 271-281.

J.M., T. and Perrin, D.M. 2009. Probing general acid catalysis in the hammerhead ribozyme. *Journal of the American Chemical Society* **131**: 1520-5126.

Khvorova, A., Lescoute, A., Westhof, E., and Jayasena, S.D. 2003. Sequence elements outside the hammerhead ribozyme catalytic core enable intracellular activity. *Nat Struct Biol* **10**(9): 708-712.

Kim, N.K., Bowman, M.K., and DeRose, V.J. 2010. Precise mapping of RNA tertiary structure via nanometer distance measurements with double electron-electron resonance spectroscopy. *J Am Chem Soc* **132**(26): 8882-8884.

Kim, N.K., Murali, A., and DeRose, V.J. 2005. Separate metal requirements for loop interactions and catalysis in the extended hammerhead ribozyme. *J Am Chem Soc* **127**(41): 14134-14135.

Kim, S.G., Lin, L.J., and Reid, B.R. 1992. Determination of Nucleic-Acid Backbone Conformation by H-1-Nmr. *Biochemistry* **31**(14): 3564-3574.

Kisseleva, N., Khvorova, A., Westhof, E., and Schiemann, O. 2005. Binding of manganese(II) to a tertiary stabilized hammerhead ribozyme as studied by electron paramagnetic resionance spectroscopy. *Rna-a Publication of the Rna Society* **11**(1): 1-6.

Klein, D.J. and Ferre-D'Amare, A.R. 2006. Structural basis of glmS ribozyme activation by glucosamine-6-phosphate. *Science* **313**(5794): 1752-1756.

Knoll, R., Bald, R., and Furste, J.P. 1997. Complete identification of nonbridging phosphate oxygens involved in hammerhead cleavage. *RNA* **3**(2): 132-140.

Kore, A.R. and Eckstein, F. 1999. Hammerhead Ribozyme Mechanism: A Ribonucleotide 5‘ to the Substrate Cleavage Site Is Not Essential&#x2020. *Biochemistry* **38**(34): 10915-10918.

Kruger, K., Grabowski, P.J., Zaug, A.J., Sands, J., Gottschling, D.E., and Cech, T.R. 1982. Self-Splicing Rna - Auto-Excision and Auto-Cyclization of the Ribosomal-Rna Intervening Sequence of Tetrahymena. *Cell* **31**(1): 147-157.

Lakowicz, J.R. 2006. *Principles of fluorescence spectroscopy*. Springer, New York.

Leclerc, F. 2010. Hammerhead ribozymes: true metal or nucleobase catalysis? Where is the catalytic power from? *Molecules* **15**(8): 5389-5407.

Lee, T.S., Giambasu, G.M., Sosa, C.P., Martick, M., Scott, W.G., and York, D.M. 2009. Threshold Occupancy and Specific Cation Binding Modes in the Hammerhead Ribozyme Active Site are Required for Active Conformation. *Journal of Molecular Biology* **388**(1): 195-206.

Lee, T.S., Lopez, C.S., Giambasu, G.M., Martick, M., Scott, W.G., and York, D.M. 2008. Role of Mg2+ in hammerhead ribozyme catalysis from molecular simulation. *Journal of the American Chemical Society* **130**(10): 3053-3064.

Maderia, M., Hunsicker, L.M., and DeRose, V.J. 2000. Metal-phosphate interactions in the hammerhead ribozyme observed by 31P NMR and phosphorothioate substitutions. *Biochemistry* **39**(40): 12113-12120.

Martell, A.E. and Hancock, R.D. 1996. *Metal Complexes in Aqueous Solutions*. Plenum, New York.

Martell, A.E. and Smith, R.E. 1971-1974. *Critical Stability Constants*. Plenum, New York.

Martick, M., Horan, L.H., Noller, H.F., and Scott, W.G. 2008a. A discontinuous hammerhead ribozyme embedded in a mammalian messenger RNA. *Nature* **454**(7206): 899-U857.

Martick, M., Lee, T.S., York, D.M., and Scott, W.G. 2008b. Solvent structure and hammerhead ribozyme catalysis. *Chemistry & Biology* **15**(4): 332-342.

Martick, M. and Scott, W.G. 2006. Tertiary contacts distant from the active site prime a ribozyme for catalysis. *Cell* **126**(2): 309-320.

McDowell, S.E., Jun, J.M., and Walter, N.G. 2010. Long-range tertiary interactions in single hammerhead ribozymes bias motional sampling toward catalytically active conformations. *RNA* **16**(12): 2414-2426.

Menger, M., Tuschl, T., Eckstein, F., and Porschke, D. 1996. Mg2+-dependent conformational changes in the hammerhead ribozyme. *Biochemistry* **35**(47): 14710-14716.

Michel, F. and Dujon, B. 1983. Conservation of Rna Secondary Structures in 2 Intron Families Including Mitochondrial-Encoded, Chloroplast-Encoded and Nuclear-Encoded Members. *Embo Journal* **2**(1): 33-38.

Misra, V.K. and Draper, D.E. 2002. The linkage between magnesium binding and RNA folding. *Journal of Molecular Biology* **317**(4): 507-521.

Mohanty, U., Spasic, A., Kim, H.D., and Chu, S. 2005. Ion atmosphere of three-way junction nucleic acid. *J Phys Chem B* **109**(45): 21369-21374.

Mohr, G., Ghanem, E., and Lambowitz, A.M. 2010. Mechanisms Used for Genomic Proliferation by Thermophilic Group II Introns. *Plos Biology* **8**(6).

Nelson, J. and Uhlenbeck, O. 2008a. Hammerhead redux: Does the new structure fit the old biochemical data? *RNA* **14**(4): 605-615.

Nelson, J.A. and Uhlenbeck, O.C. 2008b. Hammerhead redux: Does the new structure fit the old biochemical data? *Rna-a Publication of the Rna Society* **14**(4): 605-615.

Nissen, P., Hansen, J., Ban, N., Moore, P.B., and Steitz, T.A. 2000. The structural basis of ribosome activity in peptide bond synthesis. *Science* **289**(5481): 920-930.

O'Rear, J.L., Wang, S.L., Feig, A.L., Beigelman, L., Uhlenbeck, O.C., and Herschlag, D. 2001. Comparison of the hammerhead cleavage reactions stimulated by monovalent and divalent cations. *RNA* **7**(4): 537-545.

Osborne, E.M., Schaak, J.E., and DeRose, V.J. 2005a. Characterization of a native hammerhead ribozyme derived from schistosomes. *Faseb Journal* **19**(4): A293-A293.

Osborne, E.M., Schaak, J.E., and Derose, V.J. 2005b. Characterization of a native hammerhead ribozyme derived from schistosomes. *RNA* **11**(2): 187-196.

Osborne, E.M., Ward, W.L., Ruehle, M.Z., and DeRose, V.J. 2009. The identity of the nucleophile substitution may influence metal interactions with the cleavage site of the minimal hammerhead ribozyme. *Biochemistry* **48**(44): 10654-10664.

Pecoraro, V.L., Hermes, J.D., and Cleland, W.W. 1984. Stability constants of Mg2+ and Cd2+ complexes of adenine nucleotides and thionucleotides and rate constants for formation and dissociation of MgATP and MgADP. *Biochemistry* **23**(22): 5262-5271.

Penedo, J.C., Wilson, T.J., Jayasena, S.D., Khvorova, A., and Lilley, D.M. 2004. Folding of the natural hammerhead ribozyme is enhanced by interaction of auxiliary elements. *RNA* **10**(5): 880-888.

Peracchi, A., Beigelman, L., Scott, E.C., Uhlenbeck, O.C., and Herschlag, D. 1997. Involvement of a specific metal ion in the transition of the hammerhead ribozyme to its catalytic conformation. *J Biol Chem* **272**(43): 26822-26826.

Pieken, W., Olsen, D., Benseler, F., Aurup, H., and Eckstein, F. 1991. Kinetic characterization of ribonuclease-resistant 2'-modified hammerhead ribozymes. *Science* **253**: 314-317.

Pley, H.W., Flaherty, K.M., and McKay, D.B. 1994. Three-dimensional structure of a hammerhead ribozyme. *Nature* **372**(6501): 68-74.

Rachofsky, E.L., Osman, R., and Ross, J.B.A. 2001. Probing structure and dynamics of DNA with 2-aminopurine: Effects of local environment on fluorescence. *Biochemistry* **40**(4): 946-956.

Roberts, G.C.K. 1993. *NMR of Macromolecules*. Oxford University Press, Oxford.

Roychowdhury-Saha, M. and Burke, D.H. 2006. Extraordinary rates of transition metal ion-mediated ribozyme catalysis. *RNA* **12**(10): 1846-1852.

-. 2007. Distinct reaction pathway promoted by non-divalent-metal cations in a tertiary stabilized hammerhead ribozyme. *RNA-Publ RNA Soc* **13**(6): 841-848.

Rueda, D., Wick, K., McDowell, S.E., and Walter, N.G. 2003. Diffusely bound Mg2+ ions slightly reorient stems I and II of the hammerhead ribozyme to increase the probability of formation of the catalytic core. *Biochemistry* **42**(33): 9924-9936.

Ruffner, D.E., Stormo, G.D., and Uhlenbeck, O.C. 1990. Sequence requirements of the hammerhead RNA self-cleavage reaction. *Biochemistry* **29**(47): 10695-10702.

Ruffner, D.E. and Uhlenbeck, O.C. 1990. Thiophosphate interference experiments locate phosphates important for the hammerhead RNA self-cleavage reaction. *Nucleic Acids Res* **18**(20): 6025-6029.

Saksmerprome, V., Roychowdhury-Saha, M., Jayasena, S., Khvorova, A., and Burke, D.H. 2004. Artificial tertiary motifs stabilize trans-cleaving hammerhead ribozymes under conditions of submillimolar divalent ions and high temperatures. *RNA* **10**(12): 1916-1924.

Schnabl, J. and Sigel, R.K. 2010. Controlling ribozyme activity by metal ions. *Curr Opin Chem Biol* **14**(2): 269-275.

Scott, W.G., Finch, J.T., and Klug, A. 1995. The crystal structure of an all-RNA hammerhead ribozyme: a proposed mechanism for RNA catalytic cleavage. *Cell* **81**(7): 991-1002.

Shan, S., Kravchuk, A.V., Piccirilli, J.A., and Herschlag, D. 2001. Defining the catalytic metal ion interactions in the Tetrahymena ribozyme reaction. *Biochemistry* **40**(17): 5161-5171.

Shepotinovskaya, I.V. and Uhlenbeck, O.C. 2008. Catalytic diversity of extended hammerhead ribozymes. *Biochemistry* **47**(27): 7034-7042.

Sigel, R.K. and Pyle, A.M. 2007. Alternative roles for metal ions in enzyme catalysis and the implications for ribozyme chemistry. *Chem Rev* **107**(1): 97-113.

Sigel, R.K.O., Song, B., and Sigel, H. 1997. Stabilities and structures of metal ion complexes of adenosine 5'-O-thiomonophosphate (AMPS(2-)) in comparison with those of its parent nucleotide (AMP(2-)) in aqueous solution. *Journal of the American Chemical Society* **119**(4): 744-755.

Slim, G. and Gait, M.J. 1991. Configurationally defined phosphorothioate-containing oligoribonucleotides in the study of the mechanism of cleavage of hammerhead ribozymes. *Nucleic Acids Res* **19**(6): 1183-1188.

Stahley, M.R., Adams, P.L., Wang, J.M., and Strobel, S.A. 2007. Structural metals in the group I intron: A ribozyme with a multiple metal ion core. *J Mol Biol* **372**(1): 89-102.

Steitz, T.A. and Steitz, J.A. 1993. A general two-metal-ion mechanism for catalytic RNA. *Proc Natl Acad Sci U S A* **90**(14): 6498-6502.

Suzumura, K., Yoshinari, K., Tanaka, Y., Takagi, Y., Kasai, Y., Warashina, M., Kuwabara, T., Orita, M., and Taira, K. 2002. A reapprisal, based on ^{31}P NMR, of the direct coordination of a metal ion with the phosphoryl oxygen at the cleavage site of a hammerhead ribozyme. *J Am Chem Soc* **124**: 8230-8236.

Thomas, J.M. and Perrin, D.M. 2008. Probing General Base Catalysis in the Hammerhead Ribozyme. *Journal of the American Chemical Society* **130**(46): 15467-15475.

-. 2009. Probing general acid catalysis in the hammerhead ribozyme. *J Am Chem Soc* **131**(3): 1135-1143.

Uesugi, S., Miki, H., Ikehara, M., Iwahashi, H., and Kyogoku, Y. 1979. Linear relationship between electronegativity of 2'-substituents and conformation of adenine nucleosides. *Tet Lett*(42): 4073-4076.

Uhlenbeck, O.C. 1987. A small catalytic oligoribonucleotide. *Nature* **328**(6131): 596-600.

Velikyan, I., Acharya, S., Trifonova, A., Foldesi, A., and Chattopadhyaya, J. 2001. The pK(a)'s of 2'-hydroxyl group in nucleosides and nucleotides. *J Am Chem Soc* **123**(12): 2893-2894.

Verheyden, J., Wagner, D., and Moffatt, J. 1971. Synthesis of some pyrimidine 2'-amino-2'-deoxynucleosides. *J Org Chem* **37**: 250-254.

Vogt, M., Lahiri, S., Hoogstraten, C.G., Britt, R.D., and DeRose, V.J. 2006. Coordination environment of a site-bound metal ion in the hammerhead ribozyme determined by 15N and 2H ESEEM spectroscopy. *J Am Chem Soc* **128**(51): 16764-16770.

Walter, N.G., Harris, D.A., Pereira, M.J.B., and Rueda, D. 2001. In the fluorescent spotlight: Global and local conformational changes of small catalytic RNAs. *Biopolymers* **61**(3): 224-242.

Wang, S., Karbstein, K., Peracchi, A., Beigelman, L., and Herschlag, D. 1999a. Identification of the hammerhead ribozyme metal ion binding site responsible for rescue of the deleterious effect of a cleavage site phosphorothioate. *Biochemistry* **38**(43): 14363-14378.

Wang, S.L., Karbstein, K., Peracchi, A., Beigelman, L., and Herschlag, D. 1999b. Identification of the hammerhead ribozyme metal ion binding site responsible for rescue of the deleterious effect of a cleavage site phosphorothioate. *Biochemistry* **38**(43): 14363-14378.

Ward, W.L. and DeRose, V.J. 2012. Ground-state coordination of a catalytic metal to the scissile phosphate of a tertiary-stabilized Hammerhead ribozyme. *Rna-a Publication of the Rna Society* **18**(1): 16-23.

-. Submitted. Metal-Dependent Structural Transitions Measured by 2-Aminopurine in the Three Helix Junction of the Hammerhead Ribozyme.

Winkler, W.C., Nahvi, A., Roth, A., Collins, J.A., and Breaker, R.R. 2004. Control of gene expression by a natural metabolite-responsive ribozyme. *Nature* **428**(6980): 281-286.

Woodson, S.A. 2005. Metal ions and RNA folding: a highly charged topic with a dynamic future. *Curr Opin Chem Biol* **9**(2): 104-109.

-. 2010. Compact intermediates in RNA folding. *Annu Rev Biophys* **39**: 61-77.

Zhang, Y. and Epstein, L.M. 1996. Cloning and characterization of extended hammerheads from a diverse set of caudate amphibians. *Gene* **172**(2): 183-190.